SANDIA REPORT

SAND2016-3077
Unlimited Release
Printed March 2016

Assessment of the Available Drawdowns for Oil Storage Caverns at the West Hackberry SPR Site

Steven R. Sobolik

Prepared by
Sandia National Laboratories
Albuquerque, New Mexico 87185 and Livermore, California 94550

Sandia National Laboratories is a multi-program laboratory managed and operated by Sandia Corporation, a wholly owned subsidiary of Lockheed Martin Corporation, for the U.S. Department of Energy's National Nuclear Security Administration under contract DE-AC04-94AL85000.

Issued by Sandia National Laboratories, operated for the United States Department of Energy by Sandia Corporation.

Available to DOE and DOE contractors from
U.S. Department of Energy
Office of Scientific and Technical Information
P.O. Box 62
Oak Ridge, TN 37831

Telephone: (865) 576-8401
Facsimile: (865) 576-5728
E-Mail: reports@osti.gov
Online ordering: http://www.osti.gov/scitech

Available to the public from
U.S. Department of Commerce
National Technical Information Service
5301 Shawnee Rd
Alexandria, VA 22312

Telephone: (800) 553-6847
Facsimile: (703) 605-6900
E-Mail: orders@ntis.gov
Online order: http://www.ntis.gov/search

SAND2016-3077
Unlimited Release
Printed March 2016

Assessment of the Available Drawdowns for Oil Storage Caverns at the West Hackberry SPR Site

Steven R. Sobolik
Geotechnology and Engineering Department
Sandia National Laboratories
P.O. Box 5800
Albuquerque, New Mexico 87185-0751

ABSTRACT

The Department of Energy, in response to requests from the U.S. Congress, wishes to maintain an up-to-date table documenting the number of available full drawdowns of each of the caverns owned by the Strategic Petroleum Reserve. This information is important for assessing the SPR's ability to deliver oil to domestic oil companies expeditiously if national or world events dictate a rapid sale and deployment of the oil reserves. What factors go into assessing available drawdowns? The evaluation of drawdown risks require the consideration of several factors regarding cavern and wellbore integrity and stability, including stress states caused by cavern geometry and operations, salt damage caused by dilatant and tensile stresses, the effect on enhanced creep on wellbore integrity, the sympathetic stress effect of operations on neighboring caverns.

Based on the work over the past several months, a consensus has been built regarding the assessment of drawdown capabilities and risks for the SPR caverns. This paper draws upon the recently West Hackberry model upgrade and analyses to reevaluate and update the available drawdowns for each of those caverns. Similar papers for the Bryan Mound, Big Hill, and Bayou Choctaw papers will be developed as the upgrades to those analyses are completed. The rationale and documentation of the methodology is described in the remainder of this report, as are the updated estimates of available drawdowns for the West Hackberry caverns.

ACKNOWLEDGEMENTS

The author would like to thank Byoung-Yoon Park, Anna Lord, Barry Roberts, Moo Lee, and David Borns for their review and support of this work.

CONTENTS

LIST OF FIGURES

LIST OF TABLES

1. Introduction

The Department of Energy, in response to requests from the U.S. Congress, wishes to maintain an up-to-date table documenting the number of available full drawdowns of each of the caverns owned by the Strategic Petroleum Reserve. This information is important for assessing the SPR's ability to deliver oil to domestic oil companies expeditiously if national or world events dictate a rapid sale and deployment of the oil reserves. What factors go into assessing available drawdowns? The evaluation of drawdown risks require the consideration of several factors regarding cavern and wellbore integrity and stability, including stress states caused by cavern geometry and operations, salt damage caused by dilatant and tensile stresses, the effect on enhanced creep on wellbore integrity, the sympathetic stress effect of operations on neighboring caverns.

Based on the work over the past several months, a consensus has been built regarding the assessment of drawdown capabilities and risks for the SPR caverns. This paper draws upon the recently West Hackberry model upgrade and analyses (Sobolik, 2015) to reevaluate and update the available drawdowns for each of those caverns. Similar papers for the Bryan Mound, Big Hill, and Bayou Choctaw papers will be developed as the upgrades to those analyses are completed. The rationale and documentation of the methodology is described in the remainder of this report; the updated values for West Hackberry are included in Table 1-1.

Table 1-1. Updated Number of Available Drawdowns West Hackberry

Cavern	Basis				Best Estimate Basis (P/D or GM), Comments, Reference
	2D P/D < 1	3D P/D < 1	Geomechanics	Best Estimate	
WH101	3	3	5	5	GM; Sobolik, 2015
WH102	3	3	5	5	GM; Sobolik, 2015
WH103	2	4	5	5	GM; Sobolik, 2015
WH104	3	3	5	5	GM; Sobolik, 2015
WH105	2	2	5	5	GM; Sobolik, 2015
WH106	4	4	5	5	GM; Sobolik, 2015
WH107	2	5	5	5	GM; Sobolik, 2015
WH108	4	4	5	5	GM; Sobolik, 2015
WH109	2	4	5	5	GM; Sobolik, 2015
WH110	1	5	5	5	GM; Sobolik, 2015
WH111	5	5	5	5	GM; Sobolik, 2015
WH112	4	4	5	5	GM; Sobolik, 2015
WH113	4	4	5	5	GM; Sobolik, 2015
WH114	4	4	5	5	GM; Sobolik, 2015
WH115	4	5	5	5	GM; Sobolik, 2015
WH116	4	5	5	5	GM; Sobolik, 2015
WH117	5	5	5	5	GM; Sobolik, 2015
WH6	0	0	1	N/A	Cavern emptied of oil
WH7	0	0	5	5	GM; Sobolik, 2015
WH8	0	0	2	2	GM; Green, Lord et al 2013; Sobolik, 2015
WH9	0	0	1	1	GM; Yellow, Lord et al 2013; Sobolik & Ehgartner, 2009b, Sobolik, 2015
WH11	5	5	5	5	GM; Sobolik, 2015
P/D numbers from Rudeen & Lord (2013)					

1.1 Criteria for Available Drawdowns Developed by Working Group, March 26, 2014

As a follow-up to the progress of analysis detailed in Rudeen and Lord (2013) and Lord et al. (2013), a working group meeting comprising staff from DOE-SPR, Sandia, and Fluor was held in New Orleans on March 26, 2014. The agenda essentially comprised two topics: one, defining the requirements to immediately satisfy the DAT; and two, to develop project-wide agreement on criteria and rationale to be used to assign limits to a cavern's available drawdowns. In these discussions, the following questions were discussed, and definitions developed:

1. What is an available drawdown? To answer this, the following definitions were discussed and agreed upon:
   - Full Drawdown (DD) = 90% of the oil removed from a cavern with raw water
   - Partial Drawdown (PD) is defined by the change to the radius of the cavern where raw water was injected: $\frac{\Delta r_{PD}}{\Delta r_{DD}}$ at the maximum value of radius. (We later discussed that partial drawdowns would have to be logged and counted, and a mechanism to track downloads should be established.)
   - Available Drawdown: A cavern has an available drawdown if after that full drawdown, the long-term stability of the cavern, the cavern field, or the oil quality are not compromised.

2. What criteria are to be used to impose a limit on drawdowns? In these discussions, it was decided that for either a P/D condition or a geomechanical analysis to limit a drawdown, it must create a condition within the cavern that can potentially create failure. To answer this question, we had a long discussion on the three ways that a cavern may "fail":
   - Loss of cavern integrity such that oil escapes to another cavern, oil escapes to a caprock or anhydrite conduit to the environment, or the cavern collapses thus creating a sinkhole above (BC-7) or at the side (Bayou Corne) of a salt dome.
   - Loss of access to stored oil due to irreparable damage to casing, irreparable damage to hanging strings, or sufficient sagging of the roof to below the oil/brine interface.
   - Loss of casing integrity such that oil escapes to another cavern or oil escapes to a caprock or anhydrite conduit to the environment.

We also discussed the ways that field observations and measurements, and geomechanical analyses, can be used to determine the current status of a cavern and to predict future behavior. After these discussions, we created the following table of criteria (Table 1-2) that may be used to limit drawdowns, with examples caverns for each criterion and what the technical basis for each criterion would be and description of how example cavern illustrates it. This table can (and will likely) be modified before we officially address the status of the low drawdown caverns.

Table 1-2. Criteria to Limit Drawdowns

Criterion to Limit Drawdowns	Example Cavern	Technical Basis for Criterion
Sinkhole formation	BM2	Geomechanics (GM) considerations such as predicted tensile stresses above cavern roof; literature on other similar caverns and sinkholes; based on literature, large diameter, proximity to thin caprock, BM2 is SPR cavern with highest potential for sinkhole formation
Cavern coalescence (probable, not absolute)	WH6&9, BC15&17	GM prediction of tensile stresses that could cause coalescence; also operator judgment. Coalescence of WH-6, 9 would render them inoperable because of casing, GM considerations. Whereas BC-15, 17 are operated as a gallery now, so coalescence might be acceptable.
Oil leaking outside cavern system (casing issue)	BH (example of problem, not DD-based.)	GM predictions of strains, shear and collapse stresses on casings. Emphasis on how drawdown would change existing strain, stress accumulation rates. In addition, other definitions would have to be established: What is a leak (operationally, legally)? How do we factor in casing repair? How does this affect 1-DD caverns, which may require long-term post-oil monitoring and maintenance?
Emulsions	BM5	Not discussed, except that loss of a hanging string in BM-5 would present emulsion issues for removing the oil according to oil quality regulations.
Oil is unrecoverable outside of drastic action (e.g., new borehole)	WH6, BM5	Not discussed
Fluid removal rate not worth it	WH6, BM2	Does the difficulty of removing the oil based on allowable removal rates make this cavern worth additional drawdowns?
Edge of dome/property line	BC20	Regulations, literature, future GM analyses.

1.2 Determination of Available Drawdowns

The definition of a drawdown used here is the one arrived at in the March 2014 meeting: 90% of the oil removed from a cavern with raw water, which typically adds around 15% to the volume of the cavern. The process can be outlined is outlined by the following steps, after which an explanation of these steps is given:

- Step 1: Using the industry standard of keeping the P/D > 1, the drawdown limit is initially assigned the number of drawdowns before the SOCON-defined 2D P/D becomes less than 1.0.

- Step 2: The drawdown limit based on the 3D P/D ratio defined in Lord, Rudeen et al. (2009), which represents a more physically meaningful description of the pillar thickness between caverns, is compared to the 2D P/D limit.
- Step 3: The drawdown limit based on full-scale geomechanical model predictions are also compared to the 2D P/D limit. If the limits based on the 3D P/D and the geomechanical analyses are both at least at large as the 2D P/D, the 3D P/D limit is used as the best estimate for the drawdown limit. If the geomechanical analysis additionally fits certain criteria described below, and if its drawdown limit is the highest of the three, then the geomechanical limit is used as the best estimate.
- Step 4: If, after all these steps, the drawdown limit is equal to zero, the best estimate is assigned a value of 1, with comments describing the anticipated technical issues during a drawdown of that cavern. This step results from the fact that the oil must at some point be withdrawn from all the caverns.
- Step 5: Regardless of P/D or geomechanics calculations, an absolute maximum limit of 5 drawdowns has been defined, to allow for increased knowledge and experience to better inform this process in the future.

As described in Rudeen and Lord (2013), SPR joint working group meetings on cavern leaching and SOCON software training held in New Orleans, LA, in the spring of 2013 resulted in the adoption and implementation of a new definition of the P/D ratio, namely the 2D P/D. The new definition is more conservative than the definitions used in the 2009 analyses by Lord, Rudeen et al. (2009). In fact, the new definition could be summarized as using the smallest logical "pillar" thickness and the largest logical cavern "diameter." The new 2D P/D can be shown to be less than or equal to the definitions used in 2009. The first applications of these definitions are shown in the Technical Basis for 2013 SPR Remedial Leach Plan (Eldredge, Checkai et al. 2013).

A study by Park and Ehgartner (2011) justified a conservative and reasonable lower limit on the minimum 3D P/D of 1.0, based on geomechanical modeling that predicted the onset of dilatant failure of the salt as a function of P/D. Note they did not claim that cavern integrity would be compromised at P/D less than 1.0 but they highly recommended that more detailed analyses be performed on specific cavern pairs (sets) to evaluate the effects of continued leaching and reduction of the P/D on cavern stability. Using the 2D P/D to define a drawdown limit adds in nearly all cases an extra layer of conservatism.

For all of the SPR sites, large dome-scale geomechanical analyses have been performed including representations for all the caverns. All of these analyses have included drawdown or leach layers for all the Phase 1 and Phase 2 caverns with the exception of BM-5. One of the published analyses (Bryan Mound; Sobolik and Ehgartner, 2009a) has all the caverns been meshed according to the geometries obtained by sonars, and was completed before 2015; an enhanced model is currently being developed that will include more accurate dome, cavern, and drawdown geometries, and an updated salt creep model. A second model for West Hackberry (Sobolik, 2015) was recently completed; it has sonar-based geometries for all Phase 1 and Phase 2 caverns, and up to five drawdown layers built into the computational mesh. The published Big Hill and Bayou Choctaw models include cylinder and frustum representations for the caverns; these models are currently being updated with sonar-based geometries for all caverns, and their results will eventually be used to update the estimates for their available drawdowns. In general,

when assessing the potential for cavern stability problems, the following events/processes are the most critical:

- Large ΔP events such as workovers; dilatant and tensile stress conditions occur during large values of ΔP, but are driven by large values of rate of pressure change dP/dt; these events may cause salt falls and cracking.
- Length of time that the caverns are held in workover; strain rate is a function of ΔP, and most vertical strain on casings occurs during the enhanced creep resulting from a workover.
- Other phenomena which can cause casing strain, such as Big Hill caprock/salt interface.

The overriding observation from the geomechanical analyses (most of the cited Park and Sobolik references) is that the drawdown process itself rarely induces stress conditions (i.e., shear stress levels that create dilatant salt damage, tensile normal stresses that create fractures in the salt, or excessive vertical strains on the borehole casings) that cause instability issues. This is because the drawdown process uses fresh water injected at pressures not significantly different from the normal operating pressures of the cavern; therefore, the large pressure differential that causes increased cavern creep, and that can create the conditions listed above, is not present during drawdown. Therefore, for this reason as well as for ease of numerical computation, drawdown processes are modeled in the geomechanical analyses as instantaneous removal of a specified "onion layer" of material around the cavern.

Stability problems related to a drawdown would be expected to occur during a workover following the drawdown. The wellhead pressure during a workover is zero, creating the maximum pressure differential condition for a cavern, and as the cavern volume expands from leaching and the pillar thickness decreases, the potential for undesired stress conditions increases during workovers. Nearly all of the Phase 2 caverns, because of their cylindrical construction and designed spacing, are expected to be capable of having several drawdowns in their lifetime. Many of the Phase 1 caverns, however, have cavern geometry issues which will limit their available drawdowns to one or two.

The results of the geomechanical analyses are used to establish a limit to available drawdowns in the following manner. If at any time, and for any duration, during a simulated five-year period after a drawdown, which will include one workover, the maximum principal stress achieves a tensile condition, or the dilatant damage factor achieves a value less than 1.0, then that particular drawdown would be disallowed (i.e., if this condition occurs after the 3rd drawdown, then the limit due to geomechanics would be two drawdowns). This criterion is very conservative regarding the dilatant stress condition because achieving a short-term state of dilatant stress is not a distinct threshold for failure. In addition, the failure due to dilatant stress may be merely a salt fall, which is not necessarily a condition that would cause environmental or operational problems. Similarly, a tensile stress would likely result in a crack in the salt, but may not necessarily be a limiting condition depending on the severity of the crack.

Step 3 listed above stated that geomechanical analyses may be used as the overriding values for the best estimate for the drawdown limit if they fit certain criteria. The criteria are as follows: if the specific caverns have been meshed according to the sonar geometry (either an axisymmetric representation of the geometry, or the actual sonar-measured geometry), and additional

drawdown layers are built into the cavern's mesh and removed in simulated leaching processes. The cavern geometry caveat is important, because the bumps and sharp corners are the locations of stress concentrations, and thus are the most likely locales for dilatant or tensile stresses.

Using the steps listed above, a best estimate for the available drawdowns for each cavern has been determined. The best estimates for each site were documented in Sobolik (2014). This paper draws upon the recently West Hackberry model upgrade and analyses (Sobolik, 2015) to reevaluate and update the available drawdowns for each of those caverns. Similar papers for the Bryan Mound, Big Hill, and Bayou Choctaw papers will be developed as the upgrades to those analyses are completed.

2. West Hackberry Caverns

The geomechanical model and analyses for the West Hackberry SPR site that were used for the original 2014 estimation of available drawdowns (Sobolik and Ehgartner 2009b; Sobolik 2013 a, 2013b, 2014) has been updated with a more comprehensive, geometrically-accurate model (Sobolik, 2015). Using this new model, each West Hackberry cavern has been reevaluated for its number of available drawdowns. The revised numbers for all the WH caverns are listed in Tables 1-1 and 3-1; this section provide a detailed examination of each WH cavern. Because WH-6 will not be reutilized for oil storage for the foreseeable future, it has not been included in this evaluation of available cavern drawdowns.

The updated WH model and analyses (Sobolik 2015) included several upgrades. The most important included cavern geometries based on those obtained from sonar measurements, the implementation of the multi-mechanism deformation (M-D) creep model for salt behavior, and historical wellhead pressures for each cavern through April 2014. For wellbore and cavern integrity issues, the most critical times for each cavern are those during a workover, particularly at the beginning and end when large pressure and stress changes occur over a very short period of time. In the model calculations, workovers during the calculation period where actual pressure histories are used typically went from maximum (operating) to zero wellhead pressure in 1-4 day intervals. After the available historical pressures were exhausted, the previous analysis scheme of a constant wellhead pressure with workovers occurring once every five years for each cavern was implemented. In this scheme, the pressure change at the beginning and end of the workover was implemented instantaneously, resulting in a much sharper spike in the stress rate. (Caverns 6, 8, and 9 were handled differently, given more gradual pressure changes as has been previously documented (Sobolik, 2013a and 2013b).) Therefore, some of the peaks in dilatancy damage factor and maximum stress portrayed after the historical pressure period are more extreme than during that period, and this is due to the more abrupt pressure changes modeled for workovers. For the Phase 2 caverns, this extreme behavior acts as somewhat of a worst case scenario and a level of conservatism in the following evaluations.

Four design factors were used to evaluate the number of drawdowns for each cavern: dilatant safety factor, maximum principal stress, vertical casing strain, and salt falls. The salt damage factor (analogous to a safety factor) has been developed from a dilatant damage criterion based on a linear function of the hydrostatic pressure (Van Sambeek et al., 1993). Dilatancy is considered as the onset of damage to rock resulting in significant increases in permeability. Dilatant damage in salt typically occurs at a stress state where a rock reaches its minimum volume, or dilation limit, at which point microfracturing increases the volume. Dilatant criteria typically relate two stress invariants: the mean stress invariant I_1 (equal to three times the average normal stress) and the square root of the stress deviator invariant J_2, or $\sqrt{J_2}$ (a measure of the overall deviatoric or dilatant shear stress). (By convention, tensile normal stresses are positive, and compressive normal stresses are negative, hence the sign nomenclature in the following equations.) The dilatant criterion chosen here is the equation typically used from Van Sambeek et al. (1993),

$$\sqrt{J_2} = -0.27 I_1. \qquad (1)$$

The Van Sambeek damage criterion defines a linear relationship between I_1 and $\sqrt{J_2}$, and such linear relationships have been established from many suites of laboratory tests on WIPP, SPR, and other salt samples. This criterion was applied during post-processing of the analyses. A damage factor (safety factor) index was created (SF_{VS}) by normalizing I_1 by the given criterion:

$$SF_{VS} = \frac{-0.27 I_1}{\sqrt{J_2}} \tag{2}$$

Several earlier publications define that the Van Sambeek damage factor SF_{VS} indicates damage when SF_{VS}<1. In previous SPR studies, values of SF_{VS}<1.5 have been categorized as cautionary because of unknown localized heterogeneities in the salt that cannot be captured in these finite element calculations. This report will use these damage thresholds, particularly the threshold of 1.0 to indicate the onset of damage. It is important to note that a very short-term occurrence of a safety factor less than 1.0 does not necessarily result in immediate salt fracturing; in fact, the greater concern would be a value less than 1.0 over a period of several weeks or months, indicating the accumulation of damage which would cause fracture generation.

The maximum principal stress is a greater measure of the potential for immediate damage to the salt. For these calculations, tensile stress is by convention positive, compressive is negative. If a location on the wall of a cavern shows a positive or tensile stress, even for a short period of time, then that could indicate the immediate creation of a fracture in the salt at that location. If fractures are generated near the cavern ceiling or borehole, then a loss of fluid to the caprock would be an immediate concern. If the fracture propagates horizontally and intersects another cavern, then several operational pressure issues can arise. If the fracture occurs in the floor, then there are much fewer concerns, as the fluid is still contained in the salt and the fracture will likely not create any operational issues.

The predicted average axial casing strain between the casing and top of salt is another factor used in this evaluation. The baseline threshold for axial casing strain is 1.6 millistrains, which is the onset of plastic deformation for steel typically used in casings. This value does not indicate the actual strain at the point of failure; that value can be as much as 5 times higher for intact steel (Park, 2013 & 2014), or at an intermediate value at threaded connections. The predicted overall average strain is presented in the following sections, although the region above the top of each cavern, including the casing shoe, is usually predicted to have experienced localized strains above 1.6 mε by 2015 (Sobolik, 2015). Because of salt creep, casing integrity is an expected operational issue independent of the number of drawdowns for a particular cavern. For evaluation of available drawdowns, the indicator of potential casing integrity issues related directly to drawdowns would be a significant change in strain behavior resulting from the drawdowns, such as a large increase in strain rate. If successive drawdowns produce only a slight increase in the casing strain rate, then it will be assumed that there is no additional concern for the mechanical stability of the casing.

The final performance indicator that is used in these evaluations is recorded salt falls. Such incidents can affect cavern stability and operations by damaging hanging strings and generating fractures in the salt which may impact fluid isolation. Salt falls are not unusual, even for

otherwise mechanically-stable caverns, so a history of salt falls is not necessarily an indication of cavern stability problems. However, if a large number of salt falls occurs in conjunction with significant periods of dilatant or tensile stress conditions, then there would be cause to limit the number of available drawdowns for such a cavern.

Each of the following subsections focuses on an individual cavern. In each subsection, the following information is provided: sonar picture of the cavern (and date), computational mesh of the cavern based on sonar, a listing of neighboring caverns and their locations, the 2014 assessment of its available drawdowns, plot of the minimum value of dilatant safety factor around each cavern, plot of the maximum value of maximum principal stress around each cavern, contour plot highlighting the location of the min/max values (if necessary), plot of the overall average vertical casing strain, the number of salt falls recorded as of 2014, and finally an updated estimate of the number of available drawdowns.

2.1 WH Cavern 101

WH Cavern 101 is a Phase 2 cavern surrounded by other Phase 2 caverns. The previous best estimate for its number of available drawdowns was 3, based on P/D ratios with its nearby caverns. Table 2.1 summarizes the P/D and geomechanical estimates for available drawdowns for WH-101 in 2014. Figure 2.1-1 shows the volume of WH-101 in both its computational mesh geometry and its oldest available sonar geometry from 2000, and the geometries of the five drawdown layers built into the computational mesh. (The sonar geometry from 2006 is also included.) As is the case for all the Phase 2 caverns, the modeled drawdown layers extend for nearly the entire height of the cavern, and add approximately 15% to the volume of the cavern when they are removed.

Table 2.1. 2014 Estimates of available drawdowns, WH-101.

Cavern	Basis				2014 Best Estimate Basis (P/D or GM), Comments, Reference
	2D P/D < 1	3D P/D < 1	Geomechanics	Best Estimate	
WH101	3	3	5	3	P/D; Rudeen & Lord, 2013; Sobolik & Ehgartner, 2009b*
					Nearest neighbors: 105 (S), 104 (SW), 102 (NW), 103 (N)

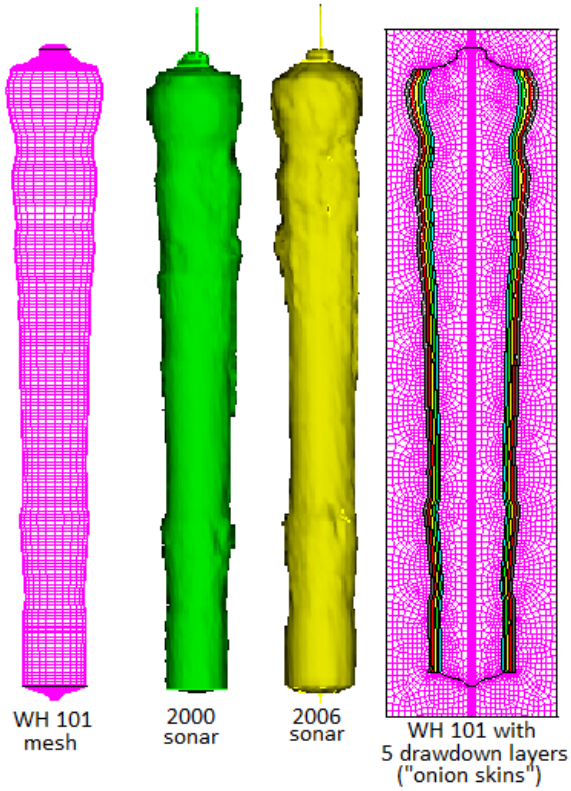

Figure 2.1-1. Computational mesh and sonar geometries for WH-101

Figure 2.1-2 plots the minimum value of dilatant damage factor, or safety factor, at any point around the cavern wall, as a function of time through five drawdowns. The lowest value for the dilatant safety factor was 1.37, recorded during a workover after the second drawdown. These

values dip below the recommended value of 1.5 for only brief periods (during a workover), and never fall below the value of 1.0 that signifies the onset of dilatant damage. Figure 2.1-3 shows the locations of the minimum values of the dilatant safety factor around WH-101. The minimum values tend to occur in two places: near the top of the cavern in the roof and in the first narrowed region; and around the base of the cavern. These general locations will tend to be the same for all the Phase 2 caverns: the ceiling undergoes the most relative pressure change compared to in situ stress; any protrusions into the cavern tend to be stress concentration points which will experience greater differential stress; and the bottom of the caverns undergo significant deformation, and also often have sharper mesh angles at a flat base which will induce stress concentrations. Also, note that the values for minimum dilatant safety factor decrease at each "instantaneous" drawdown layer removal; the actual process is more gradual, so this much of a change is not expected, but this behavior will be noted for all the other caverns to look for any indication of possible problems immediately after a drawdown.

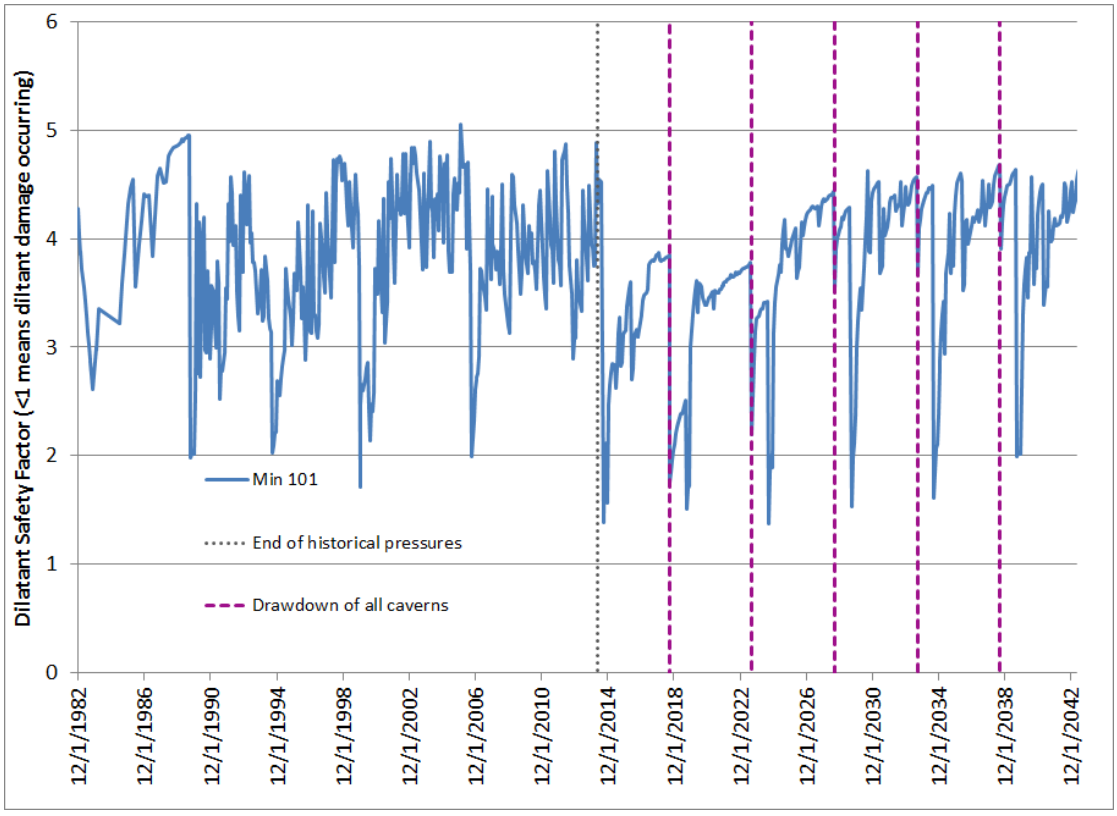

Figure 2.1-2. Minimum value of dilatant safety factor surrounding WH-101.

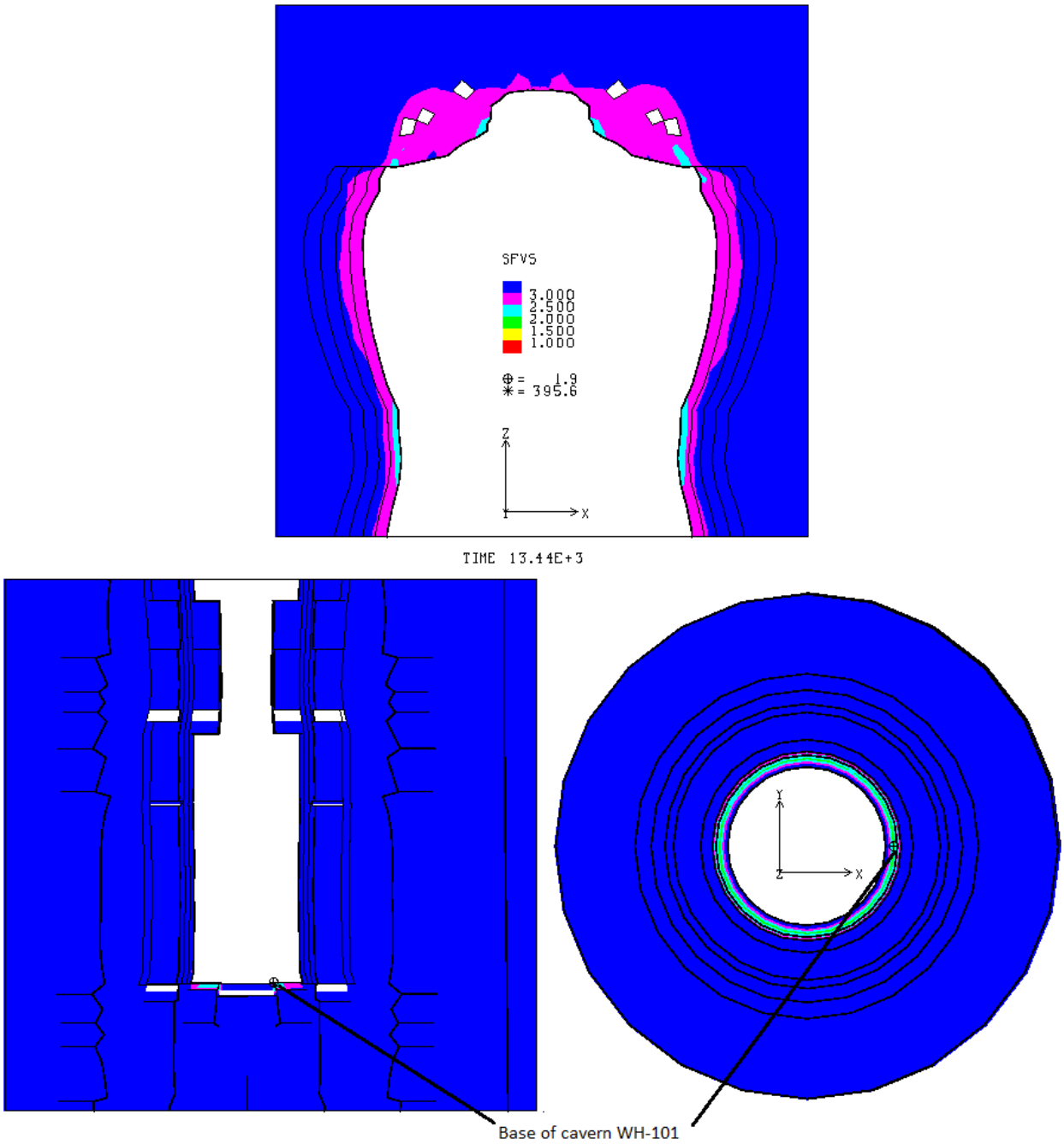

Figure 2.1-3. Locations of minimum value of dilatant safety factor surrounding WH-101.

Figure 2.1-4 plots the maximum value of maximum principal stress around WH-101. Positive values indicate tension, which if they occur would likely be in the same locations as the minimum dilatant safety factor values. The maximum pressure never reaches a positive or tensile value through five drawdowns. Figure 2.1-5 plots the predicted average axial casing strain between the casing and top of salt for WH-101. Two interesting patterns can be observed from this plot: one, beginning in 2008 the strain is predicted to decrease between workovers, and only increase during workovers; and two, the strain rates both during and between workovers increase with succeeding drawdowns. The overall average strain does not exceed 1.6

millistrains, although the region above the top of the cavern, including the casing shoe, is predicted to have experienced localized strains above 1.6 mε by 2015 (Sobolik, 2015). There is nothing in the behavior of the predicted casing strain to indicate additional concern for the mechanical stability of the cavern.

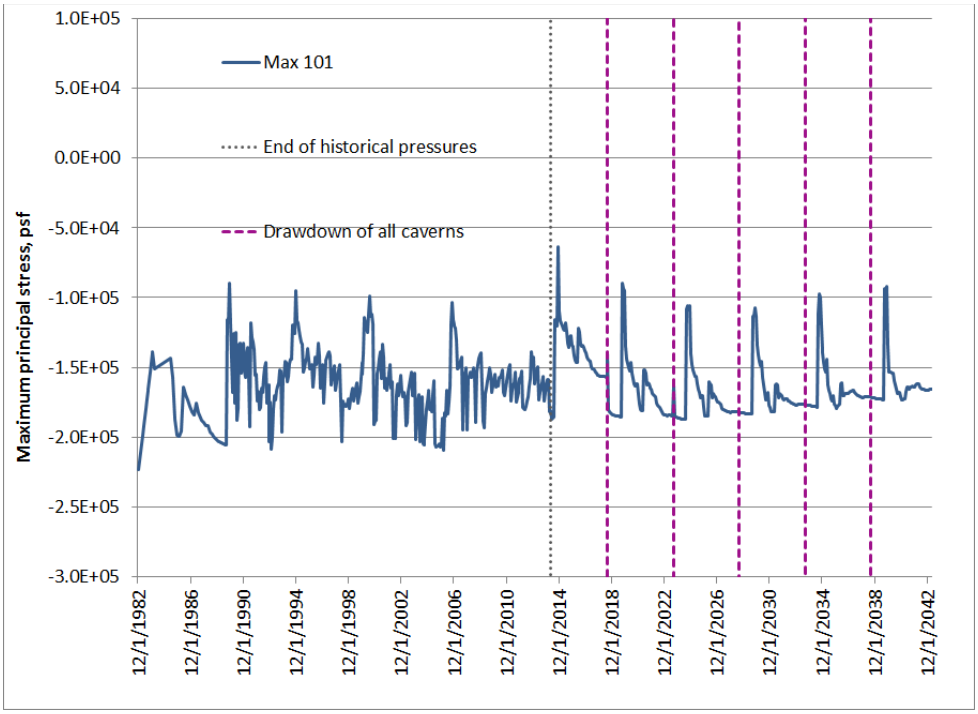

Figure 2.1-4. Maximum value of maximum principal stress surrounding WH-101.

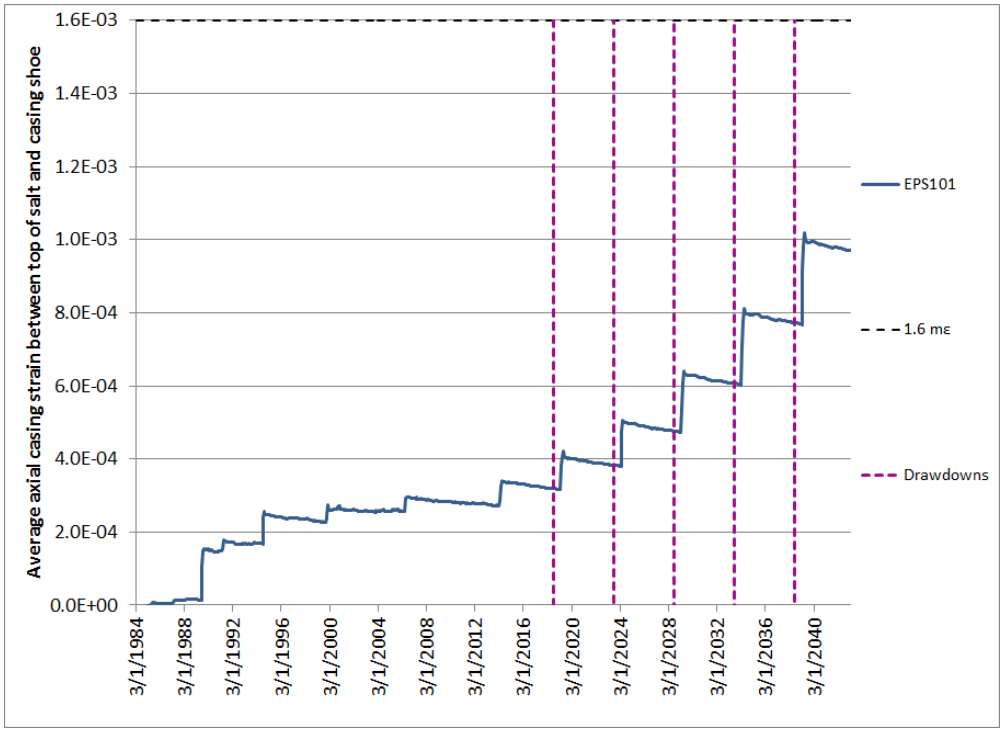

Figure 2.1-5. Predicted avg. axial casing strain between casing shoe and top of salt for WH-101.

As of July 2015, no salt falls have been recorded for WH-101 (Roberts et al., 2015). This result supports the indications from the geomechanical calculations that WH-101 should be mechanically stable through five drawdowns. Therefore:

The updated estimate for WH-101 based on geomechanical analyses is that this cavern is stable through 5 drawdowns.

2.2 WH Cavern 102

WH Cavern 102 is a Phase 2 cavern surrounded by other Phase 2 caverns. The previous best estimate for its number of available drawdowns was 3, based on P/D ratios with its nearby caverns. Table 2.2 summarizes the P/D and geomechanical estimates for available drawdowns for WH-102 in 2014. Figure 2.2-1 shows the volume of WH-102 in both its computational mesh geometry and its oldest available sonar geometry from 1983, and the geometries of the five drawdown layers built into the computational mesh. As is the case for all the Phase 2 caverns, the modeled drawdown layers extend for nearly the entire height of the cavern, and add approximately 15% to the volume of the cavern when they are removed.

Table 2.2. 2014 Estimates of available drawdowns, WH-102.

Cavern	Basis				2014 Best Estimate Basis (P/D or GM), Comments, Reference
	2D P/D < 1	3D P/D < 1	Geomechanics	Best Estimate	
WH102	3	3	5	3	P/D; Rudeen & Lord, 2013; Sobolik & Ehgartner, 2009b*
					Nearest neighbors: 104 (S), 107 (N), 103 (NE), 101 (SE)

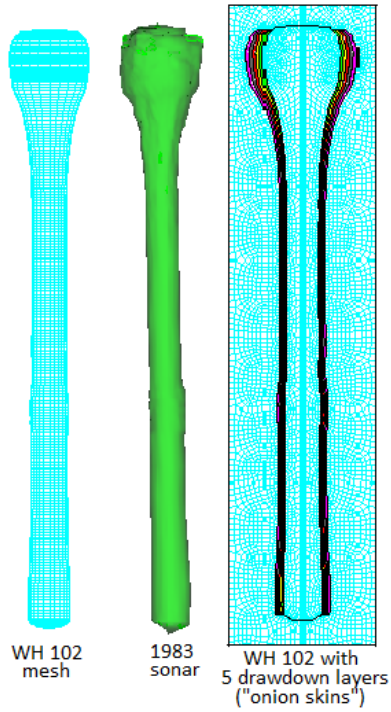

Figure 2.2-1. Computational mesh and sonar geometries for WH-102

Figure 2.2-2 plots the minimum value of dilatant damage factor, or safety factor, at any point around the cavern wall, as a function of time through five drawdowns. The lowest value for the dilatant safety factor was 1.44, recorded during a workover after the fourth drawdown. This instance coincided with the initiation date of that drawdown, so this would be a lowest expected value for the damage factor. These values dip below the recommended value of 1.5 for only brief periods (during a workover), and never fall below the value of 1.0 that signifies the onset of

dilatant damage. The minimum values tend to occur in two places: near the top of the cavern at the corner of the roof; and around the base of the cavern, particularly where the bottom of the onion layer is located. Also, note that the values for minimum dilatant safety factor decrease at each "instantaneous" drawdown layer removal; the actual process is more gradual, so this much of a change is not expected. Figure 2.2-3 plots the maximum value of maximum principal stress around WH-102. Positive values indicate tension, which if they occur would likely be in the same locations as the minimum dilatant safety factor values. The maximum stress never reaches a positive or tensile value through five drawdowns.

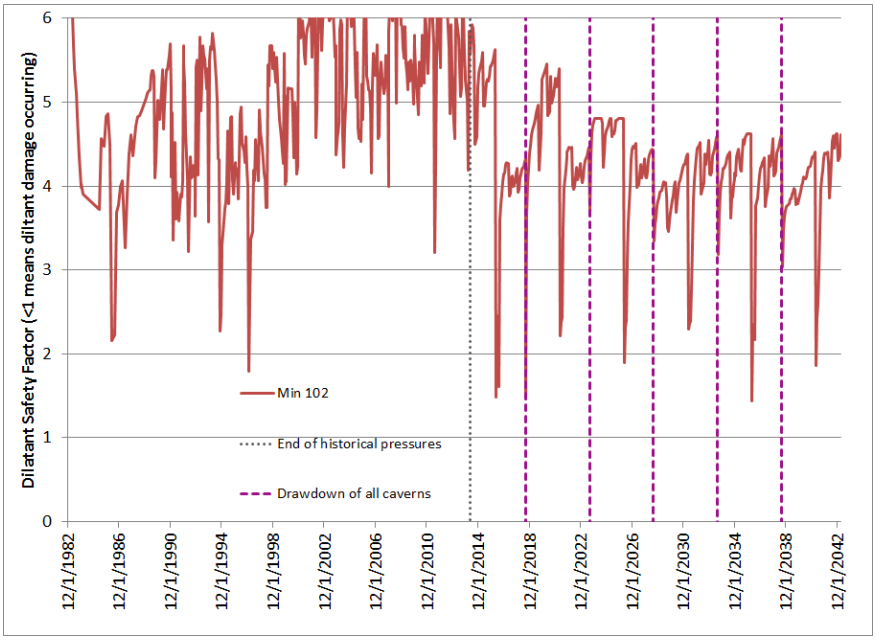

Figure 2.2-2. Minimum value of dilatant safety factor surrounding WH-102.

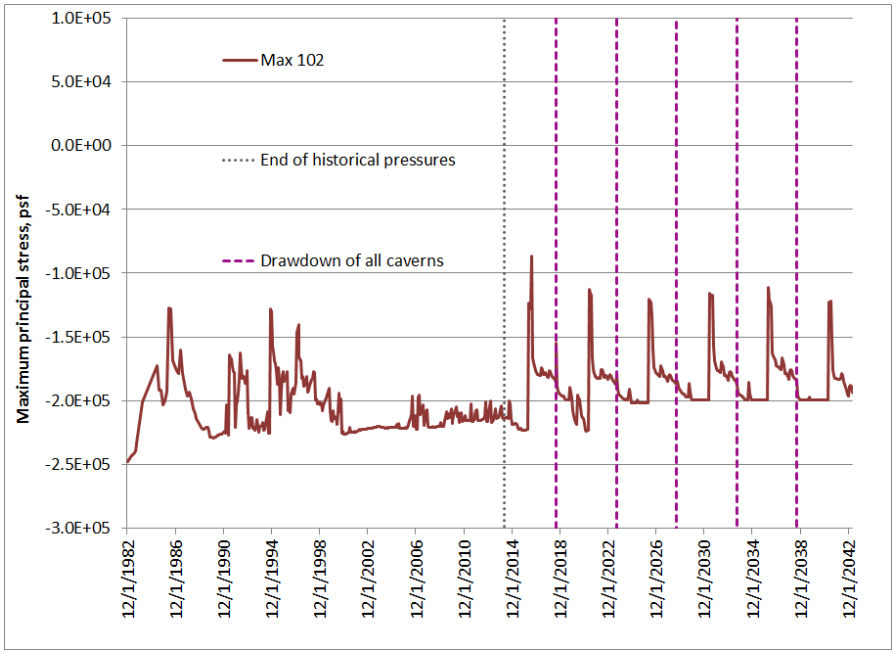

Figure 2.2-3. Maximum value of maximum principal stress surrounding WH-102.

Figure 2.2-4 plots the predicted average axial casing strain between the casing and top of salt for WH-102. The overall average strain is predicted to exceed 1.6 millistrains after the third drawdown, although the region above the top of the cavern, including the casing shoe, is predicted to have experienced localized strains above 1.6 mε by 2015 (Sobolik, 2015). The strain rate increases slightly once drawdowns begin, but not in an alarming fashion. Because of salt creep, casing integrity is an expected operational issue independent of the number of drawdowns for a particular cavern; because there is no significant change in strain behavior resulting from the drawdowns, there is nothing to indicate additional concern for the mechanical stability of the cavern.

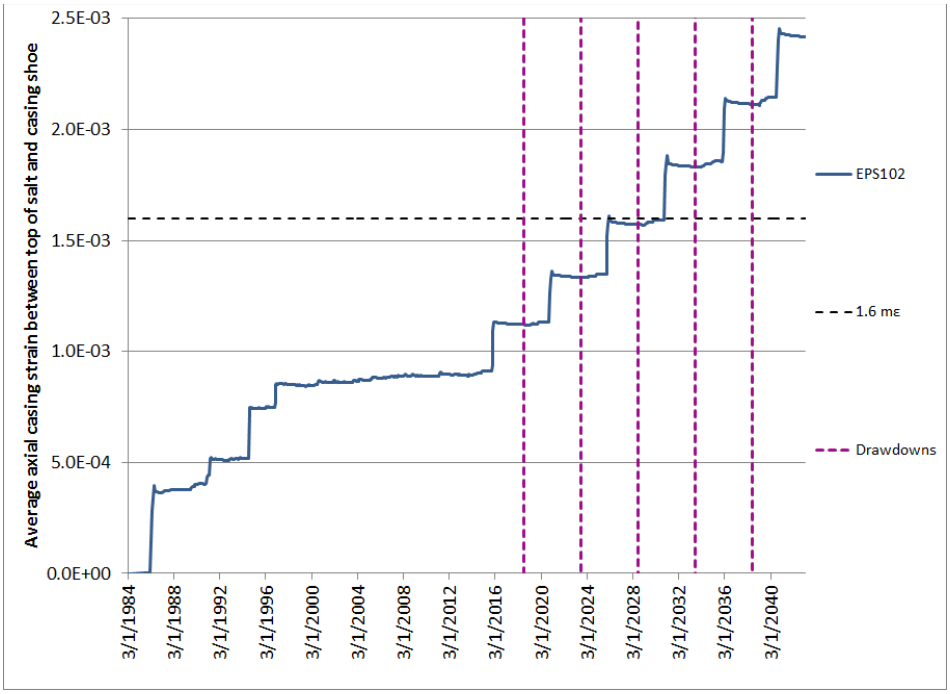

Figure 2.2-4. Predicted avg. axial casing strain between casing shoe and top of salt for WH-102.

As of July 2015, two salt falls have been recorded for WH-102 (Roberts et al., 2015). Salt falls are not unusual, even for otherwise mechanically-stable caverns, so this number of salt falls does not contradict the indications from the geomechanical calculations that WH-102 should be mechanically stable through five drawdowns. Therefore:

The updated estimate for WH-102 based on geomechanical analyses is that this cavern is stable through 5 drawdowns.

2.3 WH Cavern 103

WH Cavern 103 is a Phase 2 cavern surrounded by Phase 1 and Phase 2 caverns. It is unusual in that it is the only cavern with a welded steel casing (as opposed to threaded). The previous best estimate for its number of available drawdowns was 4, based on P/D ratios with its nearby caverns. Table 2.3 summarizes the P/D and geomechanical estimates for available drawdowns for WH-103 in 2014. Figure 2.3-1 shows the volume of WH-103 in both its computational mesh geometry and its oldest available sonar geometry from 2004, and the geometries of the five drawdown layers built into the computational mesh. As is the case for all the Phase 2 caverns, the modeled drawdown layers extend for nearly the entire height of the cavern, and add approximately 15% to the volume of the cavern when they are removed.

Table 2.3. 2014 Estimates of available drawdowns, WH-103.

Cavern	Basis				2014 Best Estimate Basis (P/D or GM), Comments, Reference
	2D P/D < 1	3D P/D < 1	Geomechanics	Best Estimate	
WH103	2	4	5	4	P/D; Rudeen & Lord, 2013; Sobolik & Ehgartner, 2009b*
					Nearest neighbors: 101 (S), 102 (SW), 107 (NW), 109 (N), 9 (NE)

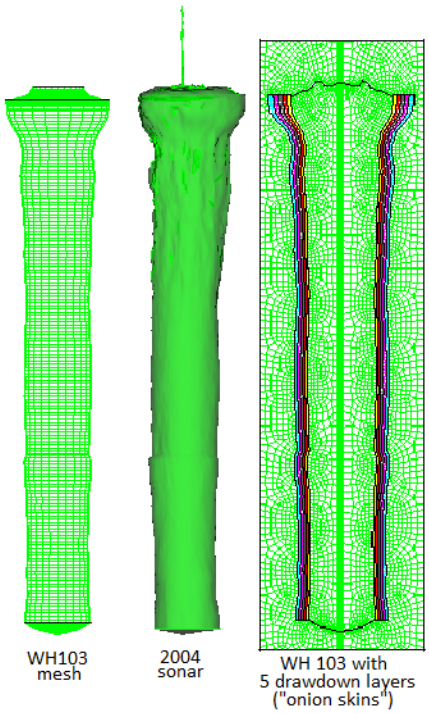

Figure 2.3-1. Computational mesh and sonar geometries for WH-103.

Figure 2.3-2 plots the minimum value of dilatant damage factor, or safety factor, at any point around the cavern wall, as a function of time through five drawdowns. The lowest predicted values for the dilatant safety factor were 1.22, recorded for a simulated workover in 2015, and 1.35 during a workover after the third drawdown. This instance coincided with the initiation date of that drawdown, so this would be a lowest expected value for the damage factor. These

values dip below the recommended value of 1.5 for only brief periods (during a workover), and never fall below the value of 1.0 that signifies the onset of dilatant damage. The minimum values tend to occur in two places: near the top of the cavern at the corner of the roof; and at a location 200-300 feet below the roof where there is a narrowing of the cavern radius. Lower values also occur around the base of the cavern, particularly where the bottom of the onion layer is located. These locations are shown in Figure 2.3-3. As usual, these values occur during workovers; the geomechanical predictions indicate that at all other times there are no excessive dilatant stress values.

Figure 2.3-4 plots the maximum value of maximum principal stress around WH-103. Positive values indicate tension, which if they occur would likely be in the same locations as the minimum dilatant safety factor values. The maximum stress never reaches a positive or tensile value through five drawdowns. Figure 2.3-5 plots the predicted average axial casing strain between the casing and top of salt for WH-103. The overall average strain is predicted to exceed 1.6 millistrains after the fourth drawdown, although the region above the top of the cavern, including the casing shoe, is predicted to have experienced localized strains above 1.6 mε by 2015 (Sobolik, 2015). The strain rate increases slightly once drawdowns begin, but not in an alarming fashion. Because of salt creep, casing integrity is an expected operational issue independent of the number of drawdowns for a particular cavern; because there is no significant change in strain behavior resulting from the drawdowns, there is nothing to indicate additional concern for the mechanical stability of the cavern.

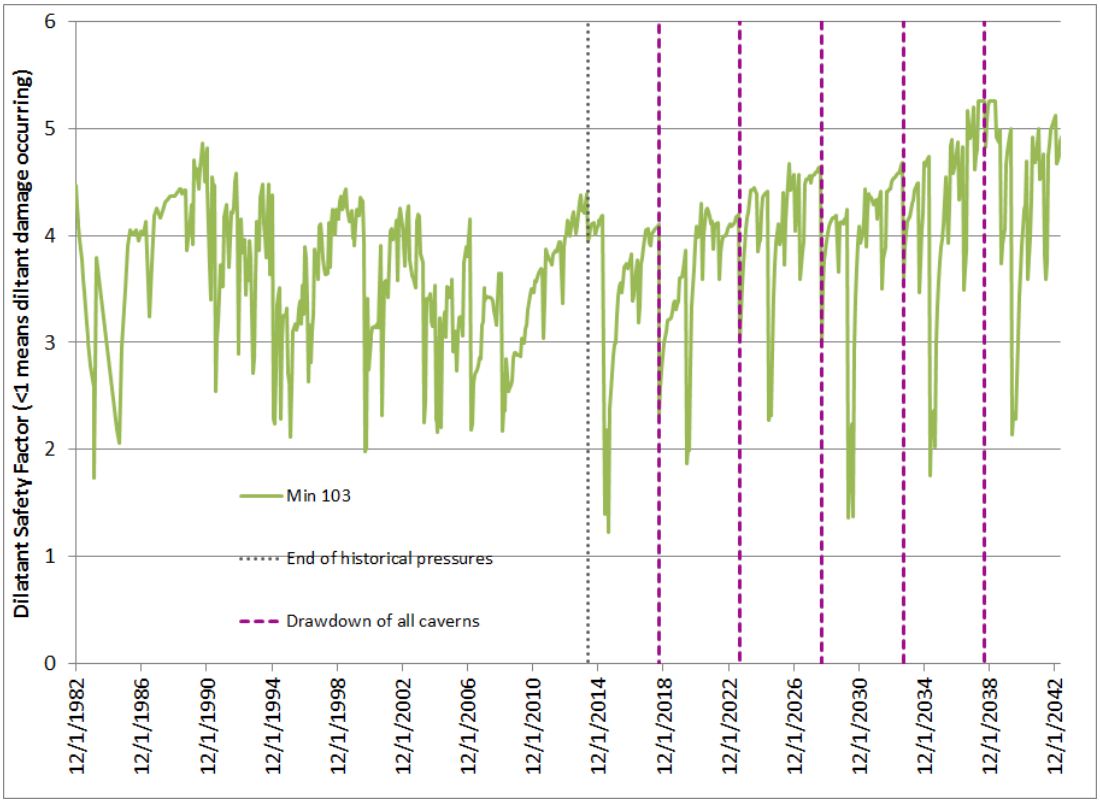

Figure 2.3-2. Minimum value of dilatant safety factor surrounding WH-103.

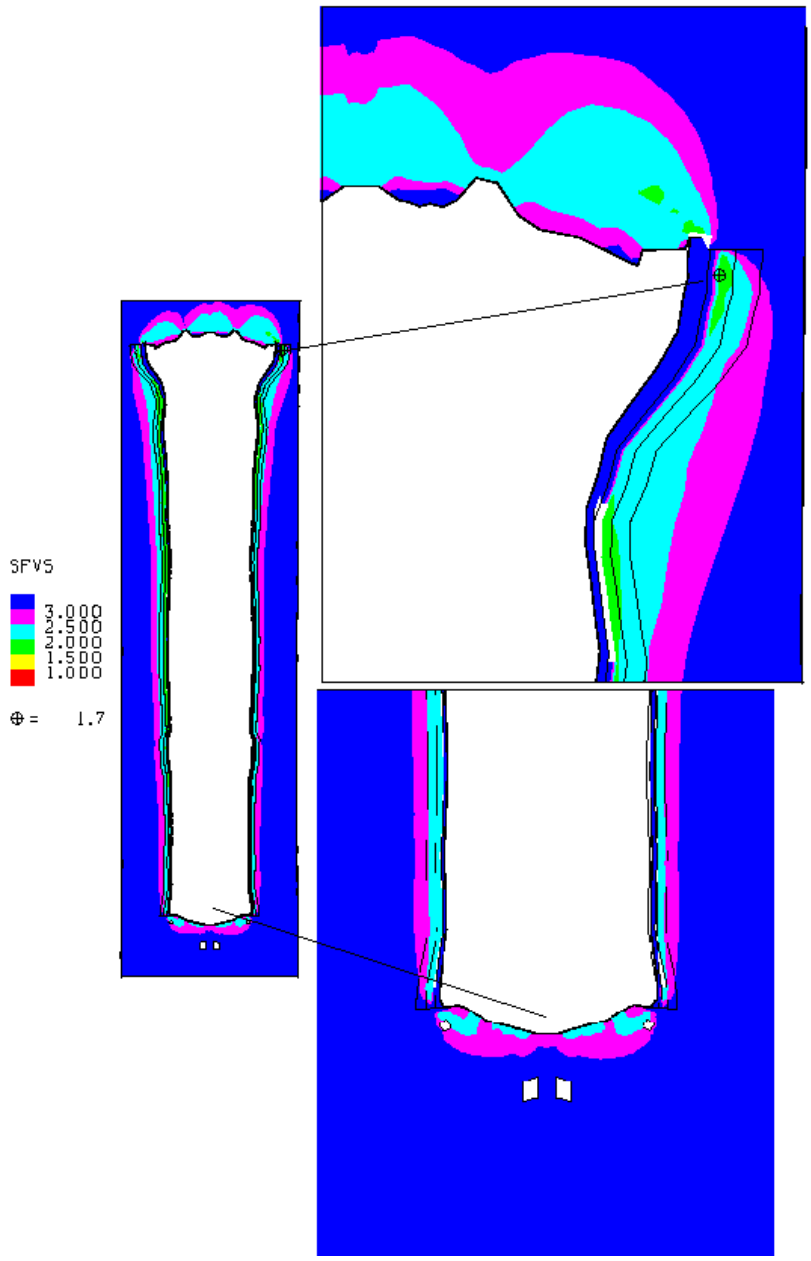

Figure 2.3-3. Locations of minimum value of dilatant safety factor surrounding WH-103.

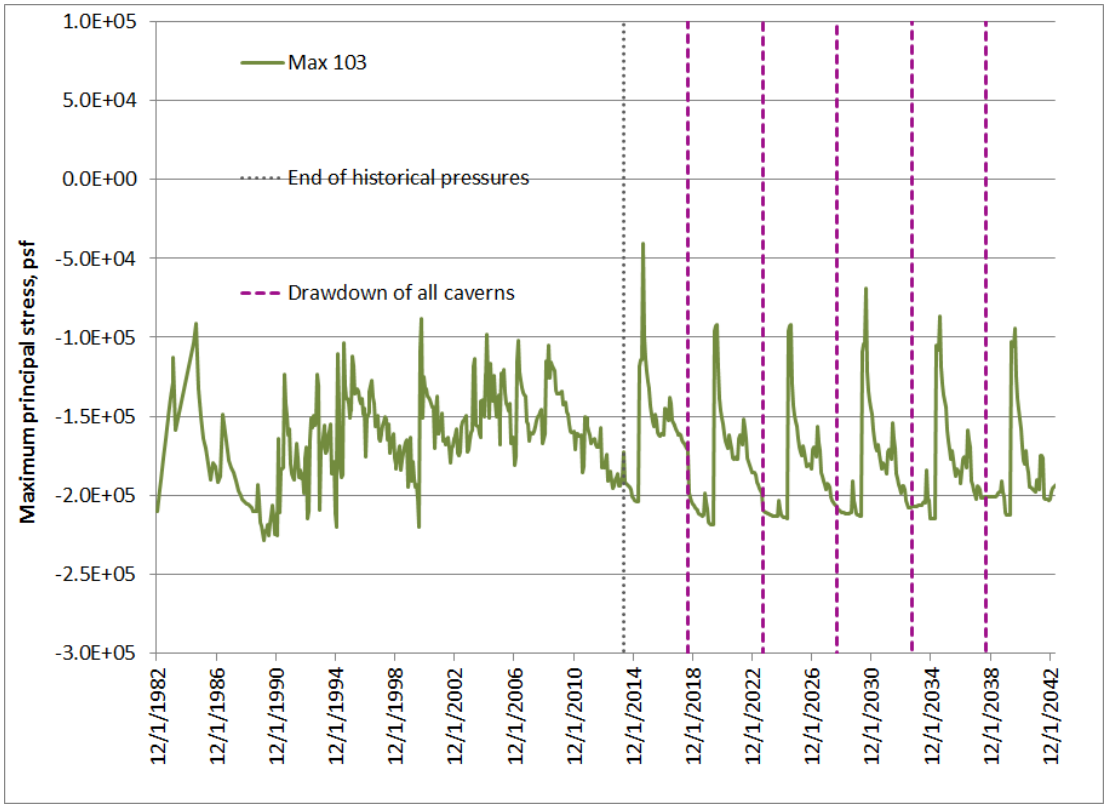

Figure 2.3-4. Maximum value of maximum principal stress surrounding WH-103.

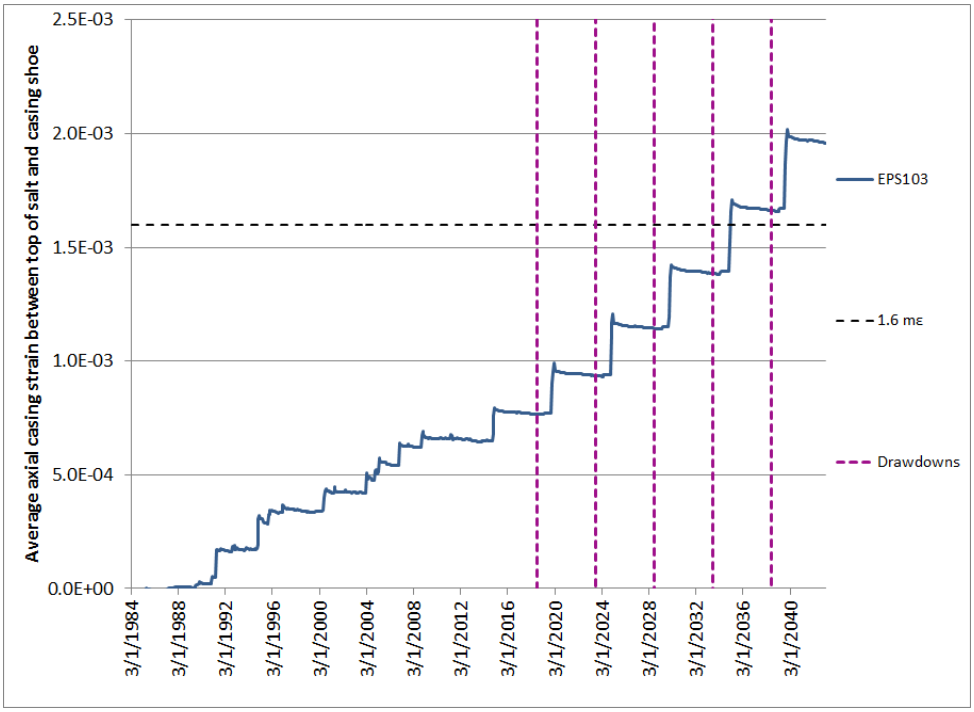

Figure 2.3-5. Predicted avg. axial casing strain between casing shoe and top of salt for WH-103.

As of July 2015, seven salt falls have been recorded for WH-103 (Roberts et al., 2015), which is the most for any cavern at West Hackberry. There are no indications why this cavern has

sustained so many salt falls, and it is speculated that the presence of a welded casing that has no threaded joints to deform may create local tensile or high shear stress in the salt resulting in fracturing and falls. Nevertheless, salt falls are not unusual, even for otherwise mechanically-stable caverns, so this number of salt falls does not necessarily contradict the indications from the geomechanical calculations that WH-103 should be mechanically stable through five drawdowns. Therefore:

The updated estimate for WH-103 based on geomechanical analyses is that this cavern is stable through 5 drawdowns. (However, as WH-103 is enlarged, the number and frequency of salt falls should be monitored to determine if drawdowns are affecting the cavern integrity.)

2.4 WH Cavern 104

WH Cavern 104 is a Phase 2 cavern surrounded by Phase 2 caverns. The previous best estimate for its number of available drawdowns was 3, based on P/D ratios with its nearby caverns. Table 2.4 summarizes the P/D and geomechanical estimates for available drawdowns for WH-104 in 2014. Figure 2.4-1 shows the volume of WH-104 in both its computational mesh geometry and its oldest available sonar geometry from 2000, and the geometries of the five drawdown layers built into the computational mesh. As is the case for all the Phase 2 caverns, the modeled drawdown layers extend for nearly the entire height of the cavern, and add approximately 15% to the volume of the cavern when they are removed.

Table 2.4. 2014 Estimates of available drawdowns, WH-104.

Cavern	Basis				2014 Best Estimate Basis (P/D or GM), Comments, Reference
	2D P/D < 1	3D P/D < 1	Geomechanics	Best Estimate	
WH104	3	3	5	3	P/D; Rudeen & Lord, 2013; Sobolik & Ehgartner, 2009b*
					Nearest neighbors: 102 (N), 101 (NE), 105 (SE), 106 (S)

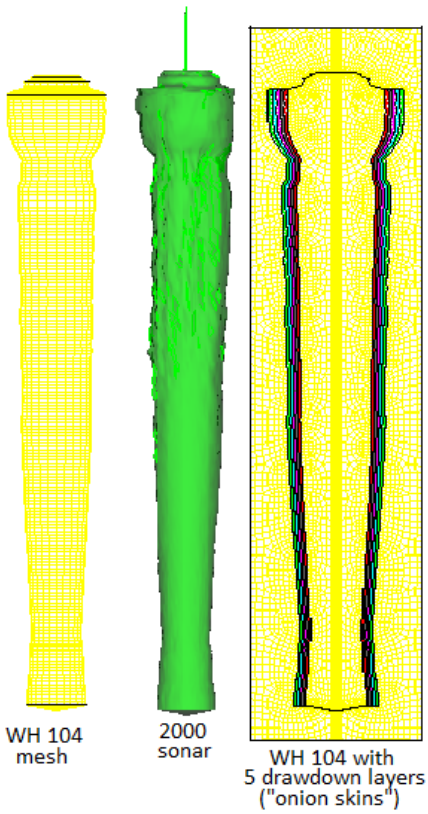

Figure 2.4-1. Computational mesh and sonar geometries for WH-104

Figure 2.4-2 plots the minimum value of dilatant damage factor, or safety factor, at any point around the cavern wall, as a function of time through five drawdowns. The lowest predicted value for the dilatant safety factor was 0.94, during a workover after the third drawdown. This

instance coincided with the initiation date of that drawdown, so this would be a lowest expected value for the damage factor. This values dips below the threshold value of 1.0 that signifies the onset of dilatant damage, and does it for only a brief period (during a workover). This minimum value occurs at the floor of the cavern, which has the similar pattern of high dilatant stresses and reduced safety factors during workovers. Two other places show noticeable, though not excessive stresses during a workover: near the top of the cavern at the corner of the roof; and at a location 200-300 feet below the roof where there is a narrowing of the cavern radius. These locations are shown in Figure 2.4-3. As usual, these values occur during workovers; the geomechanical predictions indicate that at all other times there are no excessive dilatant stress values. Because the time and location of the sub-threshold safety factor values are in the floor of the cavern, and only for a brief period at the beginning of a workover, these occurrences are not believed to be significant enough to cause microcracking in the salt of a magnitude that would affect cavern stability. This conclusion is substantiated in Figure 2.4-4, which plots the maximum value of maximum principal stress around WH-104. Positive values indicate tension, which if they occur would likely be in the same locations as the minimum dilatant safety factor values. The maximum stress never reaches a positive or tensile value through five drawdowns.

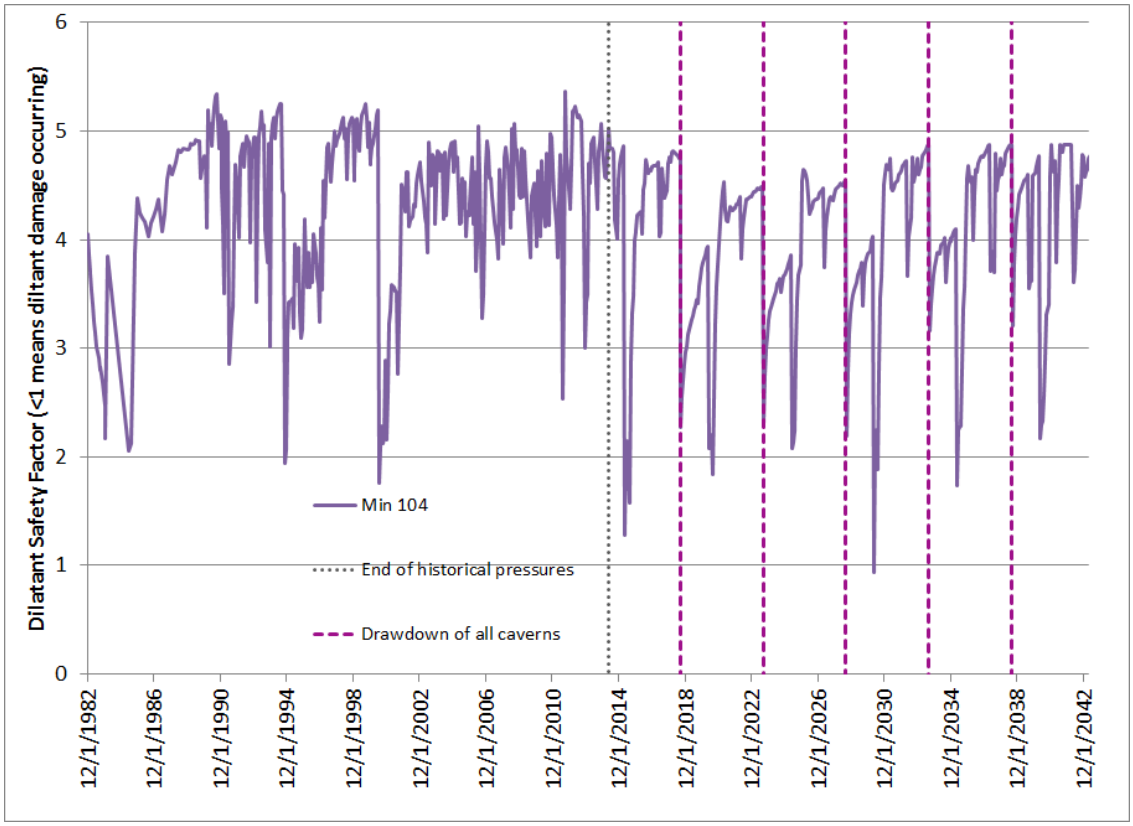

Figure 2.4-2. Minimum value of dilatant safety factor surrounding WH-104.

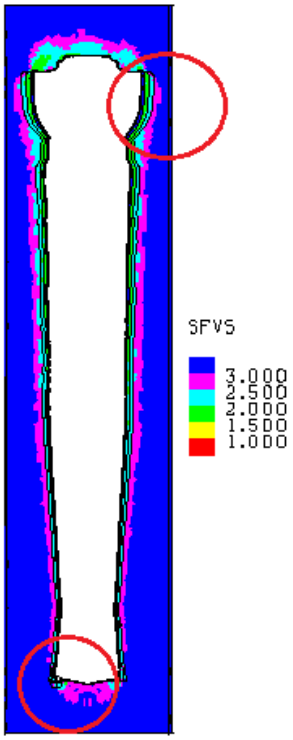

Figure 2.4-3. Locations of minimum value of dilatant safety factor surrounding WH-104.

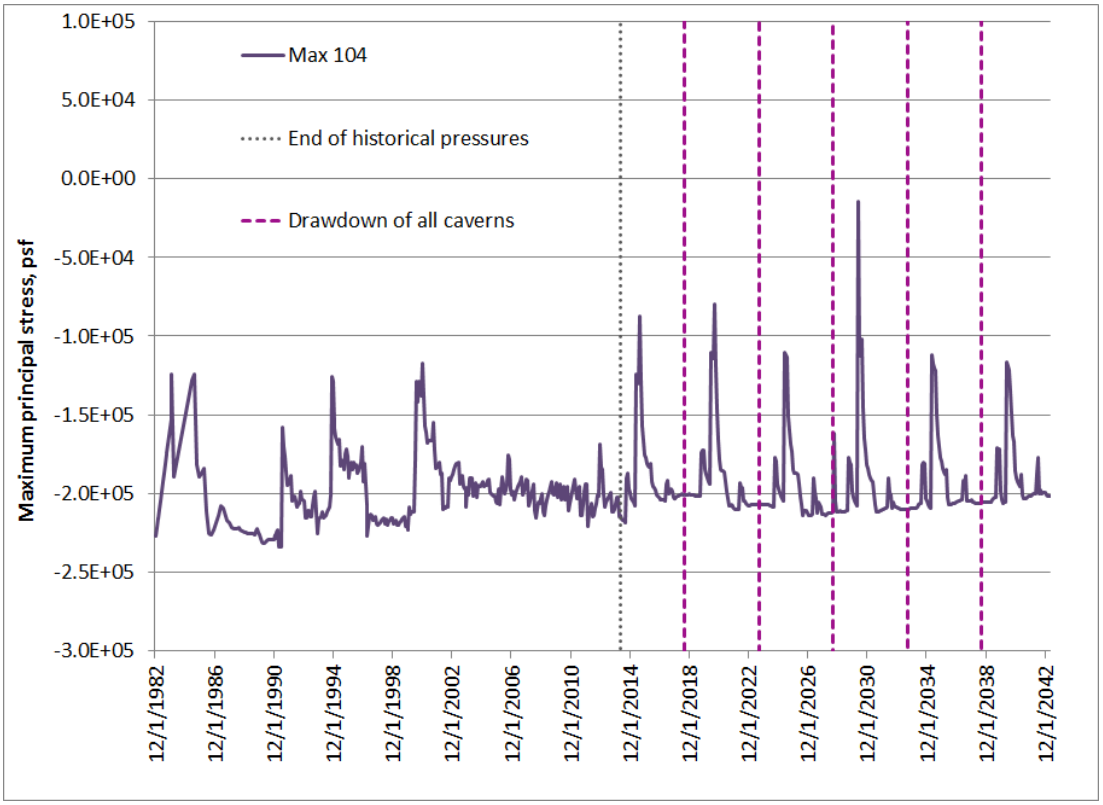

Figure 2.4-4. Maximum value of maximum principal stress surrounding WH-104.

Figure 2.4-5 plots the predicted average axial casing strain between the casing and top of salt for WH-104. The overall average strain is predicted to exceed 1.6 millistrains after the fourth drawdown, although the region above the top of the cavern, including the casing shoe, is predicted to have experienced localized strains above 1.6 mε by 2015 (Sobolik, 2015). The strain rate increases slightly once drawdowns begin, but not in an alarming fashion. Because of salt creep, casing integrity is an expected operational issue independent of the number of drawdowns for a particular cavern; because there is no significant change in strain behavior resulting from the drawdowns, there is nothing to indicate additional concern for the mechanical stability of the cavern.

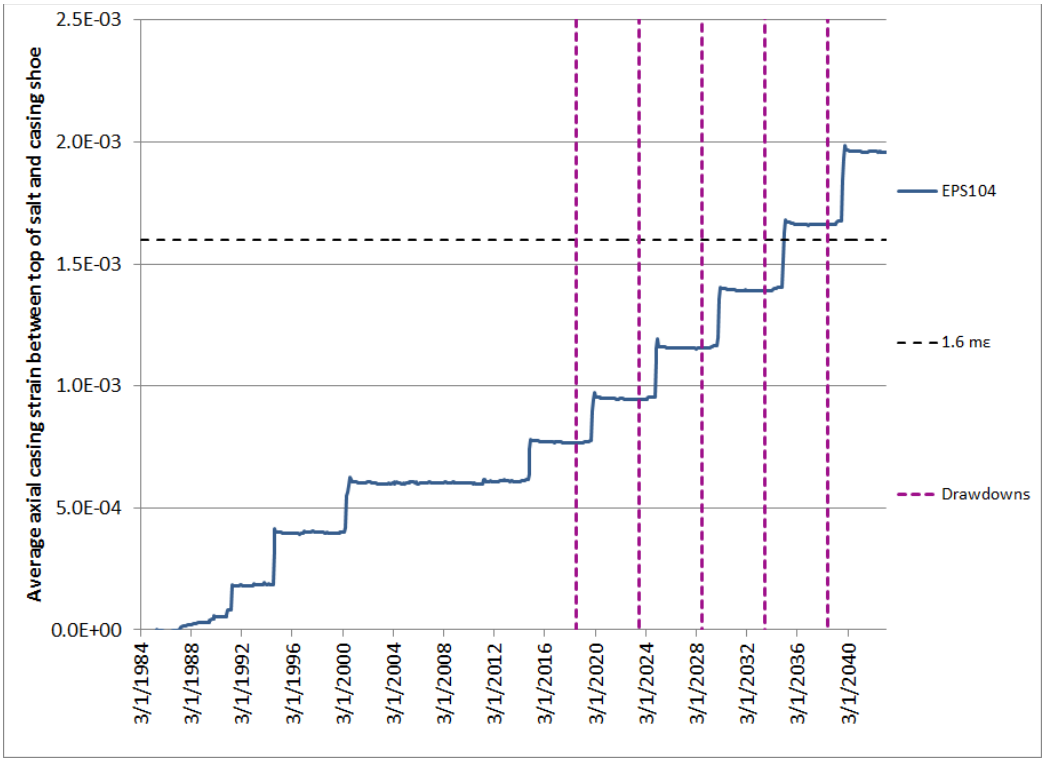

Figure 2.4-5. Predicted avg. axial casing strain between casing shoe and top of salt for WH-104.

As of July 2015, no salt falls have been recorded for WH-104 (Roberts et al., 2015). Salt falls are not unusual, even for otherwise mechanically-stable caverns, but a lack of salt falls supports the indications from the geomechanical calculations that WH-104 should be mechanically stable through five drawdowns. Therefore:

The updated estimate for WH-104 based on geomechanical analyses is that this cavern is stable through 5 drawdowns.

2.5 WH Cavern 105

WH Cavern 105 is a Phase 2 cavern surrounded by Phase 2 caverns. The previous best estimate for its number of available drawdowns was 2, based on P/D ratios with its nearby caverns. Table 2.5 summarizes the P/D and geomechanical estimates for available drawdowns for WH-105 in 2014. Figure 2.5-1 shows the volume of WH-105 in both its computational mesh geometry and its oldest available sonar geometry from 2004, and the geometries of the five drawdown layers built into the computational mesh. As is the case for all the Phase 2 caverns, the modeled drawdown layers extend for nearly the entire height of the cavern, and add approximately 15% to the volume of the cavern when they are removed.

Table 2.5. 2014 Estimates of available drawdowns, WH-105.

Cavern	Basis				2014 Best Estimate Basis (P/D or GM), Comments, Reference
	2D P/D < 1	3D P/D < 1	Geomechanics	Best Estimate	
WH105	2	2	5	2	P/D; Rudeen & Lord, 2013; Sobolik & Ehgartner, 2009b*
					Nearest neighbors: 101 (N), 101 (NW), 106 (SW), 117 (S)

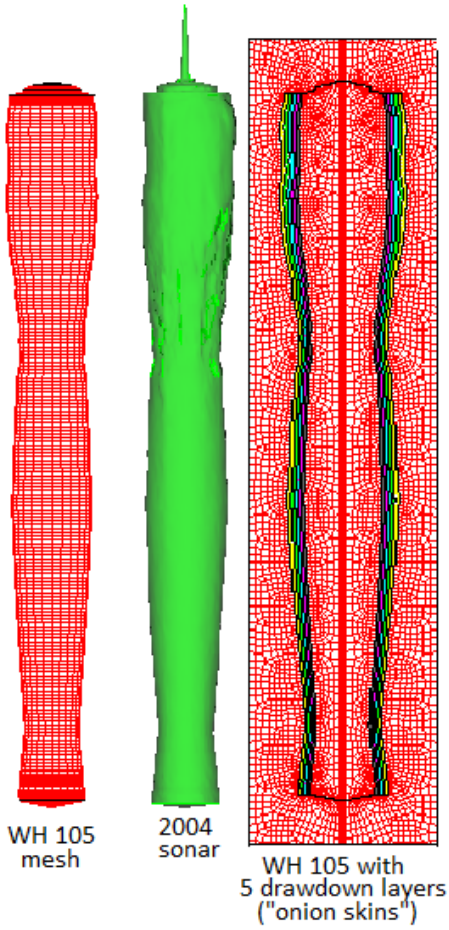

Figure 2.5-1. Computational mesh and sonar geometries for WH-105

Figure 2.5-2 plots the minimum value of dilatant damage factor, or safety factor, at any point around the cavern wall, as a function of time through five drawdowns. The lowest predicted value for the dilatant safety factor was 1.0, at the end of a workover after the historical pressure period and thus modeled more abrupt pressure changes. This minimum value occurs at the floor of the cavern, which has the similar pattern of high dilatant stresses and reduced safety factors during workovers. As usual, these values occur during workovers; the geomechanical predictions indicate that at all other times there are no excessive dilatant stress values. Because the time and location of the low safety factor values are in the floor of the cavern, and only for a brief period coincident with a workover, these occurrences are not believed to be significant enough to cause microcracking in the salt of a magnitude that would affect cavern stability. This conclusion is substantiated in Figure 2.5-3, which plots the maximum value of maximum principal stress around WH-105. Positive values indicate tension, which if they occur would likely be in the same locations as the minimum dilatant safety factor values. The maximum stress never reaches a positive or tensile value through five drawdowns.

Figure 2.5-4 plots the predicted average axial casing strain between the casing and top of salt for WH-105. The overall average strain is predicted to exceed 1.6 millistrains after the fourth drawdown, although the region above the top of the cavern, including the casing shoe, is predicted to have experienced localized strains above 1.6 mε by 2015 (Sobolik, 2015). The strain rate increases slightly once drawdowns begin, but not in an alarming fashion. Because of salt creep, casing integrity is an expected operational issue independent of the number of drawdowns for a particular cavern; because there is no significant change in strain behavior resulting from the drawdowns, there is nothing to indicate additional concern for the mechanical stability of the cavern.

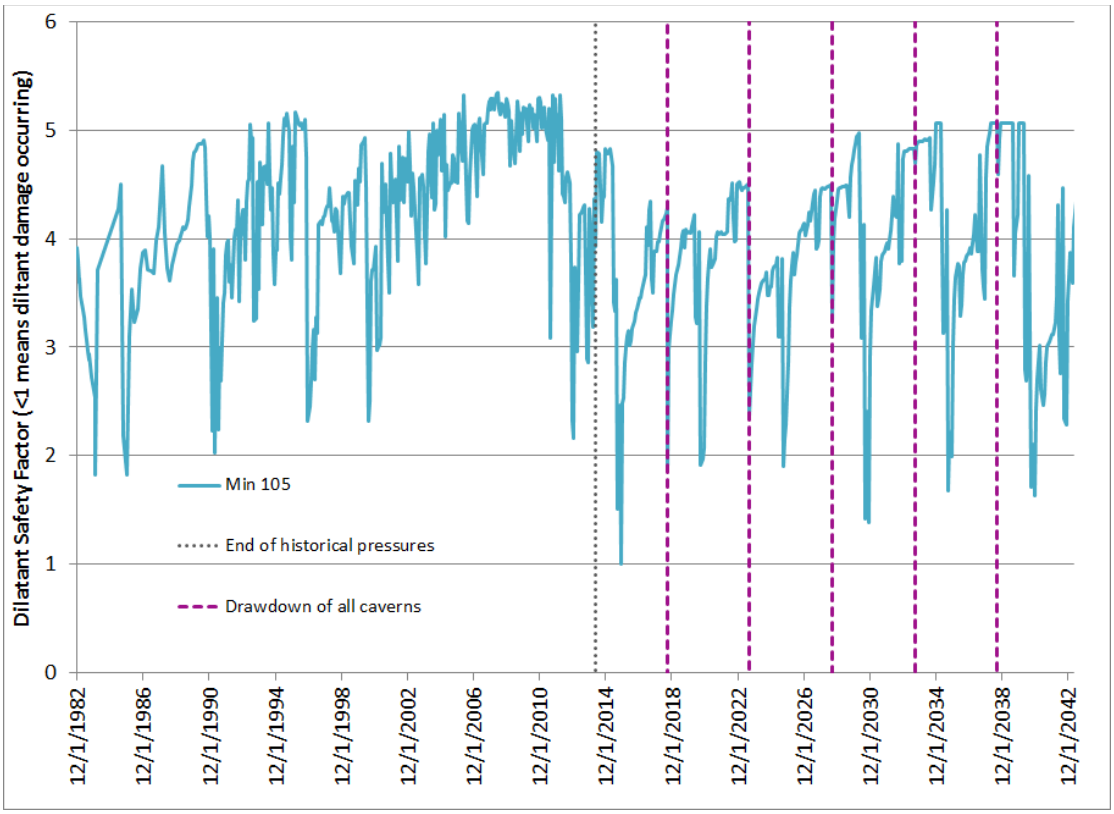

Figure 2.5-2. Minimum value of dilatant safety factor surrounding WH-105.

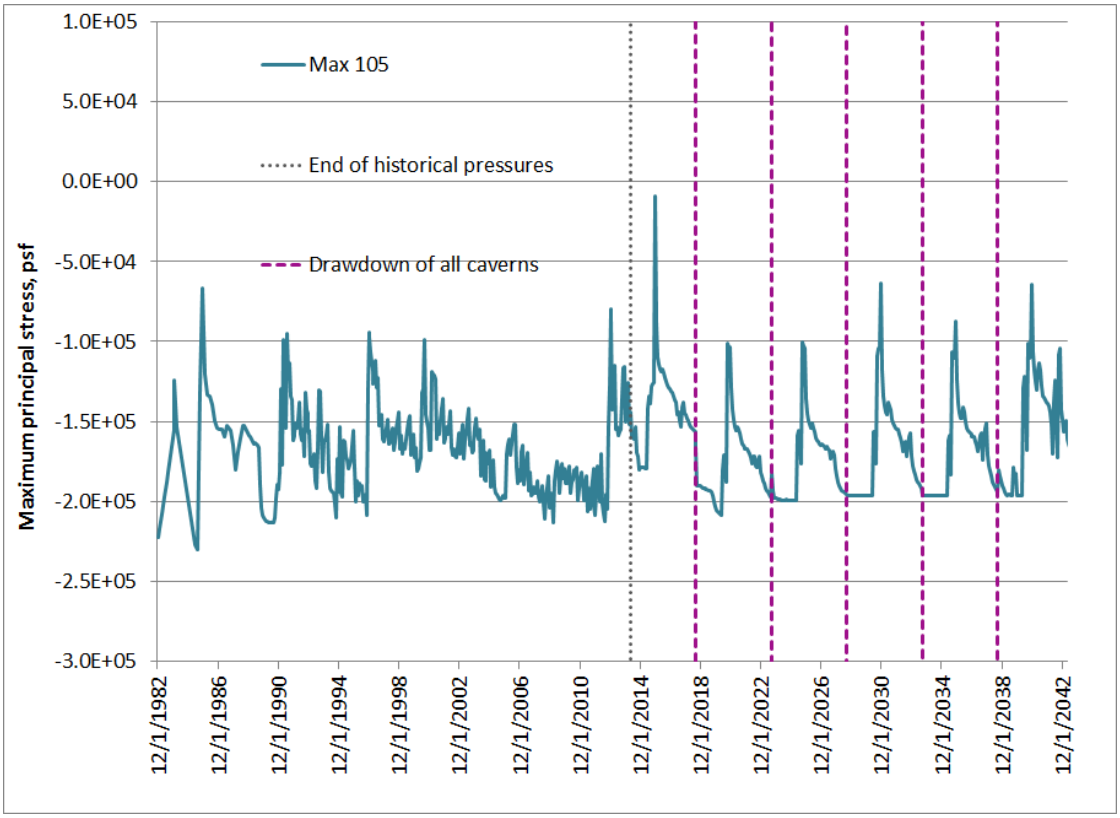

Figure 2.5-3. Maximum value of maximum principal stress surrounding WH-105.

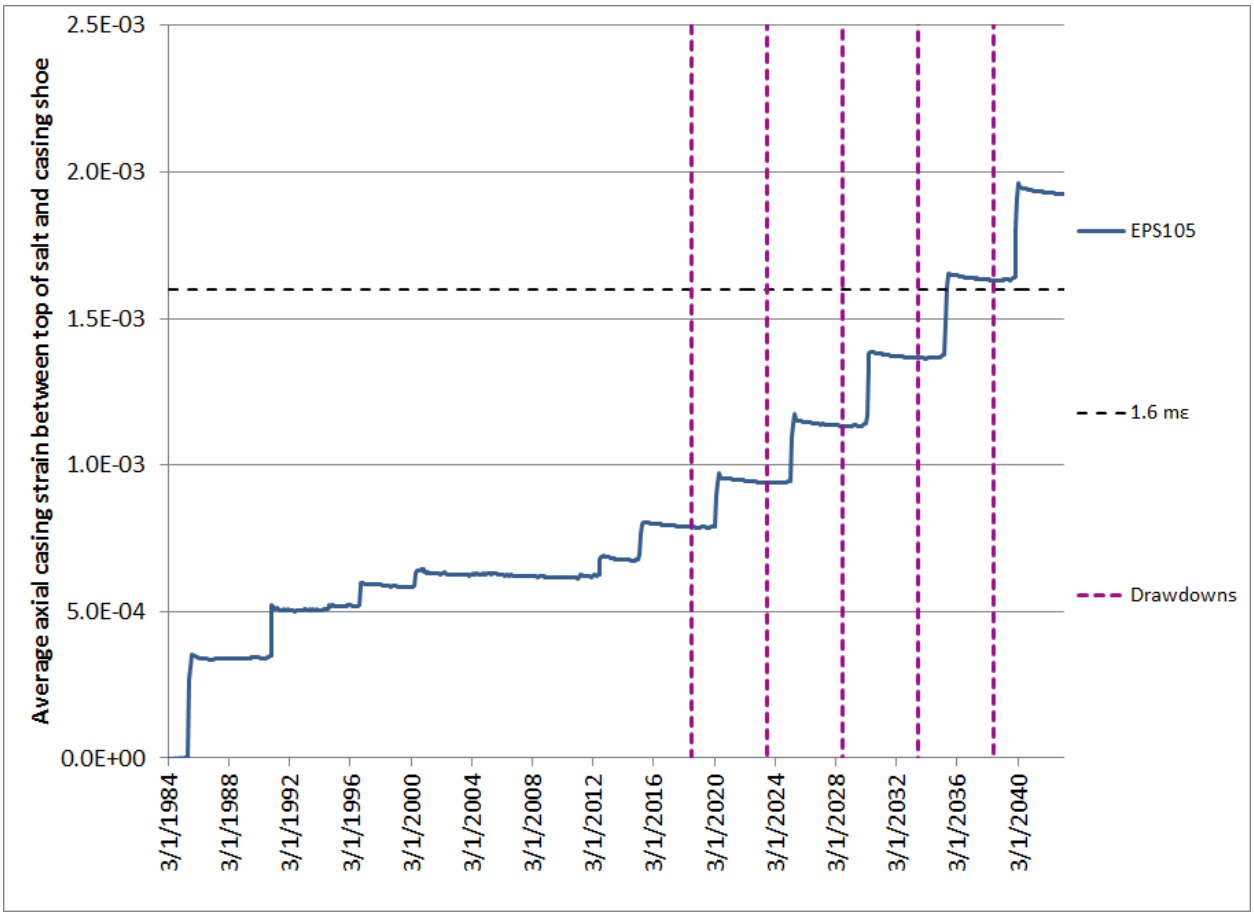

Figure 2.5-4. Predicted avg. axial casing strain between casing shoe and top of salt for WH-105.

As of July 2015, no salt falls have been recorded for WH-105 (Roberts et al., 2015). Salt falls are not unusual, even for otherwise mechanically-stable caverns, but a lack of salt falls supports the indications from the geomechanical calculations that WH-105 should be mechanically stable through five drawdowns. Therefore:

The updated estimate for WH-105 based on geomechanical analyses is that this cavern is stable through 5 drawdowns.

2.6 WH Cavern 106

WH Cavern 106 is a Phase 2 cavern surrounded by Phase 2 caverns. The previous best estimate for its number of available drawdowns was 4, based on P/D ratios with its nearby caverns. Table 2.6 summarizes the P/D and geomechanical estimates for available drawdowns for WH-106 in 2014. Figure 2.6-1 shows the volume of WH-106 in both its computational mesh geometry and its oldest available sonar geometry from 2000, and the geometries of the five drawdown layers built into the computational mesh. As is the case for all the Phase 2 caverns, the modeled drawdown layers extend for nearly the entire height of the cavern, and add approximately 15% to the volume of the cavern when they are removed.

Table 2.6. 2014 Estimates of available drawdowns, WH-106.

Cavern	Basis				2014 Best Estimate Basis (P/D or GM), Comments, Reference
	2D P/D < 1	3D P/D < 1	Geomechanics	Best Estimate	
WH106	4	4	5	4	P/D; Rudeen & Lord, 2013; Based on S&E, 2009b
					Nearest neighbors: 104 (N), 105 (NE), 117 (SE)

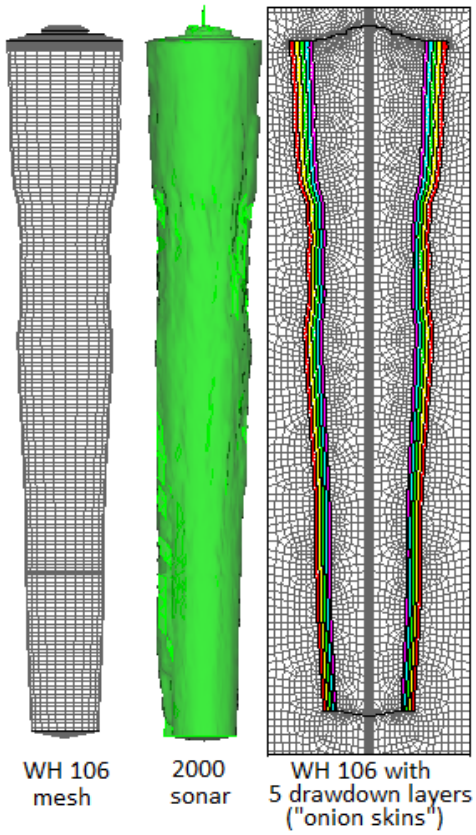

Figure 2.6-1. Computational mesh and sonar geometries for WH-106

Figure 2.6-2 plots the minimum value of dilatant damage factor, or safety factor, at any point around the cavern wall, as a function of time through five drawdowns. The lowest predicted

value for the dilatant safety factor was 1.10, at the end of a workover after the fifth drawdown. This minimum value occurs at the floor of the cavern, which has the similar pattern of high dilatant stresses and reduced safety factors during workovers. Similarly low values occur near the corner of the cavern ceiling. As usual, these values occur during workovers; the geomechanical predictions indicate that at all other times there are no excessive dilatant stress values. Because the time and location of the low safety factor values are in the floor of the cavern, and only for a brief period coincident with a workover, these occurrences are not believed to be significant enough to cause microcracking in the salt of a magnitude that would affect cavern stability. This conclusion is substantiated in Figure 2.6-3, which plots the maximum value of maximum principal stress around WH-106. Positive values indicate tension, which if they occur would likely be in the same locations as the minimum dilatant safety factor values. The maximum stress never reaches a positive or tensile value through five drawdowns.

Figure 2.6-4 plots the predicted average axial casing strain between the casing and top of salt for WH-106. The overall average strain is predicted to have exceeded 1.6 millistrains around 2003; the average strain rate actually decreases through 2018 and the five drawdowns through 2042. This behavior is among the most extreme for the West Hackberry caverns, and is likely due to the flatness and large diameter of its cavern ceiling, which are greater than for nearly all the other WH Phase 2 caverns. Because of salt creep, casing integrity is an expected operational issue independent of the number of drawdowns for a particular cavern; because there is no significant detrimental change in strain behavior resulting from the drawdowns, there is nothing to indicate additional concern for the mechanical stability of the cavern.

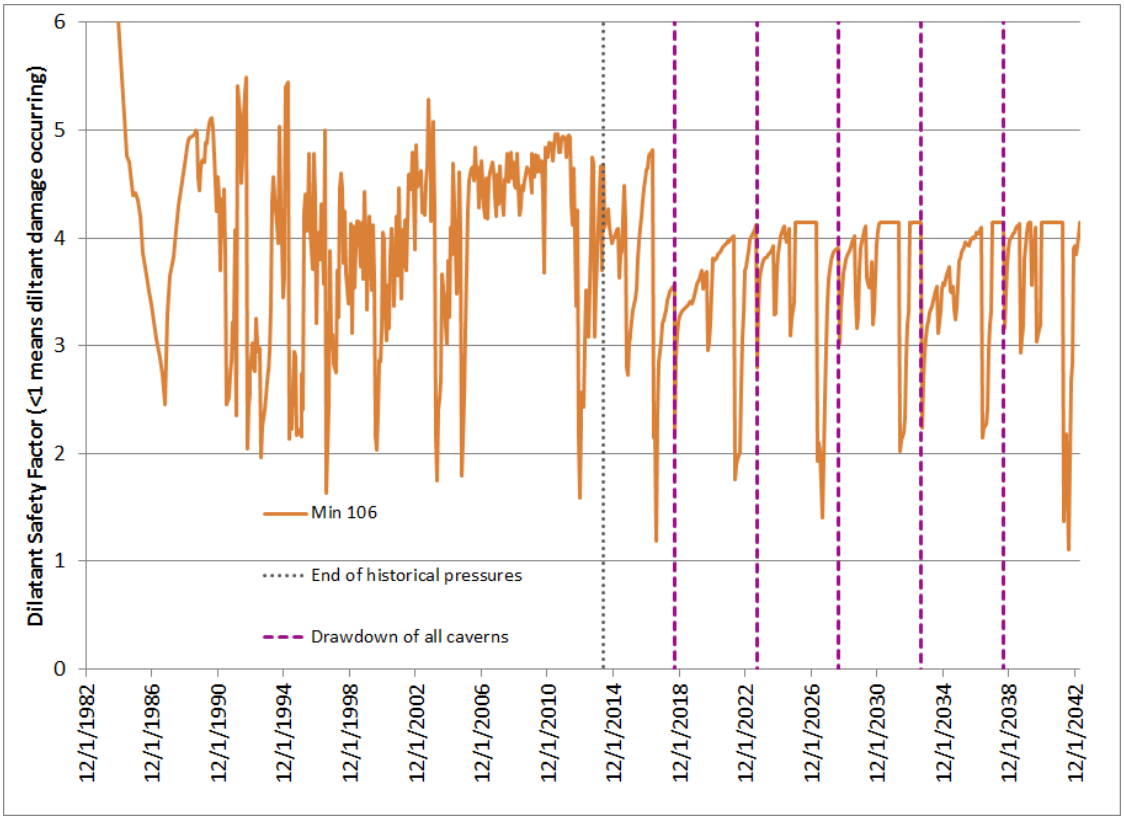

Figure 2.6-2. Minimum value of dilatant safety factor surrounding WH-106.

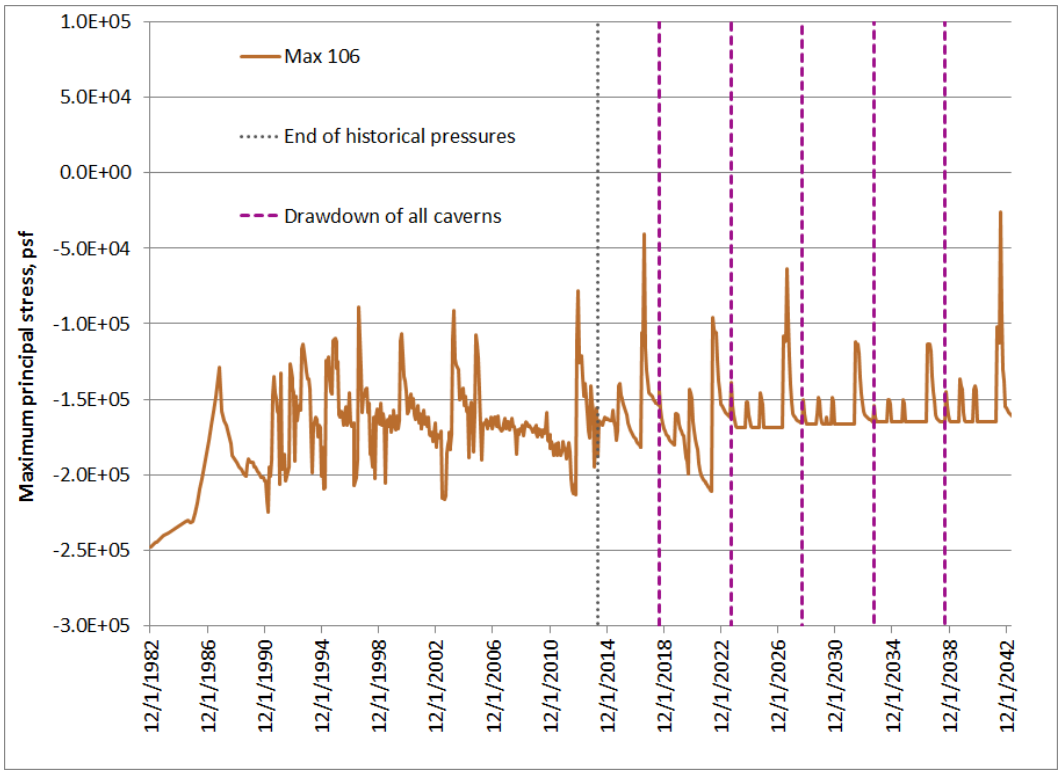

Figure 2.6-3. Maximum value of maximum principal stress surrounding WH-106.

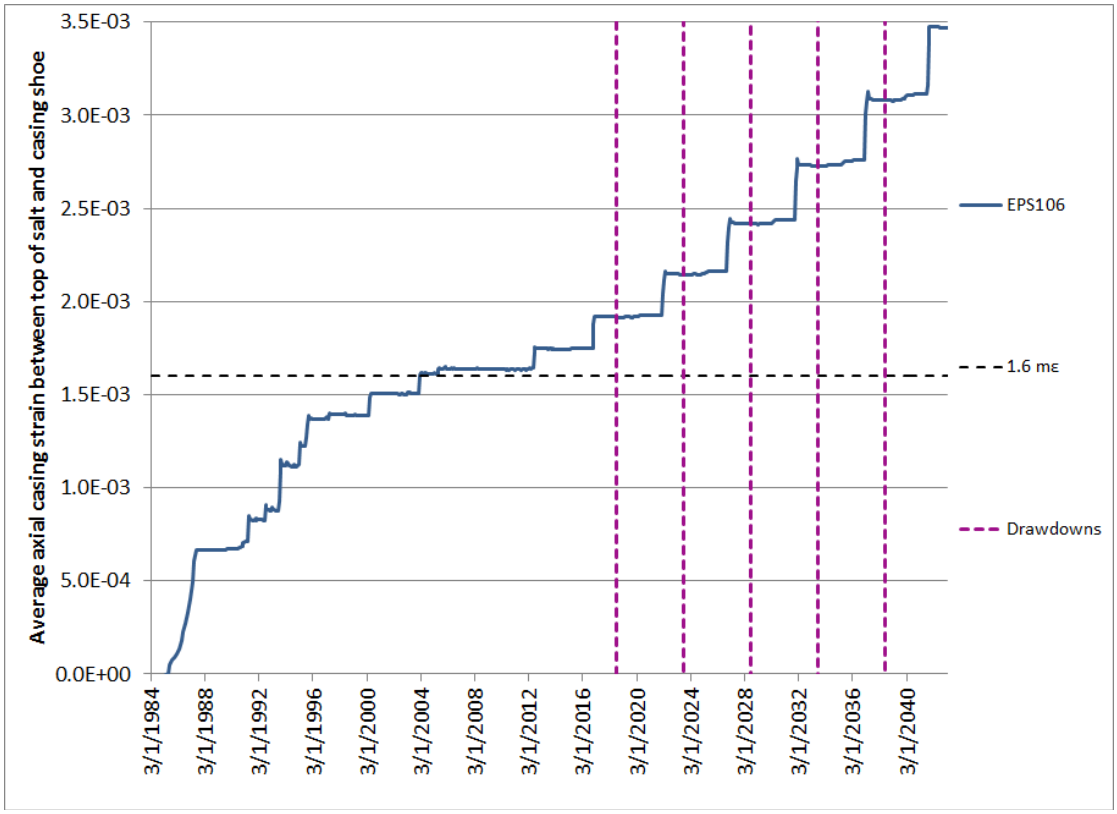

Figure 2.6-4. Predicted avg. axial casing strain between casing shoe and top of salt for WH-106.

As of July 2015, no salt falls have been recorded for WH-106 (Roberts et al., 2015). Salt falls are not unusual, even for otherwise mechanically-stable caverns, but a lack of salt falls supports the indications from the geomechanical calculations that WH-106 should be mechanically stable through five drawdowns. Therefore:

The updated estimate for WH-106 based on geomechanical analyses is that this cavern is stable through 5 drawdowns.

2.7 WH Cavern 107

WH Cavern 107 is a Phase 2 cavern surrounded by Phase 2 caverns. The previous best estimate for its number of available drawdowns was 5, based on P/D ratios with its nearby caverns. Table 2.7 summarizes the P/D and geomechanical estimates for available drawdowns for WH-107 in 2014. Figure 2.7-1 shows the volume of WH-107 in both its computational mesh geometry and its oldest available sonar geometry from 1999, and the geometries of the five drawdown layers built into the computational mesh. As is the case for all the Phase 2 caverns, the modeled drawdown layers extend for nearly the entire height of the cavern, and add approximately 15% to the volume of the cavern when they are removed.

Table 2.7. 2014 Estimates of available drawdowns, WH-107.

Cavern	Basis				2014 Best Estimate Basis (P/D or GM), Comments, Reference
	2D P/D < 1	3D P/D < 1	Geomechanics	Best Estimate	
WH107	2	5	5	5	P/D; Rudeen & Lord, 2013; Sobolik & Ehgartner, 2009b*
					Nearest neighbors: 114 (NW), 115 (N), 109 (NE), 103 (SE), 102 (S)

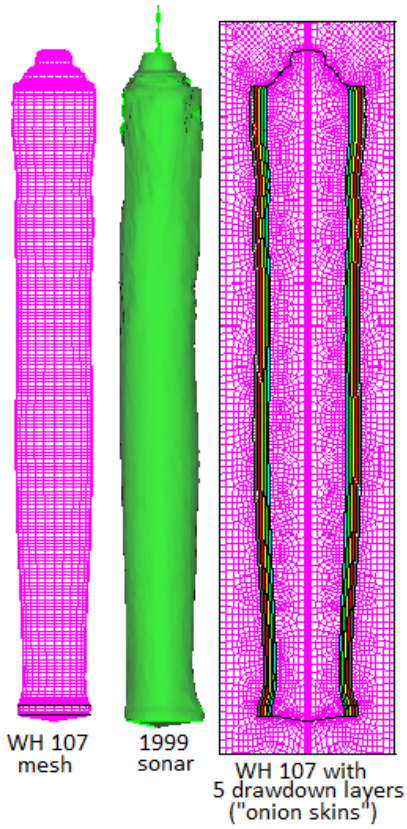

Figure 2.7-1. Computational mesh and sonar geometries for WH-107

Figure 2.7-2 plots the minimum value of dilatant damage factor, or safety factor, at any point around the cavern wall, as a function of time through five drawdowns. The lowest predicted

value for the dilatant safety factor was 0.7, during a workover after the second drawdown. This instance coincided with the initiation date of that drawdown, so this would be a lowest expected value for the damage factor. This value dips below the threshold value of 1.0 that signifies the onset of dilatant damage, and does it for only a brief period (during a workover). This minimum value occurs at the floor of the cavern, which has the similar pattern of high dilatant stresses and reduced safety factors during workovers. One other places shows noticeable, though not excessive stresses during a workover: near the top of the cavern at the corner of the roof. These locations are shown in Figure 2.7-3. As usual, these values occur during workovers; the geomechanical predictions indicate that at all other times there are no excessive dilatant stress values. Because the time and location of the sub-threshold safety factor values are in the floor of the cavern, and only for a brief period at the beginning of a workover, these occurrences are not believed to be significant enough to cause microcracking in the salt of a magnitude that would affect cavern stability. This conclusion is substantiated in Figure 2.7-4, which plots the maximum value of maximum principal stress around WH-107. Positive values indicate tension, which if they occur would likely be in the same locations as the minimum dilatant safety factor values. The maximum stress reaches a positive or tensile value at the same time as the extreme dilatancy condition. Because of the short time duration and the location of the stress condition as the cavern floor, this incidence is not expected to have any detrimental effect on cavern integrity and stability

Figure 2.7-5 plots the predicted average axial casing strain between the casing and top of salt for WH-107. The overall average strain is predicted to never exceed 1.6 millistrains even after five drawdowns, although the region above the top of the cavern, including the casing shoe, is predicted to have experienced localized strains above 1.6 mε by 2015 (Sobolik, 2015). The strain rate increases slightly once drawdowns begin, but not in an alarming fashion. Because of salt creep, casing integrity is an expected operational issue independent of the number of drawdowns for a particular cavern; because there is no significant change in strain behavior resulting from the drawdowns, there is nothing to indicate additional concern for the mechanical stability of the cavern.

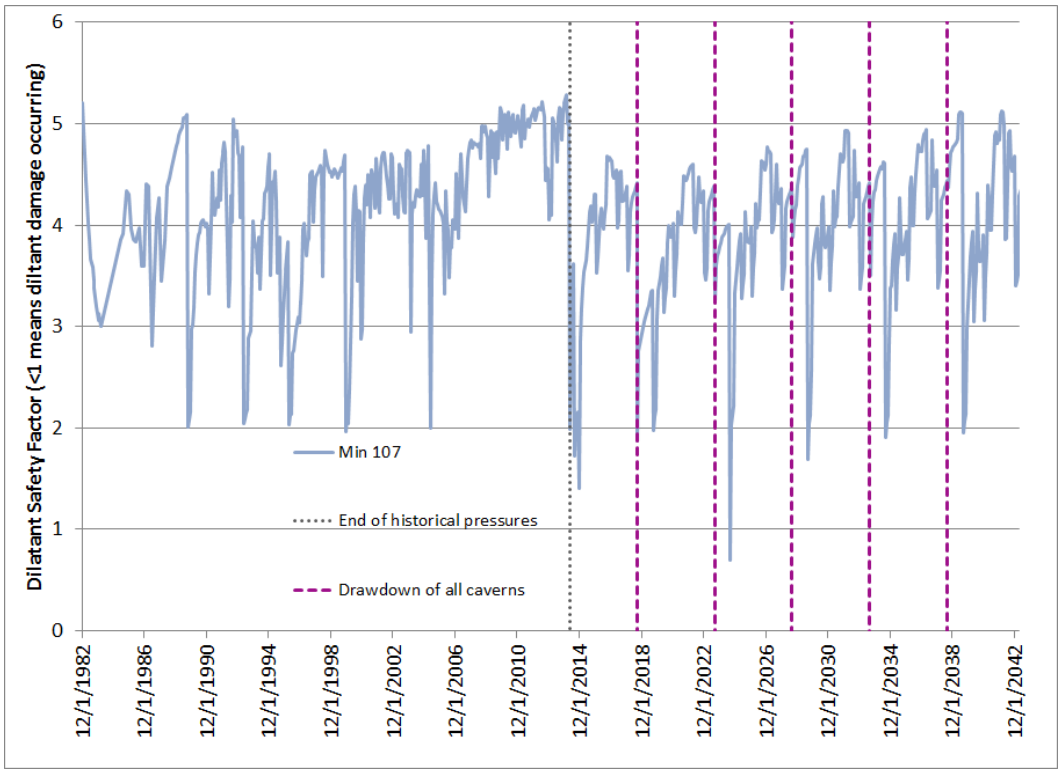

Figure 2.7-2. Minimum value of dilatant safety factor surrounding WH-107.

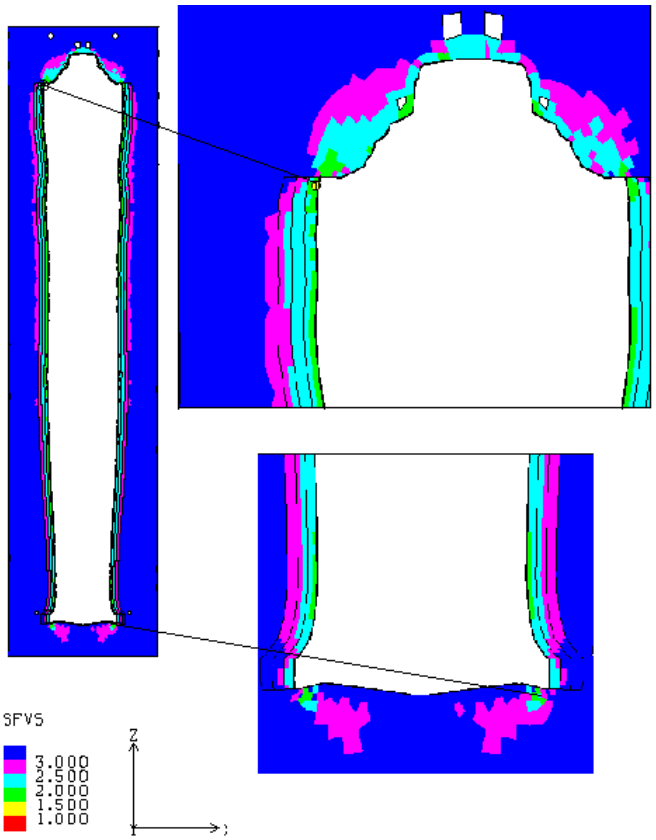

Figure 2.7-3. Locations of minimum value of dilatant safety factor surrounding WH-107.

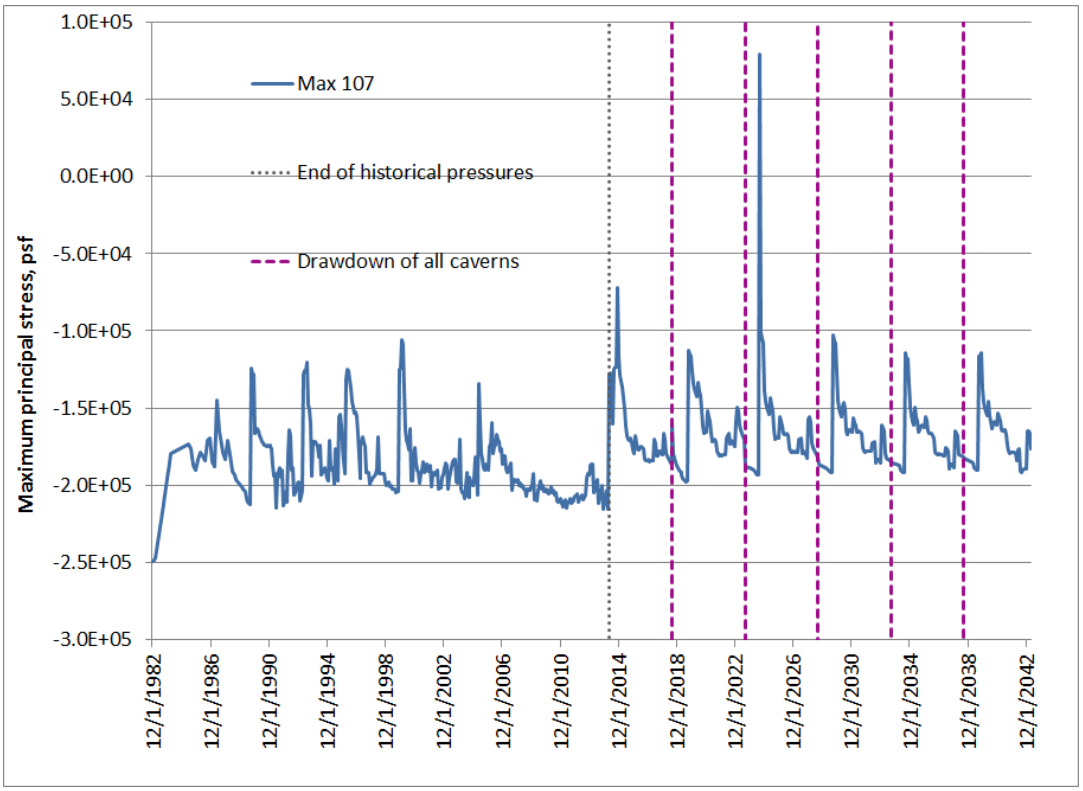

Figure 2.7-4. Maximum value of maximum principal stress surrounding WH-107.

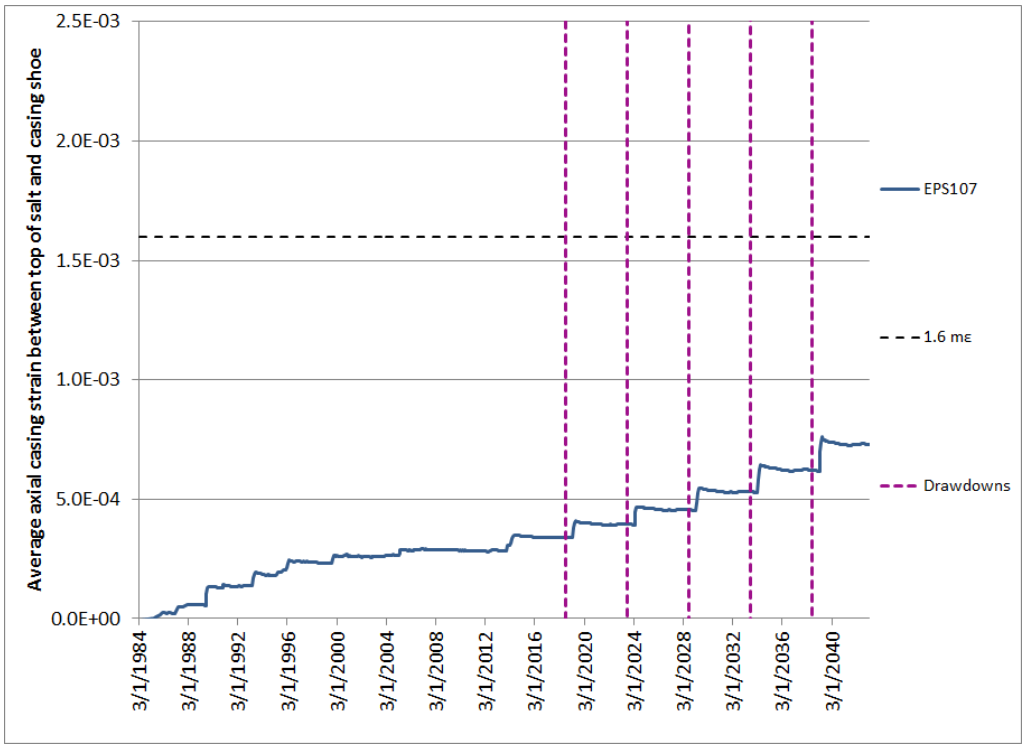

Figure 2.7-5. Predicted avg. axial casing strain between casing shoe and top of salt for WH-107.

As of July 2015, one salt fall has been recorded for WH-107 (Roberts et al., 2015). Salt falls are not unusual, even for otherwise mechanically-stable caverns, so this number of salt falls does not contradict the indications from the geomechanical calculations that WH-107 should be mechanically stable through five drawdowns. Therefore:

The updated estimate for WH-107 based on geomechanical analyses is that this cavern is stable through 5 drawdowns.

2.8 WH Cavern 108

WH Cavern 108 is a Phase 2 cavern surrounded by Phase 1 and 2 caverns. The previous best estimate for its number of available drawdowns was 4, based on P/D ratios with its nearby caverns. Table 2.8 summarizes the P/D and geomechanical estimates for available drawdowns for WH-108 in 2014. Figure 2.8-1 shows the volume of WH-108 in both its computational mesh geometry and its oldest available sonar geometry from 2003, and the geometries of the five drawdown layers built into the computational mesh. As is the case for all the Phase 2 caverns, the modeled drawdown layers extend for nearly the entire height of the cavern, and add approximately 15% to the volume of the cavern when they are removed.

Table 2.8. 2014 Estimates of available drawdowns, WH-108.

Cavern	Basis				2014 Best Estimate Basis (P/D or GM), Comments, Reference
	2D P/D < 1	3D P/D < 1	Geomechanics	Best Estimate	
WH108	4	4	5	4	P/D; Rudeen & Lord, 2013; Sobolik & Ehgartner, 2009b*
					Nearest neighbors: 11 (NE), 112 (E), 117 (NW)

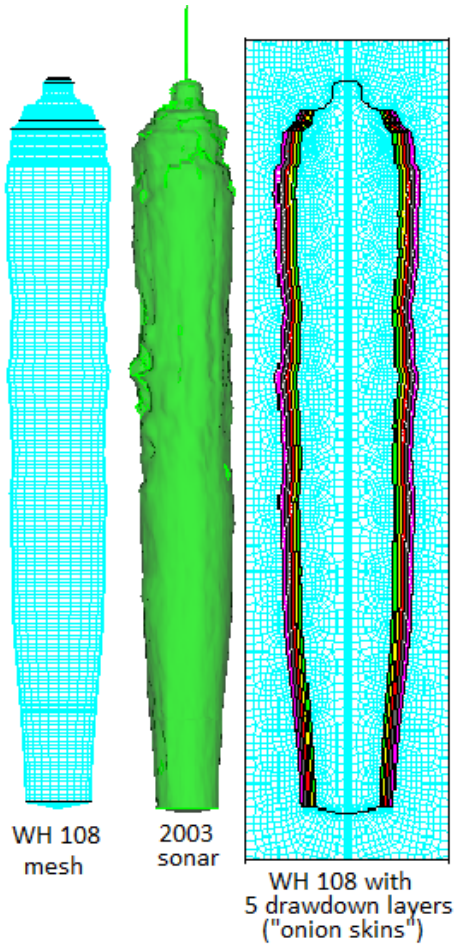

Figure 2.8-1. Computational mesh and sonar geometries for WH-108

Figure 2.8-2 plots the minimum value of dilatant damage factor, or safety factor, at any point around the cavern wall, as a function of time through five drawdowns. The lowest predicted value for the dilatant safety factor was 1.11, at the end of a workover after the fourth drawdown. This minimum value occurs at the floor of the cavern, which has the similar pattern of high dilatant stresses and reduced safety factors during workovers. Similarly low values occur near the corner of the cavern ceiling. As usual, these values occur during workovers; the geomechanical predictions indicate that at all other times there are no excessive dilatant stress values. Because the time and location of the low safety factor values are in the floor of the cavern, and only for a brief period coincident with a workover, these occurrences are not believed to be significant enough to cause microcracking in the salt of a magnitude that would affect cavern stability. This conclusion is substantiated in Figure 2.8-3, which plots the maximum value of maximum principal stress around WH-108. Positive values indicate tension, which if they occur would likely be in the same locations as the minimum dilatant safety factor values. The maximum stress never reaches a positive or tensile value through five drawdowns.

Figure 2.8-4 plots the predicted average axial casing strain between the casing and top of salt for WH-108. The overall average strain is predicted to never exceed 1.6 millistrains even after five drawdowns, although the region above the top of the cavern, including the casing shoe, is predicted to have experienced localized strains above 1.6 mε by 2015 (Sobolik, 2015). The strain rate increases slightly once drawdowns begin, but not in an alarming fashion. Because of salt creep, casing integrity is an expected operational issue independent of the number of drawdowns for a particular cavern; because there is no significant change in strain behavior resulting from the drawdowns, there is nothing to indicate additional concern for the mechanical stability of the cavern.

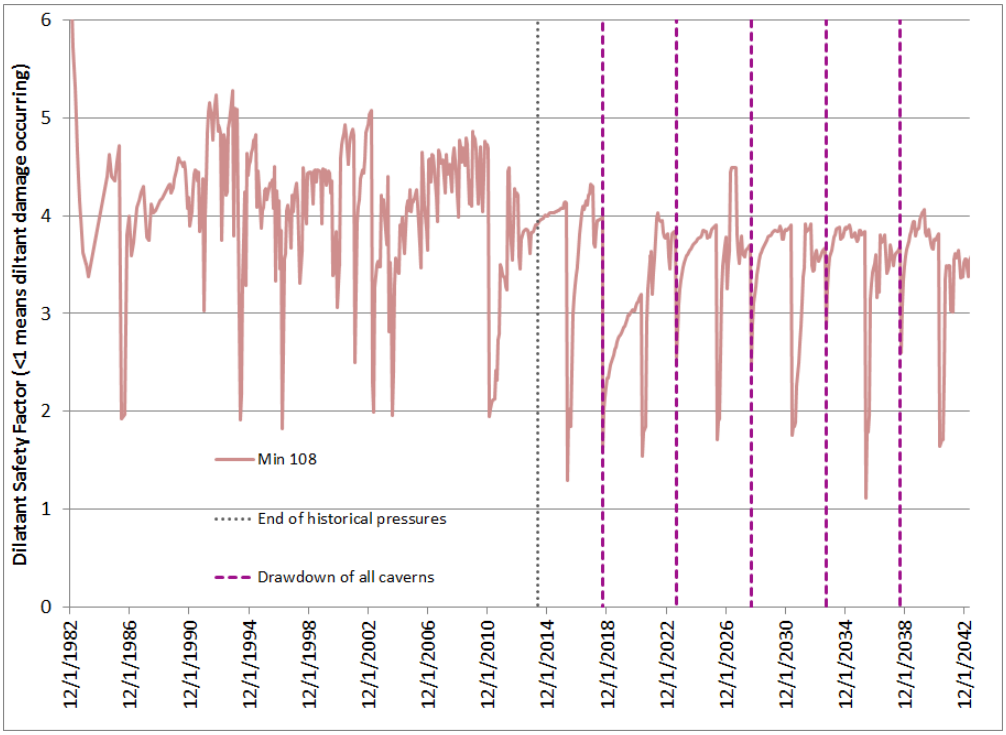

Figure 2.8-2. Minimum value of dilatant safety factor surrounding WH-108.

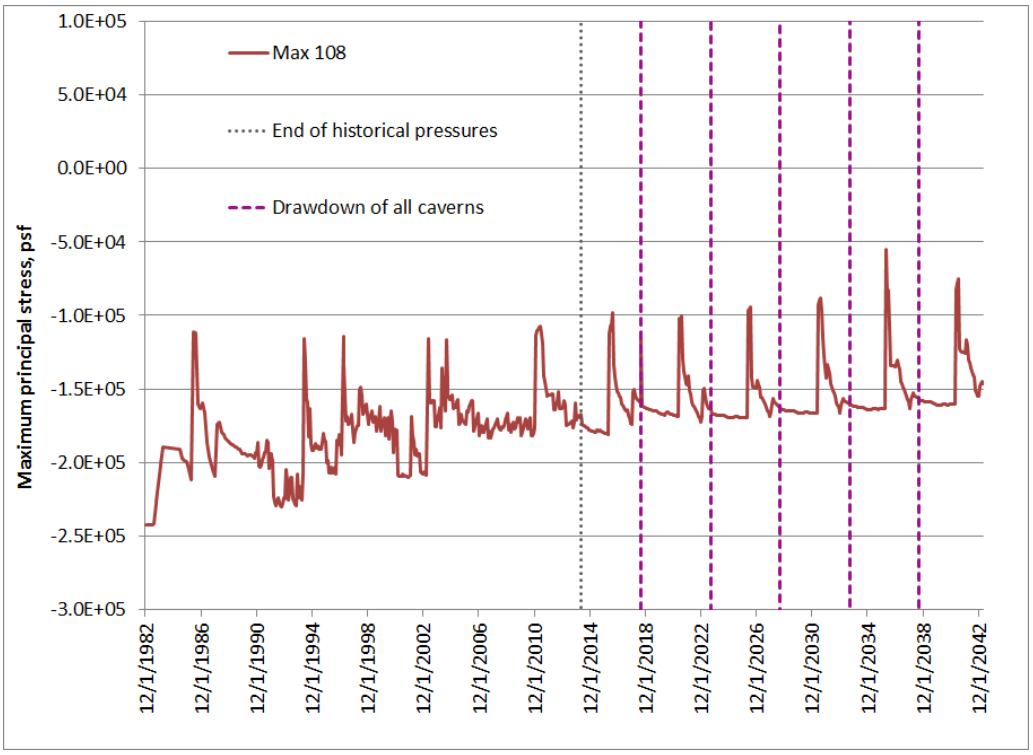

Figure 2.8-3. Maximum value of maximum principal stress surrounding WH-108.

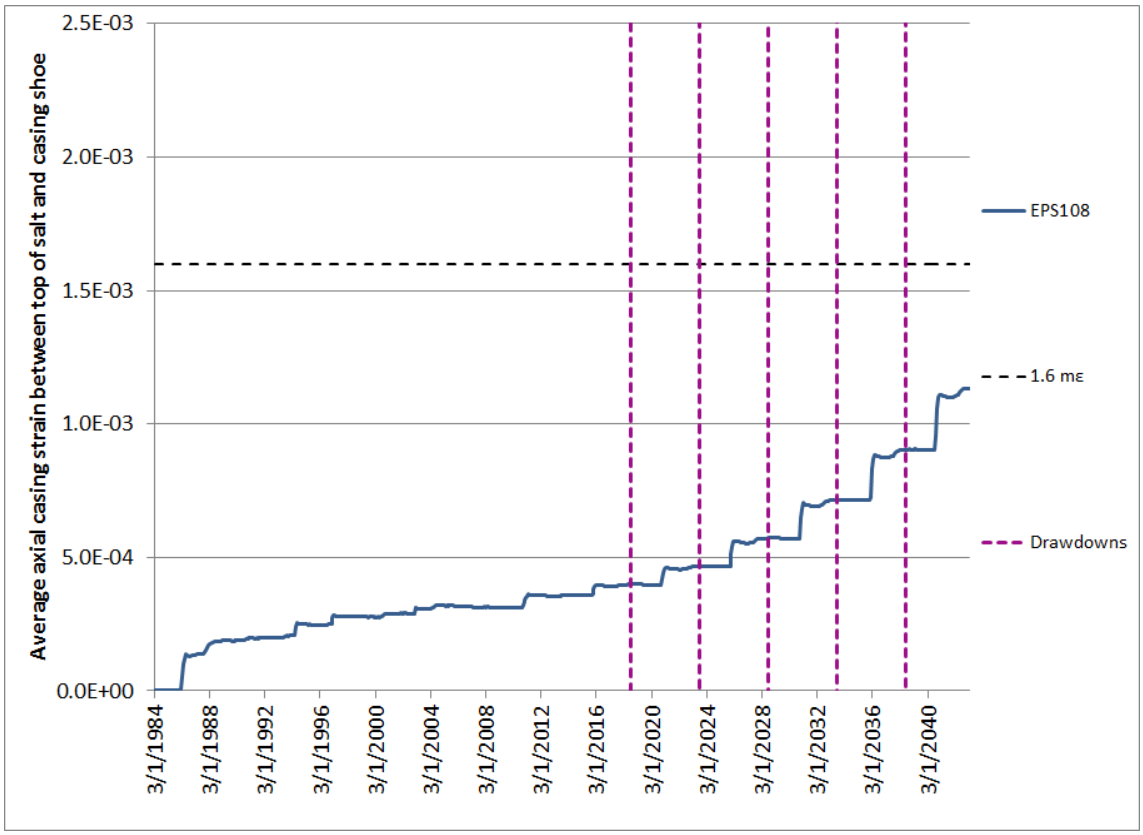

Figure 2.8-4. Predicted avg. axial casing strain between casing shoe and top of salt for WH-108.

As of July 2015, four salt falls have been recorded for WH-108 (Roberts et al., 2015). The vast majority of WH caverns have zero or one recorded salt fall; there are no indications why this cavern has experienced several more salt falls. Nevertheless, salt falls are not unusual, even for otherwise mechanically-stable caverns, so this number of salt falls does not contradict the indications from the geomechanical calculations that WH-108 should be mechanically stable through five drawdowns. Therefore:

The updated estimate for WH-108 based on geomechanical analyses is that this cavern is stable through 5 drawdowns.

2.9 WH Cavern 109

WH Cavern 109 is a Phase 2 cavern surrounded by Phase 1 and 2 caverns. The previous best estimate for its number of available drawdowns was 4, based on P/D ratios with its nearby caverns. Table 2.9 summarizes the P/D and geomechanical estimates for available drawdowns for WH-109 in 2014. Figure 2.9-1 shows the volume of WH-109 in both its computational mesh geometry and its oldest available sonar geometry from 1997, and the geometries of the five drawdown layers built into the computational mesh. As is the case for all the Phase 2 caverns, the modeled drawdown layers extend for nearly the entire height of the cavern, and add approximately 15% to the volume of the cavern when they are removed.

Table 2.9. 2014 Estimates of available drawdowns, WH-109.

Cavern	Basis				2014 Best Estimate Basis (P/D or GM), Comments, Reference
	2D P/D < 1	3D P/D < 1	Geomechanics	Best Estimate	
WH109	2	4	5	4	P/D; Rudeen & Lord, 2013; Sobolik & Ehgartner, 2009b*
					Nearest neighbors: 103 (S), 107 (SW), 115 (NW), 110 (N), 9 (E)

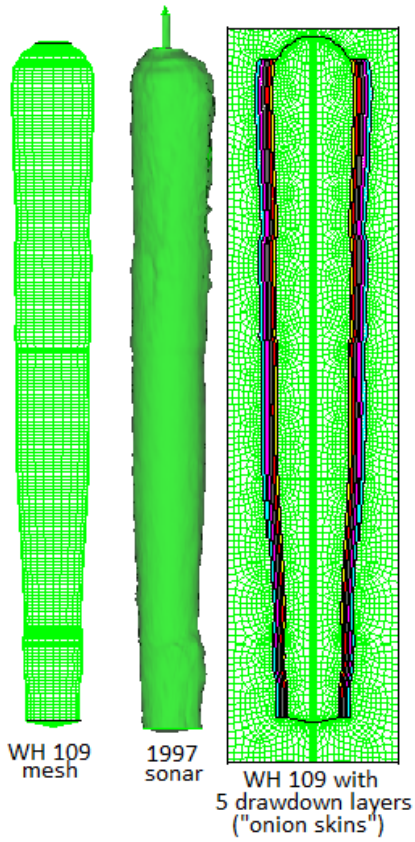

Figure 2.9-1. Computational mesh and sonar geometries for WH-109

Figure 2.9-2 plots the minimum value of dilatant damage factor, or safety factor, at any point around the cavern wall, as a function of time through five drawdowns. The lowest predicted value for the dilatant safety factor was 1.33, at the end of a workover prior to the first drawdown. This minimum value occurs at the floor of the cavern, which has the similar pattern of high dilatant stresses and reduced safety factors during workovers. Similarly low values occur near the corner of the cavern ceiling. As usual, these values occur during workovers; the geomechanical predictions indicate that at all other times there are no excessive dilatant stress values. Because the time and location of the low safety factor values are in the floor of the cavern, and only for a brief period coincident with a workover, these occurrences are not believed to be significant enough to cause microcracking in the salt of a magnitude that would affect cavern stability. This conclusion is substantiated in Figure 2.9-3, which plots the maximum value of maximum principal stress around WH-109. Positive values indicate tension, which if they occur would likely be in the same locations as the minimum dilatant safety factor values. The maximum stress never reaches a positive or tensile value through five drawdowns.

Figure 2.9-4 plots the predicted average axial casing strain between the casing and top of salt for WH-109. The overall average strain is predicted to never exceed 1.6 millistrains even after five drawdowns, although the region above the top of the cavern, including the casing shoe, is predicted to have experienced localized strains above 1.6 mε by 2015 (Sobolik, 2015). The strain rate increases slightly once drawdowns begin, but not in an alarming fashion. Because of salt creep, casing integrity is an expected operational issue independent of the number of drawdowns for a particular cavern; because there is no significant change in strain behavior resulting from the drawdowns, there is nothing to indicate additional concern for the mechanical stability of the cavern.

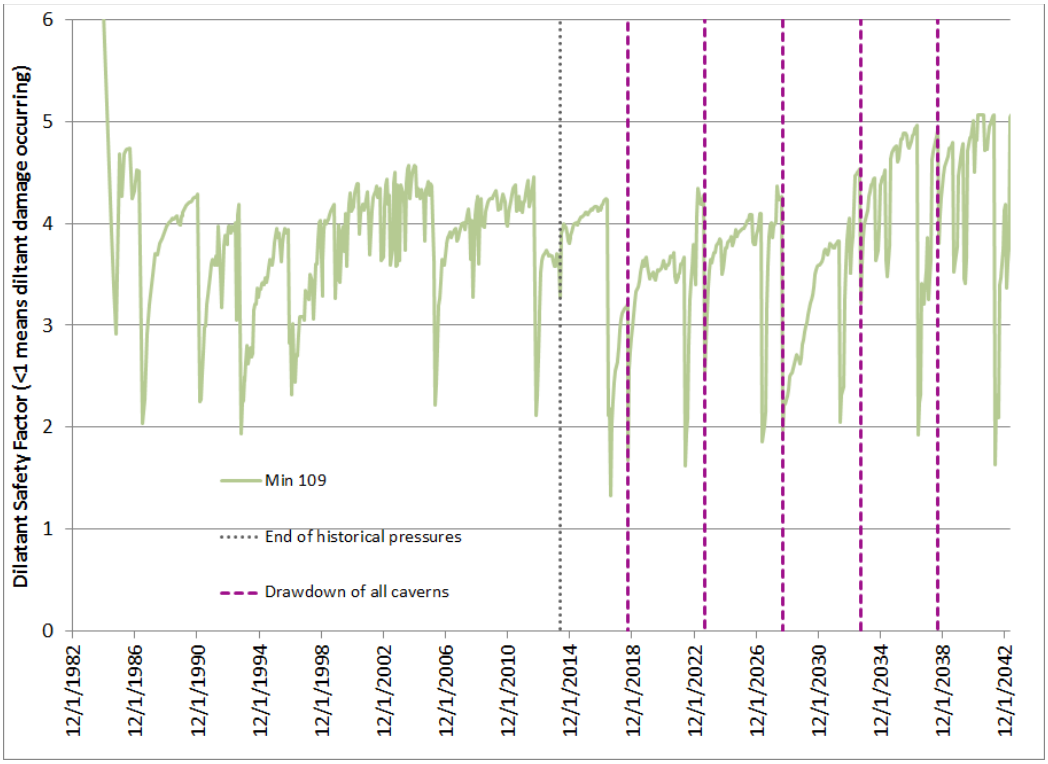

Figure 2.9-2. Minimum value of dilatant safety factor surrounding WH-109.

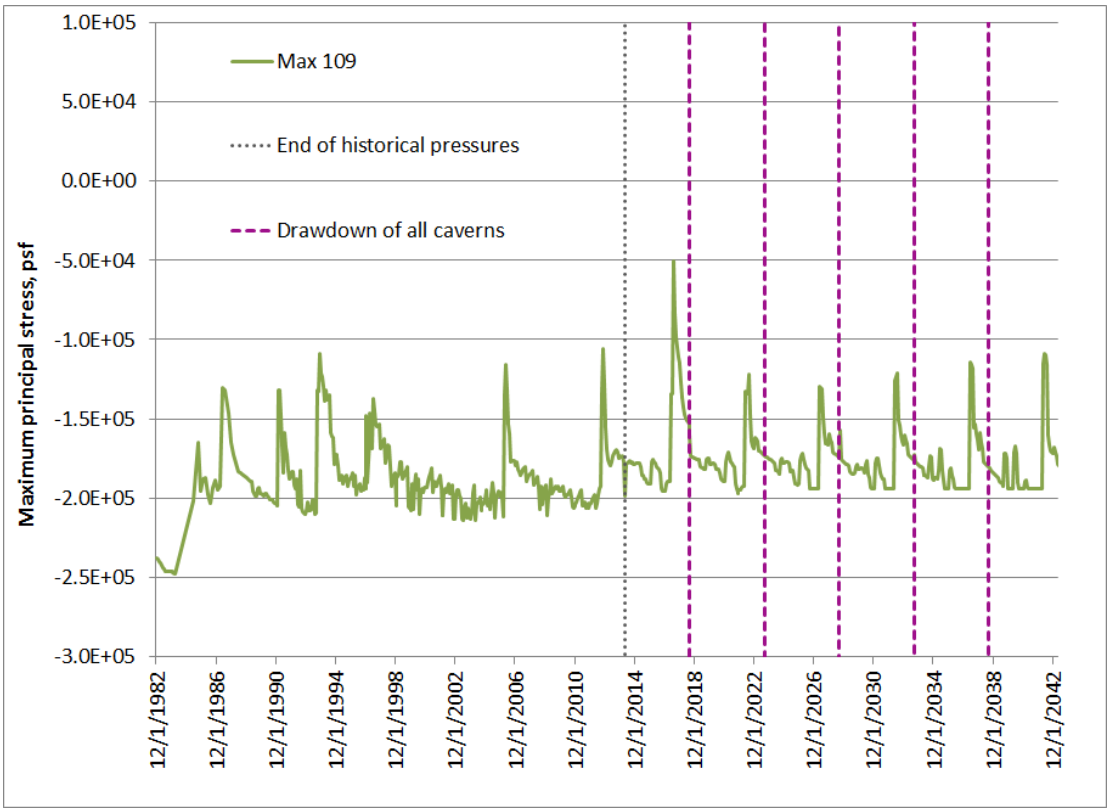

Figure 2.9-3. Maximum value of maximum principal stress surrounding WH-109.

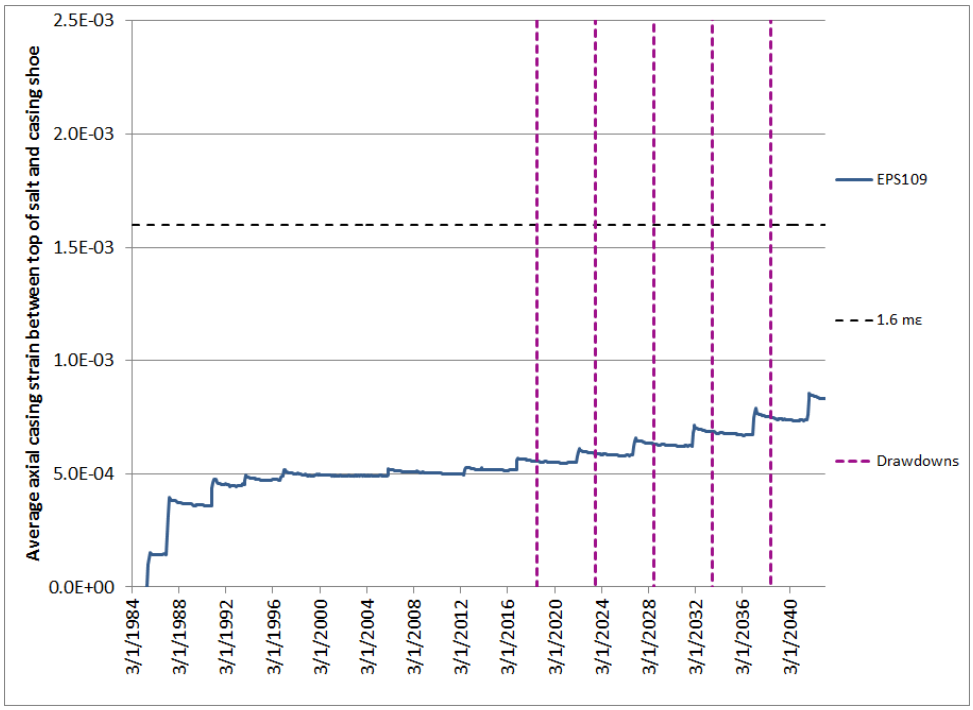

Figure 2.9-4. Predicted avg. axial casing strain between casing shoe and top of salt for WH-109.

As of July 2015, two salt falls have been recorded for WH-109 (Roberts et al., 2015). Salt falls are not unusual, even for otherwise mechanically-stable caverns, so this number of salt falls does not contradict the indications from the geomechanical calculations that WH-109 should be mechanically stable through five drawdowns. Therefore:

The updated estimate for WH-109 based on geomechanical analyses is that this cavern is stable through 5 drawdowns.

2.10 WH Cavern 110

WH Cavern 110 is a Phase 2 cavern surrounded by Phase 1 and 2 caverns. The previous best estimate for its number of available drawdowns was 5, based on P/D ratios with its nearby caverns. Table 2.10 summarizes the P/D and geomechanical estimates for available drawdowns for WH-110 in 2014. Figure 2.10-1 shows the volume of WH-110 in both its computational mesh geometry and its oldest available sonar geometry from 2003, and the geometries of the five drawdown layers built into the computational mesh. As is the case for all the Phase 2 caverns, the modeled drawdown layers extend for nearly the entire height of the cavern, and add approximately 15% to the volume of the cavern when they are removed.

Table 2.10. 2014 Estimates of available drawdowns, WH-110.

Cavern	Basis				2014 Best Estimate Basis (P/D or GM), Comments, Reference
	2D P/D < 1	3D P/D < 1	Geomechanics	Best Estimate	
WH110	1	5	5	5	P/D; Rudeen & Lord, 2013; Sobolik & Ehgartner, 2009b*
					Nearest neighbors: 109 (S), 115 (SW), 111 (NW), 6 (NE), 9 (SE)

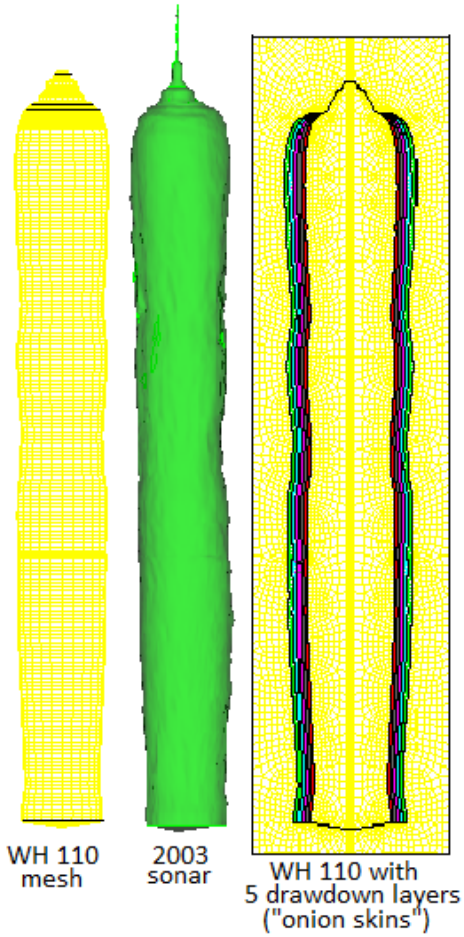

Figure 2.10-1. Computational mesh and sonar geometries for WH-110

Figure 2.10-2 plots the minimum value of dilatant damage factor, or safety factor, at any point around the cavern wall, as a function of time through five drawdowns. WH-110 exhibits one of the most bizarre behaviors of all the WH caverns, as it has extended periods where the minimum damage factor is below 1, and even equal to zero. Similarly, the maximum value of maximum principal stress plotted in Figure 2.10-3 shows extended period where tensile stress is recorded somewhere on the wall of the cavern. These results are initially alarming, and require further investigation into the spatial extent of the extreme stress states. Figure 2.10-4 shows the locations of the minimum safety factor and maximum principal stress around WH-110 at several times through a workover. A close examination reveals that the extreme stress states occur at the edge of the floor of the cavern, where there is a sharp corner in the mesh. The mesh geometry at this location is likely creating an artificially high stress concentration that exaggerates the stress at the bottom of the cavern. These occurrences are not believed to be significant enough to cause microcracking in the salt of a magnitude that would affect cavern stability.

Figure 2.10-5 plots the predicted average axial casing strain between the casing and top of salt for WH-110. The overall average strain is predicted to never exceed 1.6 millistrains even after five drawdowns, although the region above the top of the cavern, including the casing shoe, is predicted to have experienced localized strains above 1.6 mε by 2015 (Sobolik, 2015). The strain rate increases slightly once drawdowns begin, but not in an alarming fashion. Because of salt creep, casing integrity is an expected operational issue independent of the number of drawdowns for a particular cavern; because there is no significant change in strain behavior resulting from the drawdowns, there is nothing to indicate additional concern for the mechanical stability of the cavern.

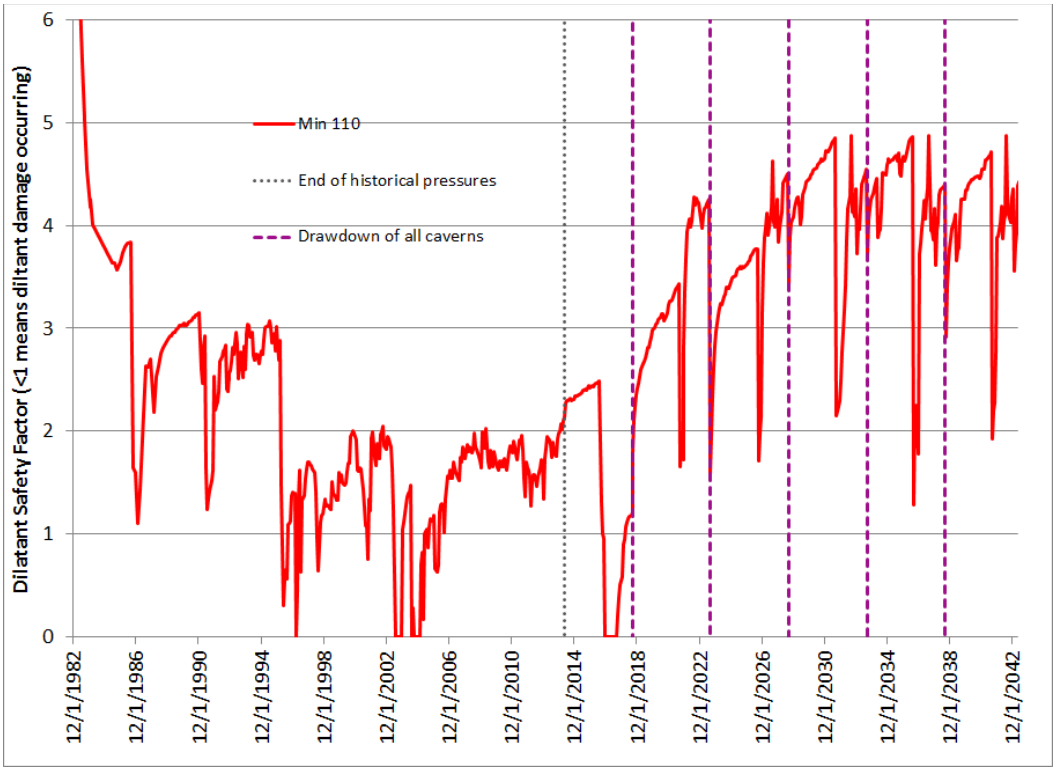

Figure 2.10-2. Minimum value of dilatant safety factor surrounding WH-110.

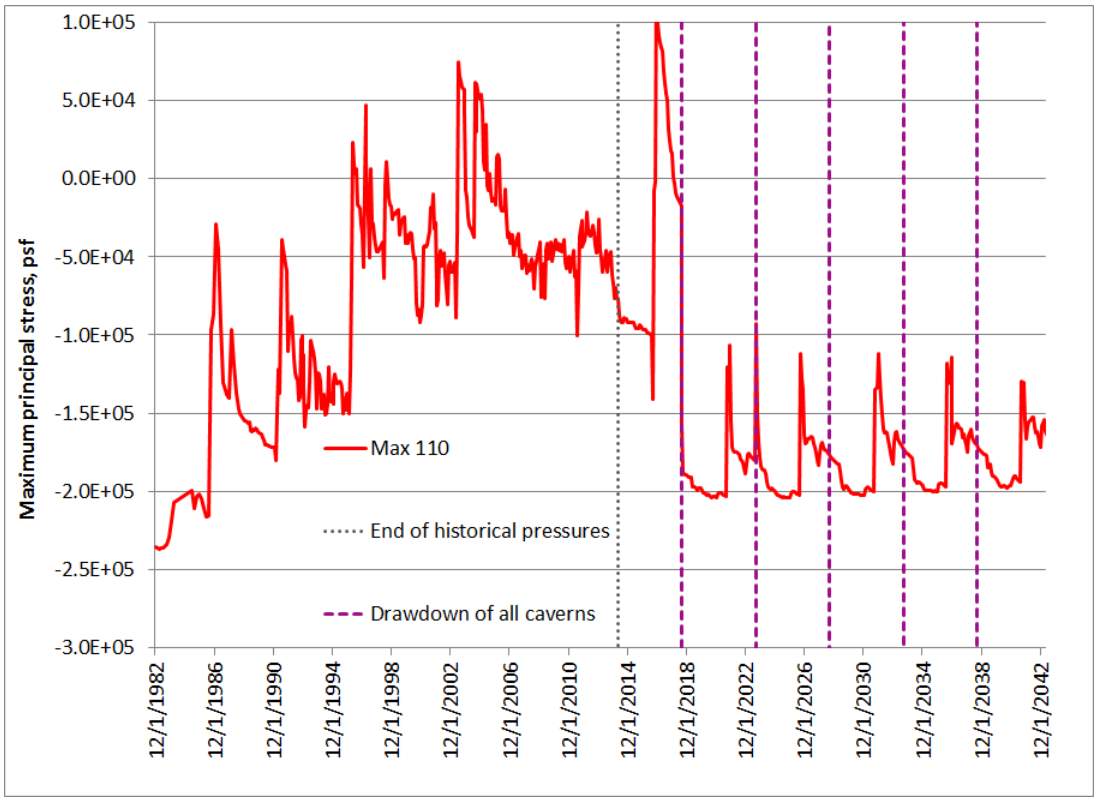

Figure 2.10-3. Maximum value of maximum principal stress surrounding WH-110.

Figure 2.10-4. Locations of minimum value of dilatant safety factor and maximum principal stress surrounding WH-110.

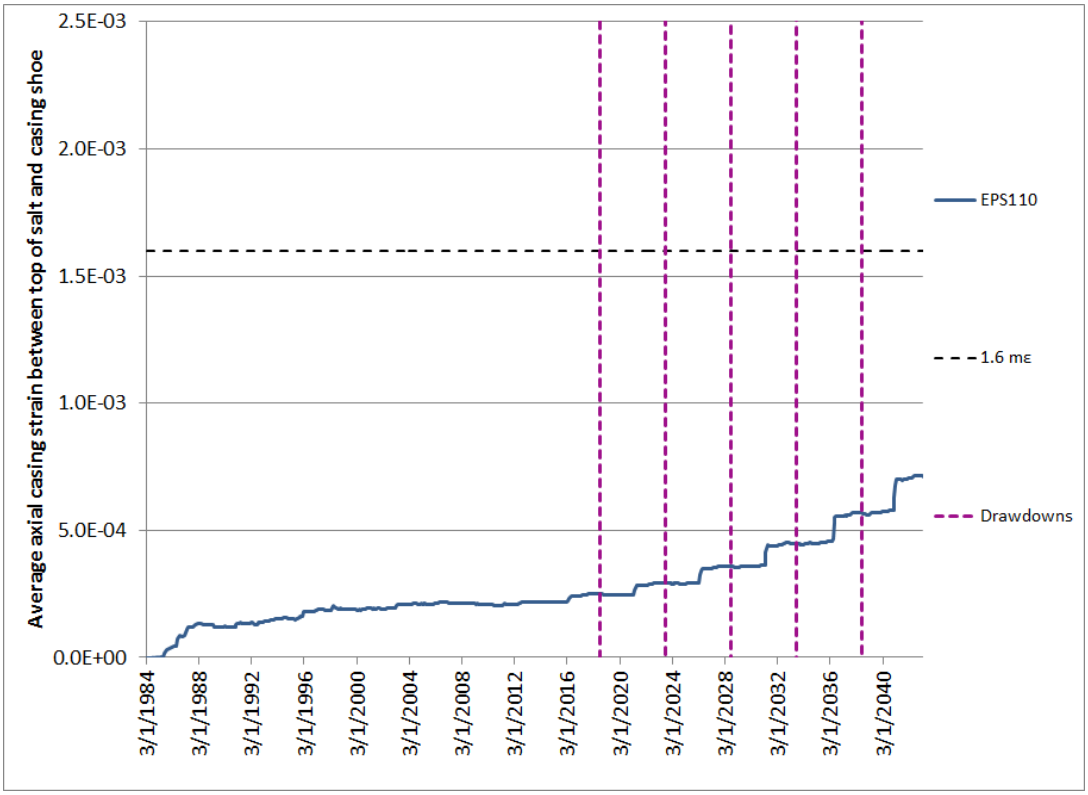

Figure 2.10-5. Predicted avg. axial casing strain between casing shoe and top of salt for WH-110.

As of July 2015, three salt falls have been recorded for WH-110 (Roberts et al., 2015). Salt falls are not unusual, even for otherwise mechanically-stable caverns, so this number of salt falls does not contradict the indications from the geomechanical calculations that WH-110 should be mechanically stable through five drawdowns. Therefore:

The updated estimate for WH-110 based on geomechanical analyses is that this cavern is stable through 5 drawdowns.

2.11 WH Cavern 111

WH Cavern 111 is a Phase 2 cavern surrounded by Phase 2 caverns. The previous best estimate for its number of available drawdowns was 5, based on P/D ratios with its nearby caverns. Table 2.11 summarizes the P/D and geomechanical estimates for available drawdowns for WH-111 in 2014. Figure 2.11-1 shows the volume of WH-111 in both its computational mesh geometry and its oldest available sonar geometry from 2006, and the geometries of the five drawdown layers built into the computational mesh. As is the case for all the Phase 2 caverns, the modeled drawdown layers extend for nearly the entire height of the cavern, and add approximately 15% to the volume of the cavern when they are removed.

Table 2.11. 2014 Estimates of available drawdowns, WH-111.

Cavern	Basis				2014 Best Estimate Basis (P/D or GM), Comments, Reference
	2D P/D < 1	3D P/D < 1	Geomechanics	Best Estimate	
WH111	5	5	5	5	P/D; Rudeen & Lord, 2013; Based on S&E, 2009b
					Nearest neighbors: 113 (SW), 110 (SE)

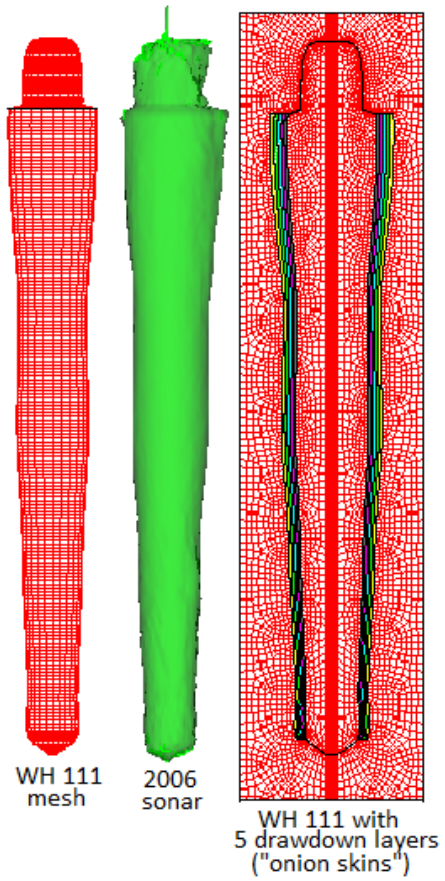

Figure 2.11-1. Computational mesh and sonar geometries for WH-111

Figure 2.11-2 plots the minimum value of dilatant damage factor, or safety factor, at any point around the cavern wall, as a function of time through five drawdowns. The lowest predicted value for the dilatant safety factor was 1.2, at the beginning of workovers before the first and after the fifth drawdown. This minimum value occurs at the floor of the cavern, which has the similar pattern of high dilatant stresses and reduced safety factors during workovers. Similarly low values occur near the corner of the cavern ceiling. As usual, these values occur during workovers; the geomechanical predictions indicate that at all other times there are no excessive dilatant stress values. Because the time and location of the low safety factor values are in the floor of the cavern, and only for a brief period coincident with a workover, these occurrences are not believed to be significant enough to cause microcracking in the salt of a magnitude that would affect cavern stability. This conclusion is substantiated in Figure 2.11-3, which plots the maximum value of maximum principal stress around WH-111. Positive values indicate tension, which if they occur would likely be in the same locations as the minimum dilatant safety factor values. The maximum stress never reaches a positive or tensile value through five drawdowns.

Figure 2.11-4 plots the predicted average axial casing strain between the casing and top of salt for WH-111. The overall average strain is predicted to exceed 1.6 millistrains after the third drawdown, although the region above the top of the cavern, including the casing shoe, is predicted to have experienced localized strains above 1.6 mε by 2015 (Sobolik, 2015). The strain rate increases slightly once drawdowns begin, but not in an alarming fashion. Because of salt creep, casing integrity is an expected operational issue independent of the number of drawdowns for a particular cavern; because there is no significant change in strain behavior resulting from the drawdowns, there is nothing to indicate additional concern for the mechanical stability of the cavern.

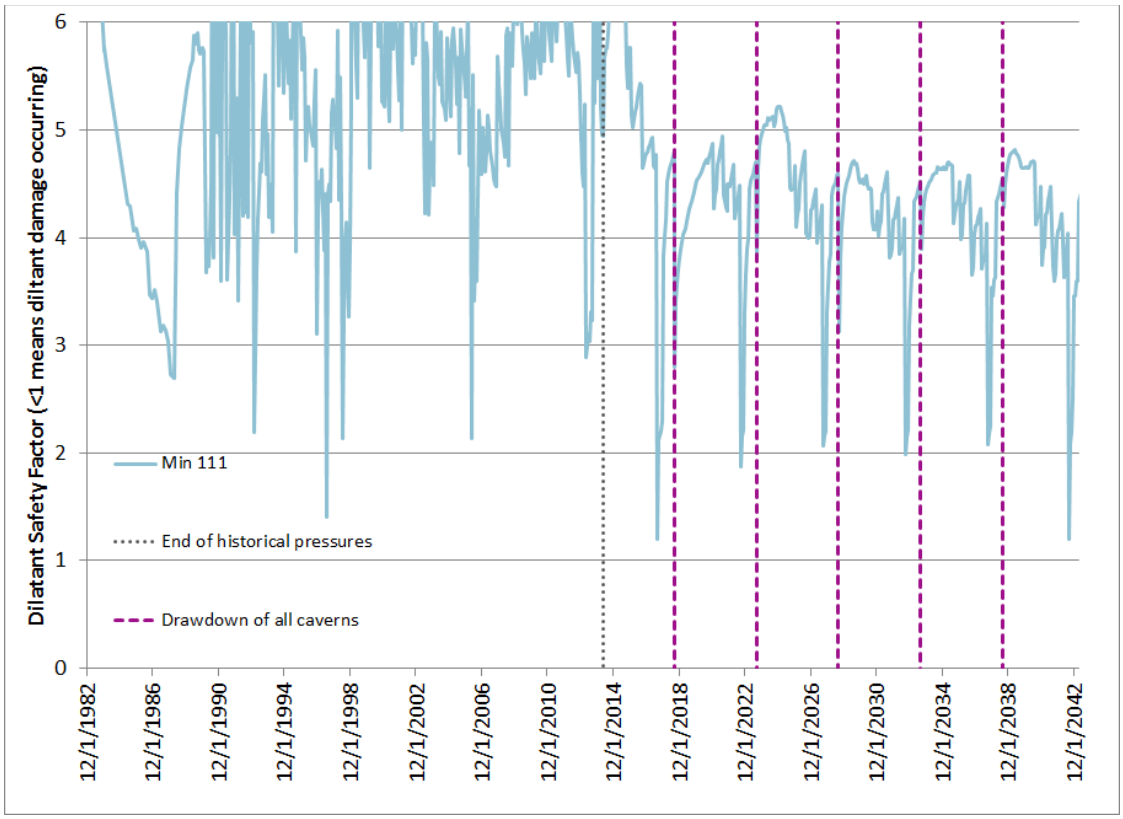

Figure 2.11-2. Minimum value of dilatant safety factor surrounding WH-111.

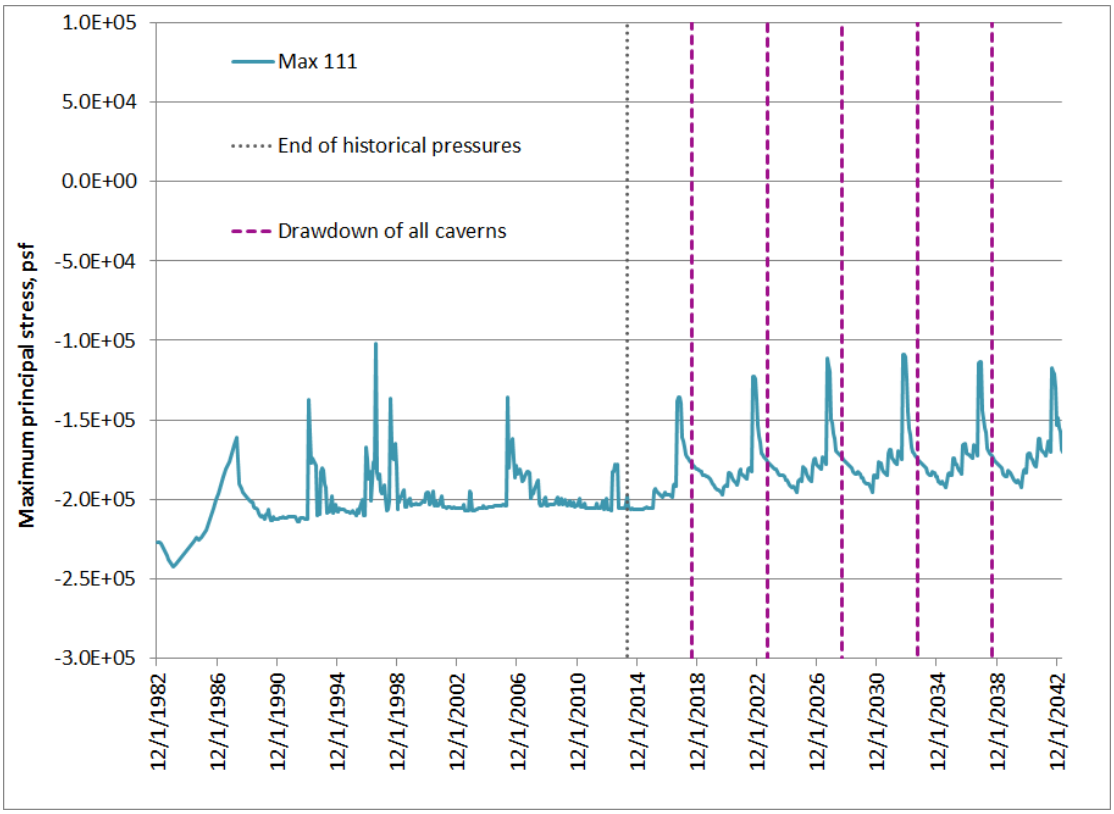

Figure 2.11-3. Maximum value of maximum principal stress surrounding WH-111.

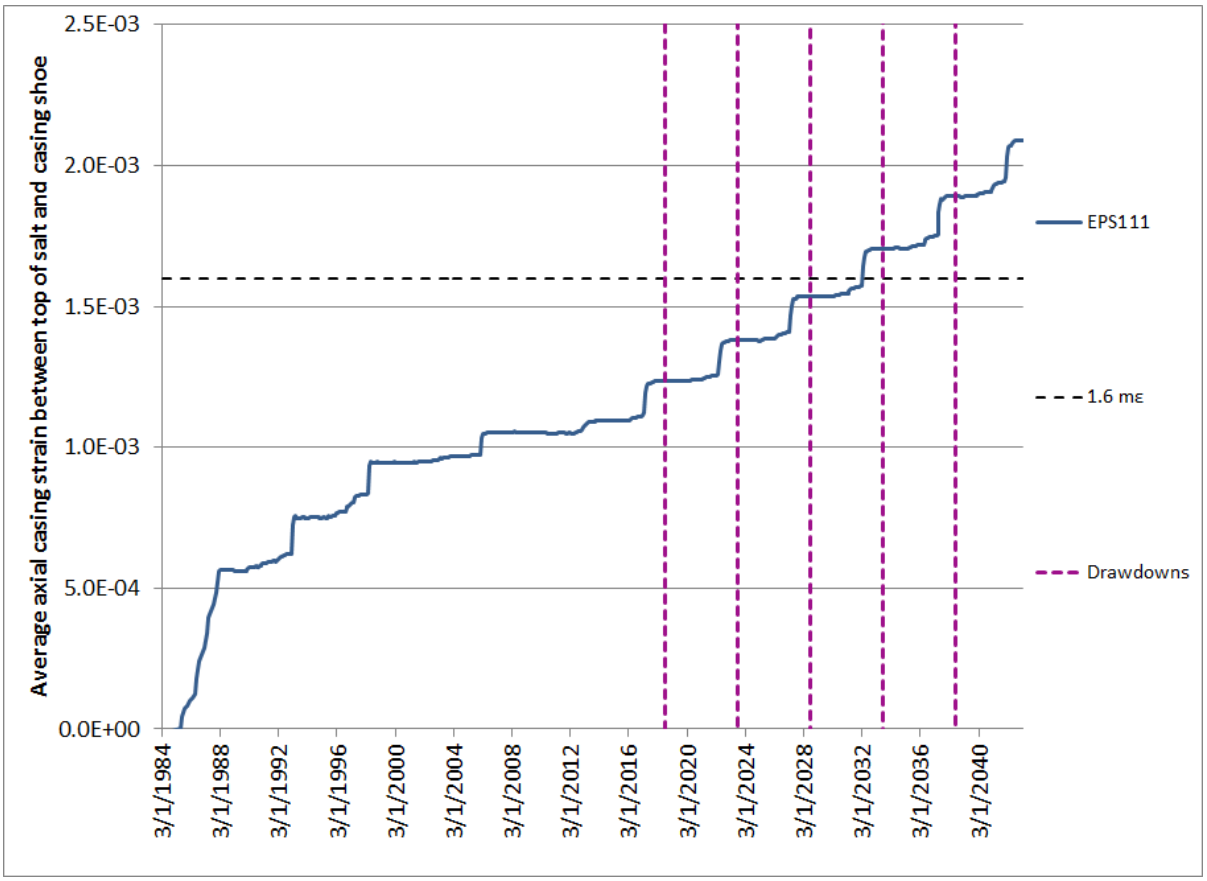

Figure 2.11-4. Predicted avg. axial casing strain between casing shoe and top of salt for WH-111.

As of July 2015, one salt fall has been recorded for WH-111 (Roberts et al., 2015). Salt falls are not unusual, even for otherwise mechanically-stable caverns, so this number of salt falls does not contradict the indications from the geomechanical calculations that WH-111 should be mechanically stable through five drawdowns. Therefore:

The updated estimate for WH-111 based on geomechanical analyses is that this cavern is stable through 5 drawdowns.

2.12 WH Cavern 112

WH Cavern 112 is a Phase 2 cavern surrounded by Phase 1 and 2 caverns. The previous best estimate for its number of available drawdowns was 5, based on P/D ratios with its nearby caverns. Table 2.12 summarizes the P/D and geomechanical estimates for available drawdowns for WH-112 in 2014. Figure 2.12-1 shows the volume of WH-112 in both its computational mesh geometry and its oldest available sonar geometry from 2000, and the geometries of the five drawdown layers built into the computational mesh. As is the case for all the Phase 2 caverns, the modeled drawdown layers extend for nearly the entire height of the cavern, and add approximately 15% to the volume of the cavern when they are removed.

Table 2.12. 2014 Estimates of available drawdowns, WH-112.

Cavern	Basis				2014 Best Estimate Basis (P/D or GM), Comments, Reference
	2D P/D < 1	3D P/D < 1	Geomechanics	Best Estimate	
WH112	4	4	5	4	P/D; Rudeen & Lord, 2013; Based on S&E, 2009b
					Nearest neighbors: 108 (SW), 11 (N)

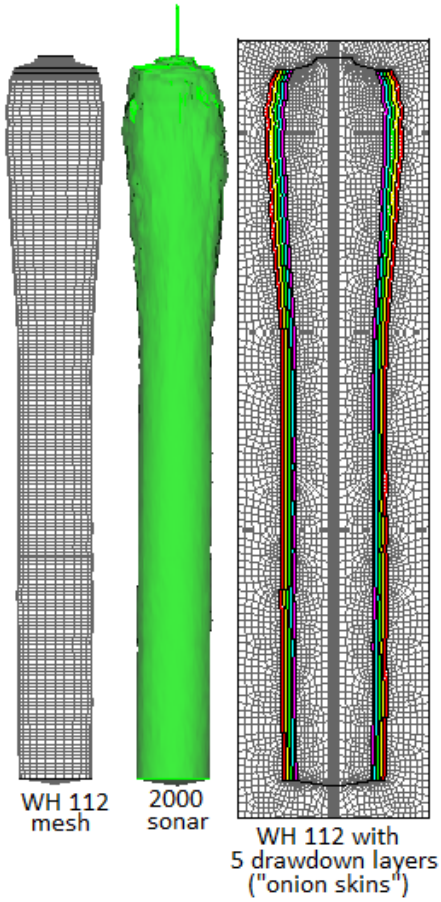

Figure 2.12-1. Computational mesh and sonar geometries for WH-112

Figure 2.12-2 plots the minimum value of dilatant damage factor, or safety factor, at any point around the cavern wall, as a function of time through five drawdowns. The lowest predicted value for the dilatant safety factor was 1.5, at the end of workovers before the first and after the fifth drawdown. This minimum value occurs at the floor of the cavern, which has the similar pattern of high dilatant stresses and reduced safety factors during workovers. Similarly low values occur near the corner of the cavern ceiling. As usual, these values occur during workovers; the geomechanical predictions indicate that at all other times there are no excessive dilatant stress values. Because the time and location of the low safety factor values are in the floor of the cavern, and only for a brief period coincident with a workover, these occurrences are not believed to be significant enough to cause microcracking in the salt of a magnitude that would affect cavern stability. This conclusion is substantiated in Figure 2.12-3, which plots the maximum value of maximum principal stress around WH-112. Positive values indicate tension, which if they occur would likely be in the same locations as the minimum dilatant safety factor values. The maximum stress never reaches a positive or tensile value through five drawdowns.

Figure 2.12-4 plots the predicted average axial casing strain between the casing and top of salt for WH-112. The overall average strain is predicted to exceed 1.6 millistrains after the first drawdown, although the region above the top of the cavern, including the casing shoe, is predicted to have experienced localized strains above 1.6 mε by 2015 (Sobolik, 2015). The strain rate increases slightly once drawdowns begin, but not in an alarming fashion. Because of salt creep, casing integrity is an expected operational issue independent of the number of drawdowns for a particular cavern; because there is no significant change in strain behavior resulting from the drawdowns, there is nothing to indicate additional concern for the mechanical stability of the cavern.

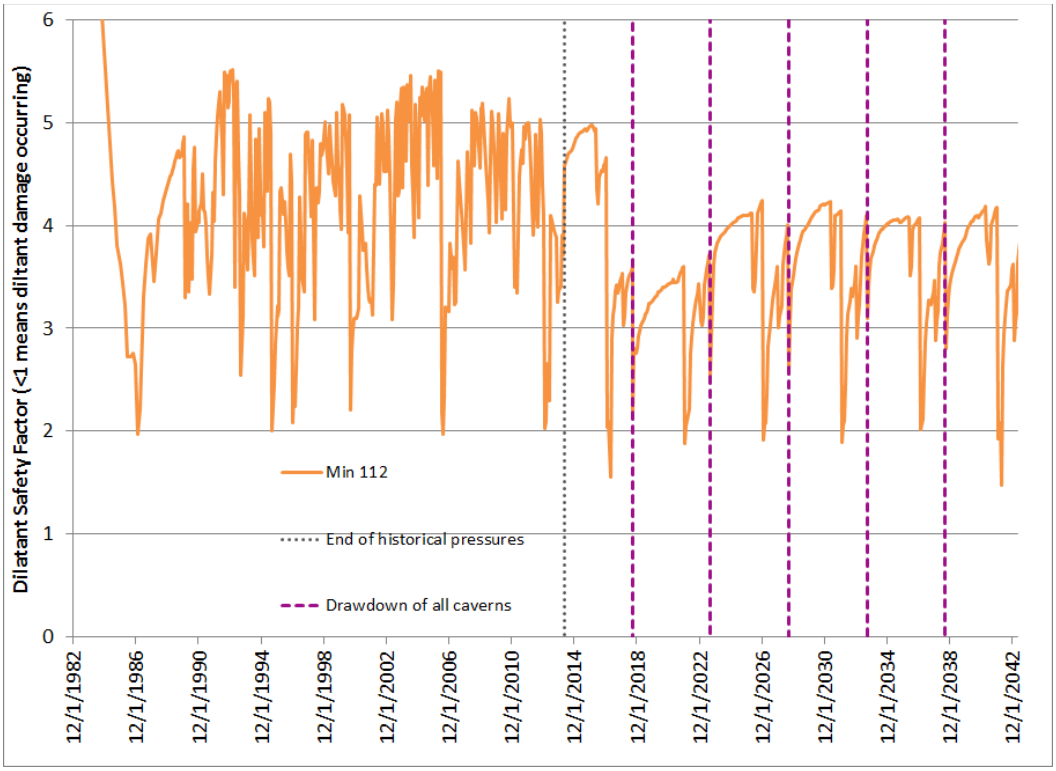

Figure 2.12-2. Minimum value of dilatant safety factor surrounding WH-112.

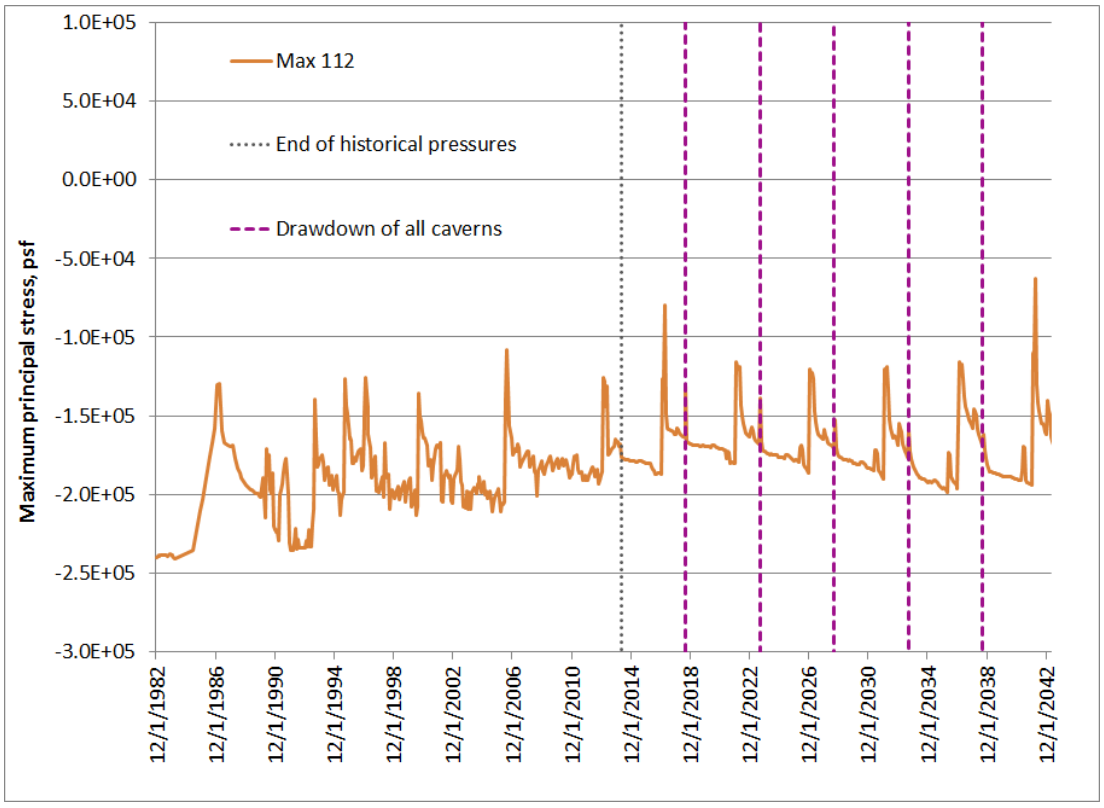

Figure 2.12-3. Maximum value of maximum principal stress surrounding WH-112.

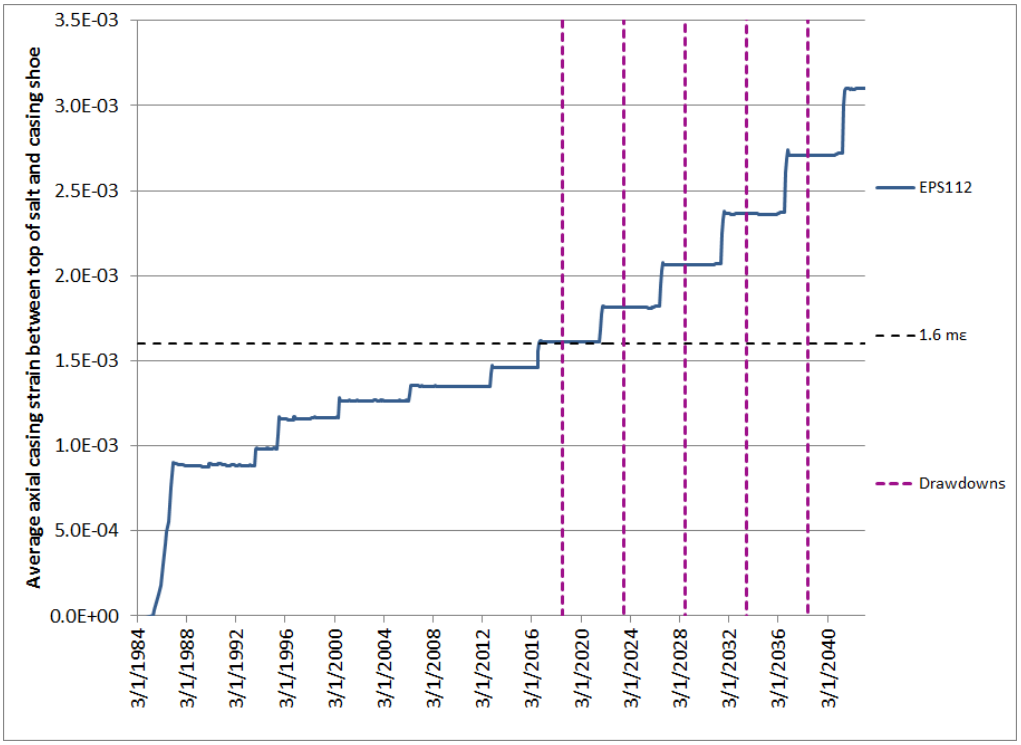

Figure 2.12-4. Predicted avg. axial casing strain between casing shoe and top of salt for WH-112.

As of July 2015, no salt falls have been recorded for WH-112 (Roberts et al., 2015). Salt falls are not unusual, even for otherwise mechanically-stable caverns, but a lack of salt falls supports the indications from the geomechanical calculations that WH-112 should be mechanically stable through five drawdowns. Therefore:

The updated estimate for WH-112 based on geomechanical analyses is that this cavern is stable through 5 drawdowns.

2.13 WH Cavern 113

WH Cavern 113 is a Phase 2 cavern surrounded by Phase 2 caverns. The previous best estimate for its number of available drawdowns was 4, based on P/D ratios with its nearby caverns. Table 2.13 summarizes the P/D and geomechanical estimates for available drawdowns for WH-113 in 2014. Figure 2.13-1 shows the volume of WH-113 in both its computational mesh geometry and its oldest available sonar geometry from 2000, and the geometries of the five drawdown layers built into the computational mesh. As is the case for all the Phase 2 caverns, the modeled drawdown layers extend for nearly the entire height of the cavern, and add approximately 15% to the volume of the cavern when they are removed.

Table 2.13. 2014 Estimates of available drawdowns, WH-113.

Cavern	Basis				2014 Best Estimate Basis (P/D or GM), Comments, Reference
	2D P/D < 1	3D P/D < 1	Geomechanics	Best Estimate	
WH113	4	4	5	4	P/D; Rudeen & Lord, 2013; Based on S&E, 2009b
					Nearest neighbors: 116 (SW), 114 (S), 111 (NE)

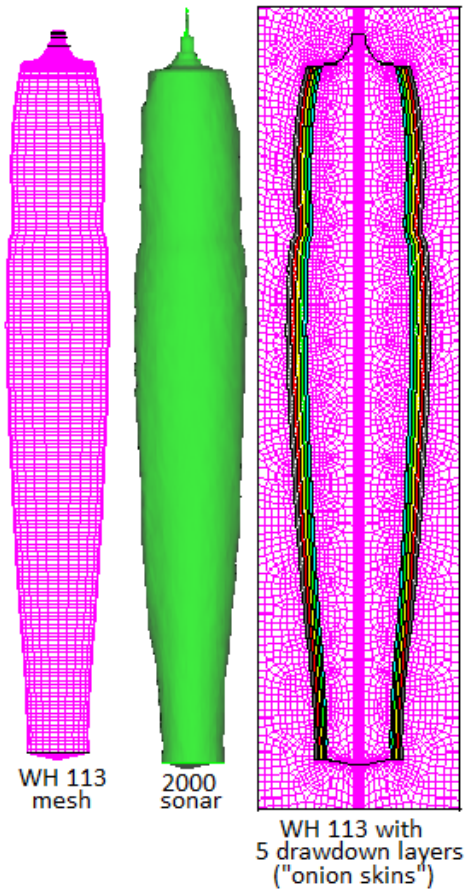

Figure 2.13-1. Computational mesh and sonar geometries for WH-113

Figure 2.13-2 plots the minimum value of dilatant damage factor, or safety factor, at any point around the cavern wall, as a function of time through five drawdowns. WH-113 has several instances when the minimum damage factor is below 1, all prior to the first drawdown. Similarly, the maximum value of maximum principal stress plotted in Figure 2.13-3 shows instances when tensile stress is recorded somewhere on the wall of the cavern. These results are curious, and require further investigation into the spatial extent of the extreme stress states. Figure 2.13-4 shows the locations of the minimum safety factor and maximum principal stress around WH-113. A close examination reveals that the extreme stress states occur at the edge of the floor of the cavern, where there is a sharp corner in the mesh. The mesh geometry at this location is likely creating an artificially high stress concentration that exaggerates the stress at the bottom of the cavern. These occurrences are not believed to be significant enough to cause microcracking in the salt of a magnitude that would affect cavern stability.

Figure 2.13-5 plots the predicted average axial casing strain between the casing and top of salt for WH-113. The overall average strain is predicted to never exceed 1.6 millistrains even after five drawdowns, although the region above the top of the cavern, including the casing shoe, is predicted to have experienced localized strains above 1.6 mε by 2015 (Sobolik, 2015). The strain rate increases slightly once drawdowns begin, but not in an alarming fashion. Because of salt creep, casing integrity is an expected operational issue independent of the number of drawdowns for a particular cavern; because there is no significant change in strain behavior resulting from the drawdowns, there is nothing to indicate additional concern for the mechanical stability of the cavern.

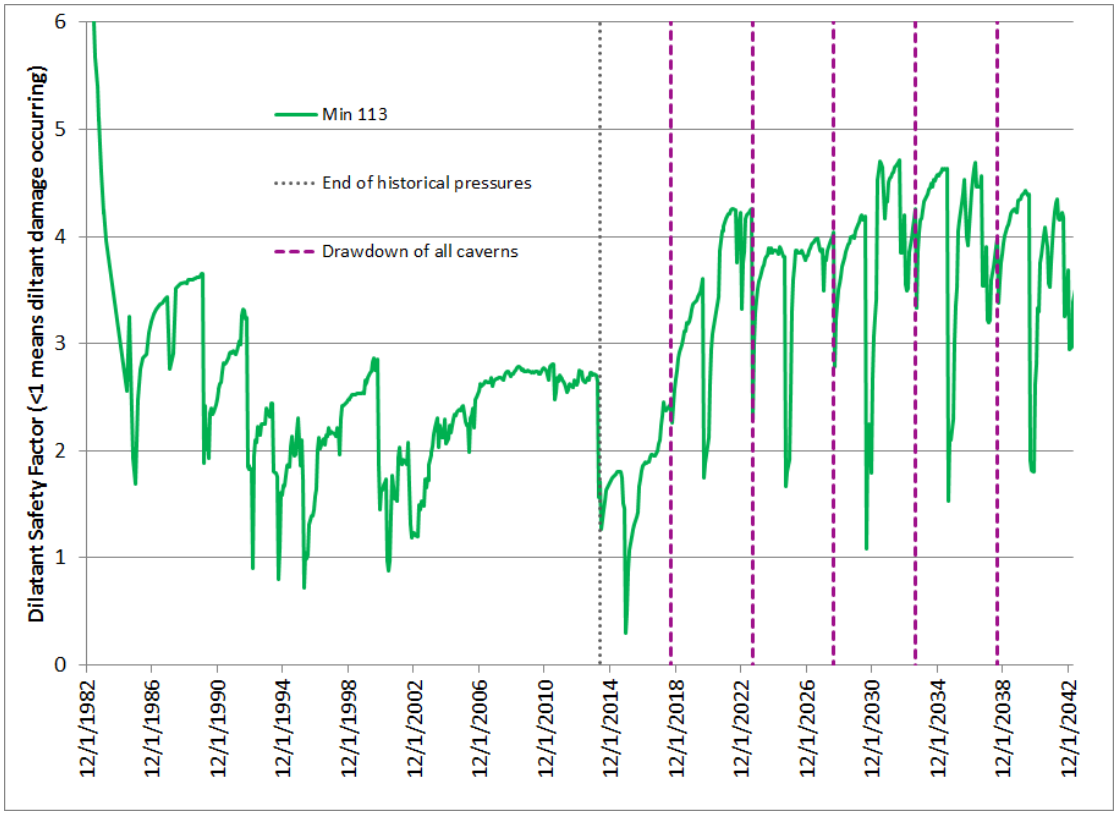

Figure 2.13-2. Minimum value of dilatant safety factor surrounding WH-113.

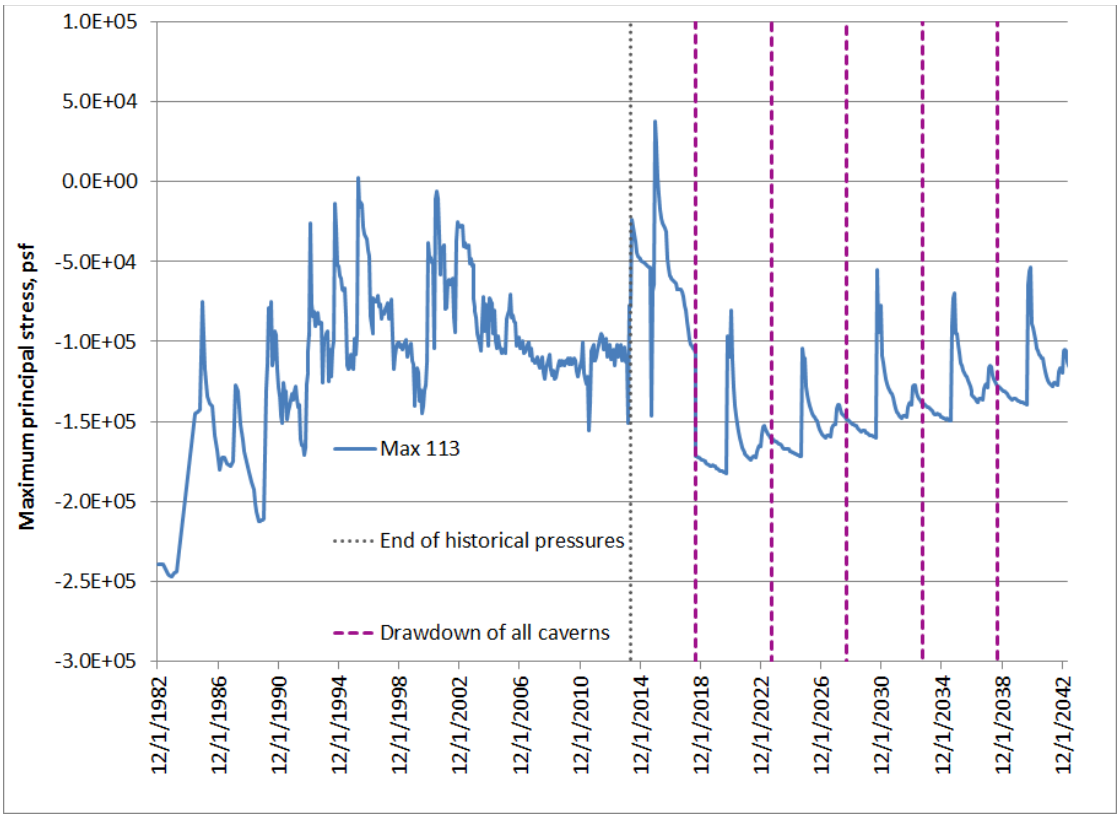

Figure 2.13-3. Maximum value of maximum principal stress surrounding WH-113.

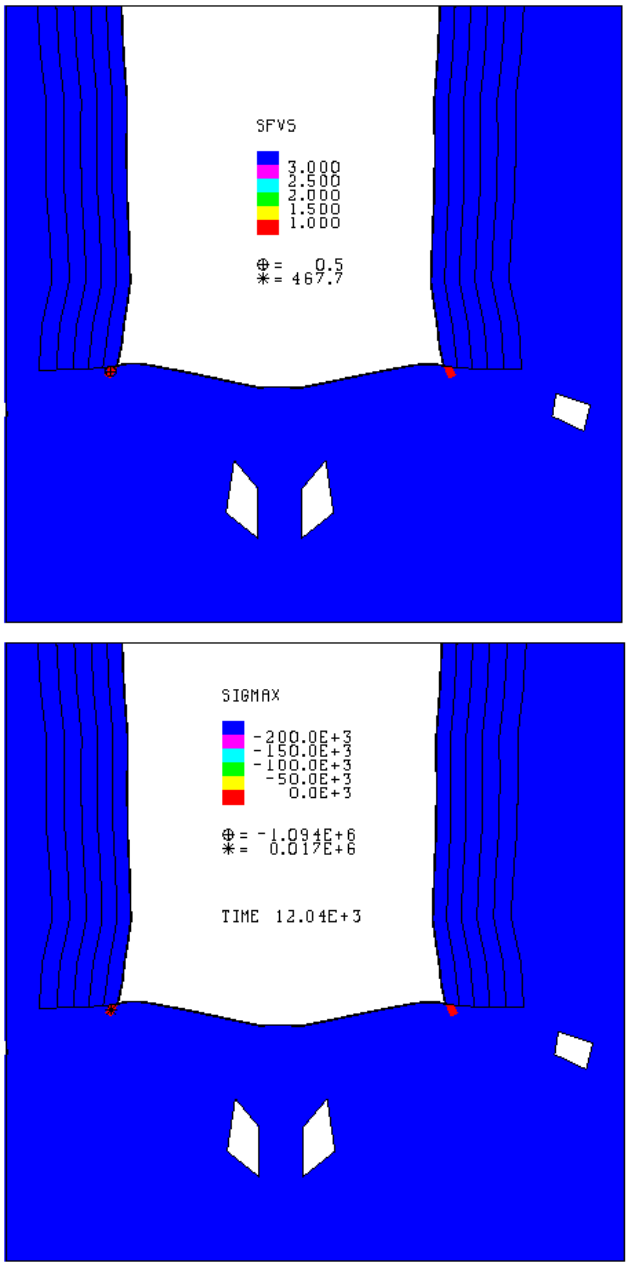

Figure 2.13-4. Locations of minimum value of dilatant safety factor and maximum principal stress at the floor of WH-113.

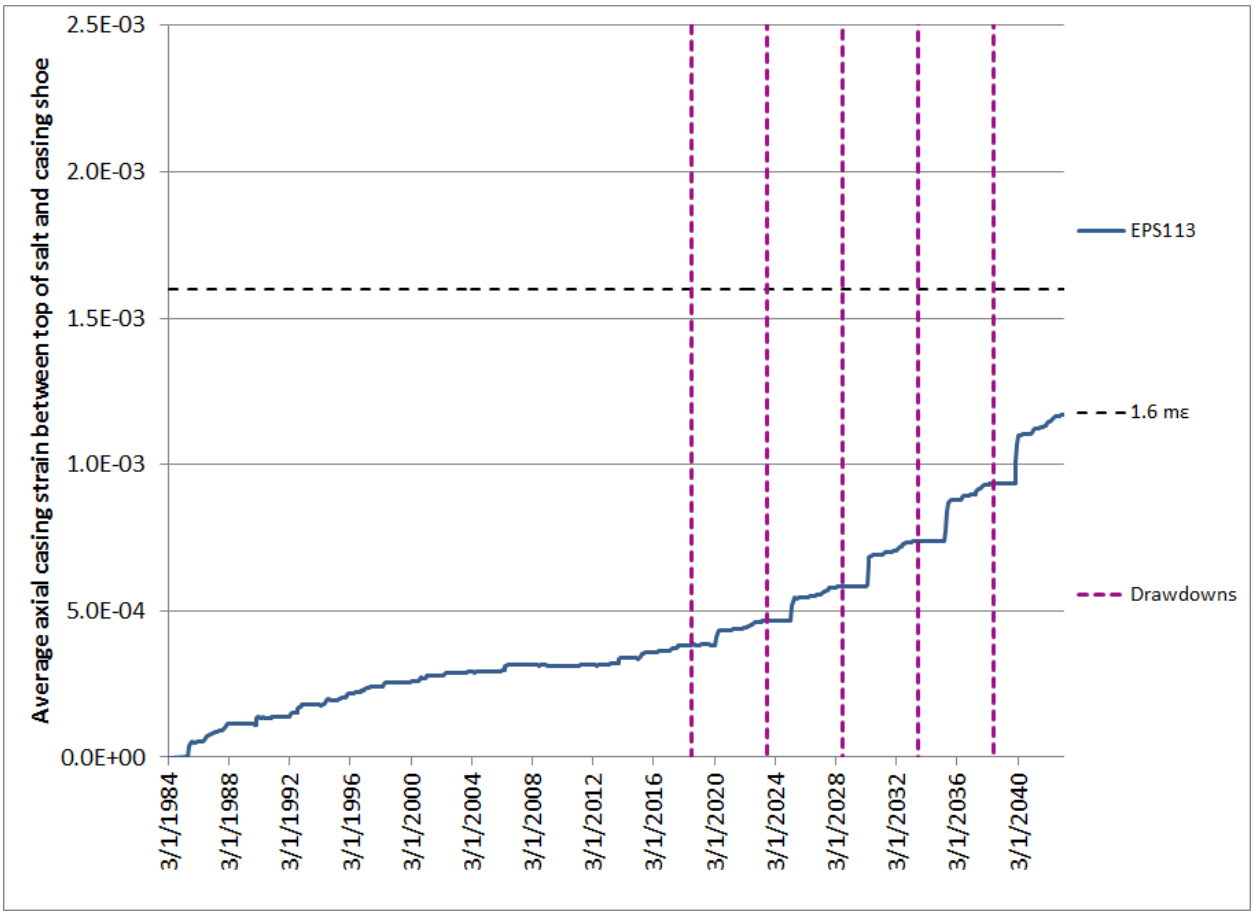

Figure 2.13-5. Predicted avg. axial casing strain between casing shoe and top of salt for WH-113.

As of July 2015, three salt falls have been recorded for WH-113 (Roberts et al., 2015). Salt falls are not unusual, even for otherwise mechanically-stable caverns, so this number of salt falls does not contradict the indications from the geomechanical calculations that WH-113 should be mechanically stable through five drawdowns. Therefore:

The updated estimate for WH-113 based on geomechanical analyses is that this cavern is stable through 5 drawdowns.

2.14 WH Cavern 114

WH Cavern 114 is a Phase 2 cavern surrounded by Phase 2 caverns. The previous best estimate for its number of available drawdowns was 4, based on P/D ratios with its nearby caverns. Table 2.14 summarizes the P/D and geomechanical estimates for available drawdowns for WH-114 in 2014. Figure 2.14-1 shows the volume of WH-114 in both its computational mesh geometry and its oldest available sonar geometry from 2000, and the geometries of the five drawdown layers built into the computational mesh. As is the case for all the Phase 2 caverns, the modeled drawdown layers extend for nearly the entire height of the cavern, and add approximately 15% to the volume of the cavern when they are removed.

Table 2.14. 2014 Estimates of available drawdowns, WH-114.

Cavern	Basis				2014 Best Estimate Basis (P/D or GM), Comments, Reference
	2D P/D < 1	3D P/D < 1	Geomechanics	Best Estimate	
WH114	4	4	5	4	P/D; Rudeen & Lord, 2013; Based on S&E, 2009b
					Nearest neighbors: 116 (W), 113 (N), 115 (E)

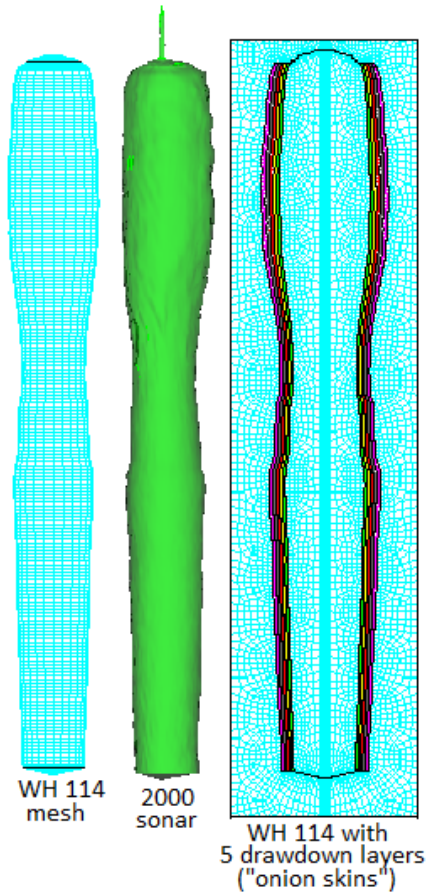

Figure 2.14-1. Computational mesh and sonar geometries for WH-114

Figure 2.14-2 plots the minimum value of dilatant damage factor, or safety factor, at any point around the cavern wall, as a function of time through five drawdowns. The lowest predicted value for the dilatant safety factor was 1.06, at the end of a workover before the first drawdown. This minimum value occurs at the floor of the cavern, which has the similar pattern of high dilatant stresses and reduced safety factors during workovers. Similarly low values occur near the corner of the cavern ceiling. As usual, these values occur during workovers; the geomechanical predictions indicate that at all other times there are no excessive dilatant stress values. Because the time and location of the low safety factor values are in the floor of the cavern, and only for a brief period coincident with a workover, these occurrences are not believed to be significant enough to cause microcracking in the salt of a magnitude that would affect cavern stability. This conclusion is substantiated in Figure 2.14-3, which plots the maximum value of maximum principal stress around WH-114. Positive values indicate tension, which if they occur would likely be in the same locations as the minimum dilatant safety factor values. The maximum stress never reaches a positive or tensile value through five drawdowns.

Figure 2.14-4 plots the predicted average axial casing strain between the casing and top of salt for WH-114. The overall average strain is predicted to never exceed 1.6 millistrains even after five drawdowns, although the region above the top of the cavern, including the casing shoe, is predicted to have experienced localized strains above 1.6 mε by 2015 (Sobolik, 2015). The strain rate increases slightly once drawdowns begin, but not in an alarming fashion. Because of salt creep, casing integrity is an expected operational issue independent of the number of drawdowns for a particular cavern; because there is no significant change in strain behavior resulting from the drawdowns, there is nothing to indicate additional concern for the mechanical stability of the cavern.

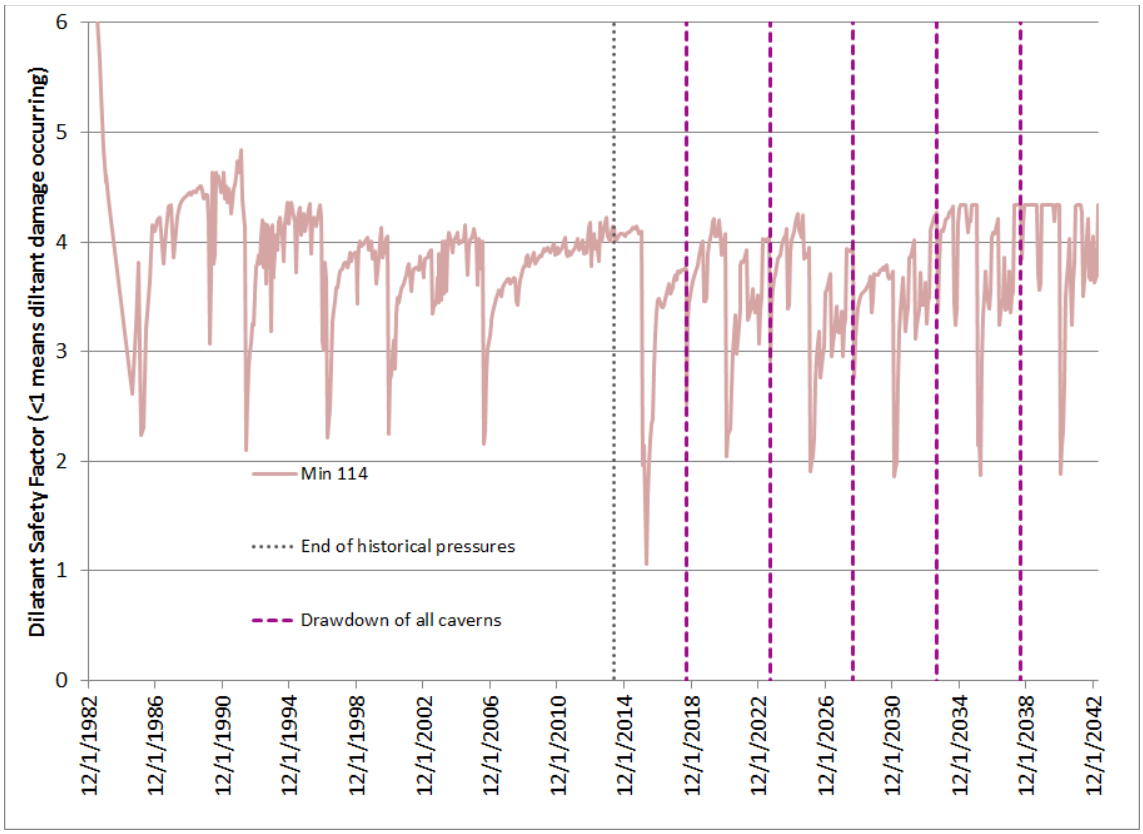

Figure 2.14-2. Minimum value of dilatant safety factor surrounding WH-114.

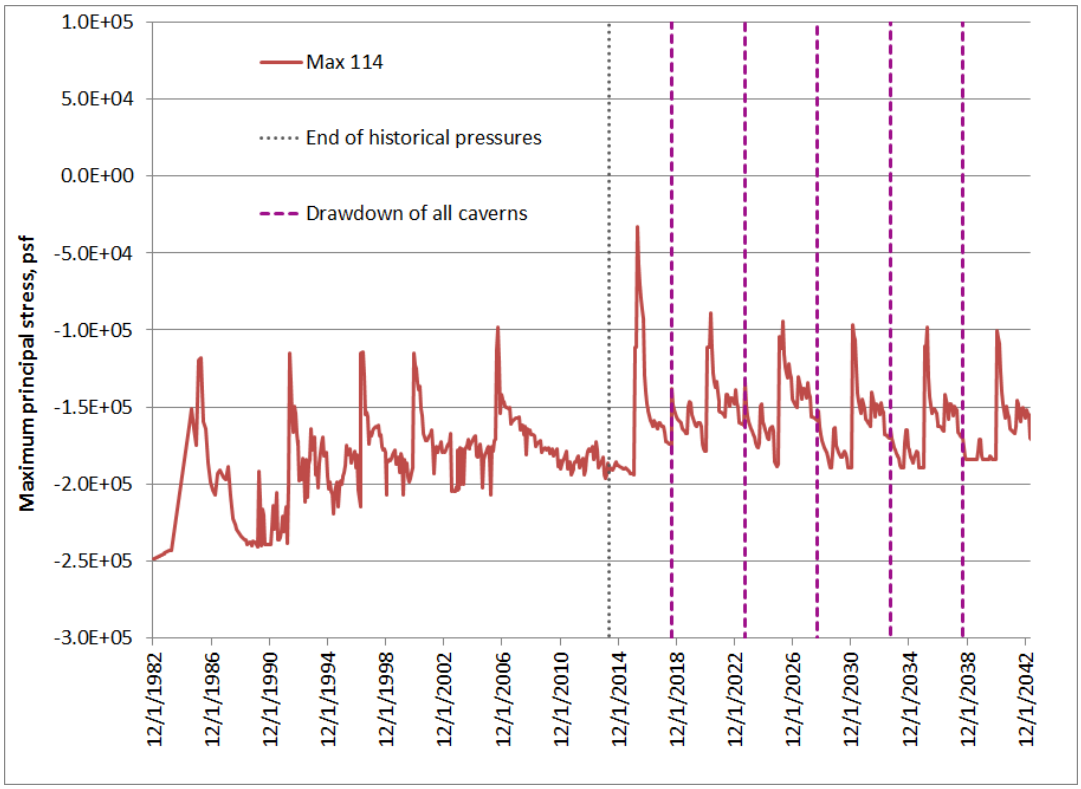

Figure 2.14-3. Maximum value of maximum principal stress surrounding WH-114.

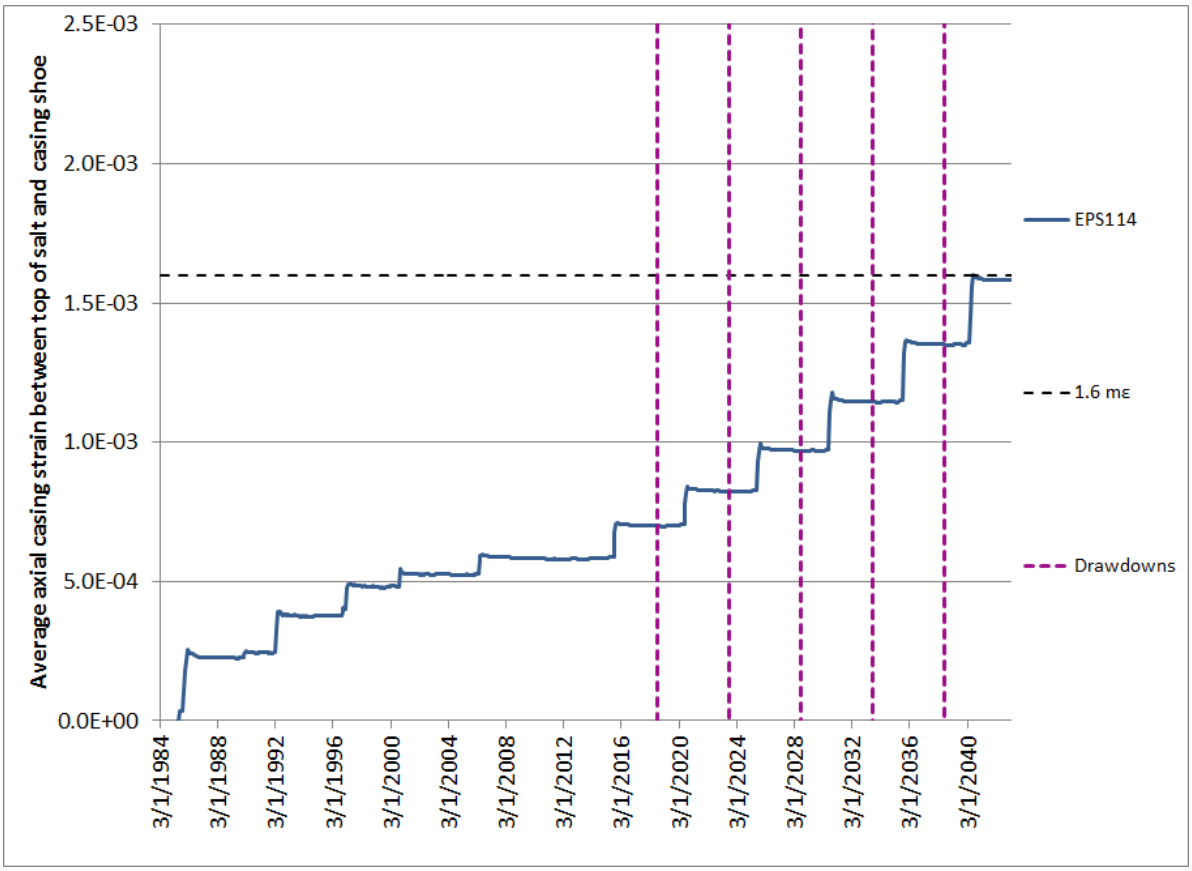

Figure 2.14-4. Predicted avg. axial casing strain between casing shoe and top of salt for WH-114.

As of July 2015, two salt falls have been recorded for WH-114 (Roberts et al., 2015). Salt falls are not unusual, even for otherwise mechanically-stable caverns, so this number of salt falls does not contradict the indications from the geomechanical calculations that WH-114 should be mechanically stable through five drawdowns. Therefore:

The updated estimate for WH-114 based on geomechanical analyses is that this cavern is stable through 5 drawdowns.

2.15 WH Cavern 115

WH Cavern 115 is a Phase 2 cavern surrounded by Phase 2 caverns. The previous best estimate for its number of available drawdowns was 5, based on P/D ratios with its nearby caverns. Table 2.15 summarizes the P/D and geomechanical estimates for available drawdowns for WH-115 in 2014. Figure 2.15-1 shows the volume of WH-115 in both its computational mesh geometry and its oldest available sonar geometry from 2006, and the geometries of the five drawdown layers built into the computational mesh. As is the case for all the Phase 2 caverns, the modeled drawdown layers extend for nearly the entire height of the cavern, and add approximately 15% to the volume of the cavern when they are removed.

Table 2.15. 2014 Estimates of available drawdowns, WH-115.

Cavern	Basis				2014 Best Estimate Basis (P/D or GM), Comments, Reference
	2D P/D < 1	3D P/D < 1	Geomechanics	Best Estimate	
WH115	4	5	5	5	P/D; Rudeen & Lord, 2013; Based on S&E, 2009b
					Nearest neighbors: 114 (W), 113 (NW), 111 (N), 110 (NE), 109 (SE), 107 (S)

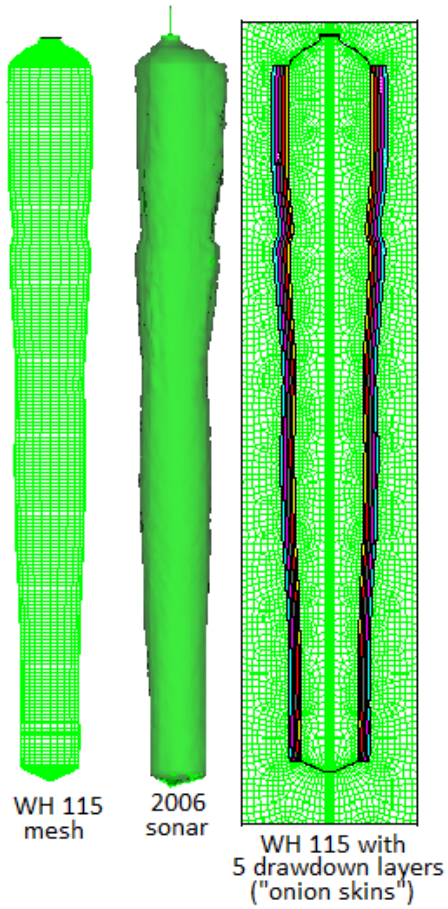

Figure 2.15-1. Computational mesh and sonar geometries for WH-115

Figure 2.15-2 plots the minimum value of dilatant damage factor, or safety factor, at any point around the cavern wall, as a function of time through five drawdowns. The lowest predicted value for the dilatant safety factor was 1.51, very early in its operational life; after this time, the minimum safety factor only barely reaches occasional values under 2.0. This minimum value occurs at the floor of the cavern, which has the similar pattern of high dilatant stresses and reduced safety factors during workovers. Similarly low values occur near the corner of the cavern ceiling. As usual, these values occur during workovers; the geomechanical predictions indicate that at all other times there are no excessive dilatant stress values. Because the time and location of the low safety factor values are in the floor of the cavern, and only for a brief period coincident with a workover, these occurrences are not believed to be significant enough to cause microcracking in the salt of a magnitude that would affect cavern stability. This conclusion is substantiated in Figure 2.15-3, which plots the maximum value of maximum principal stress around WH-115. Positive values indicate tension, which if they occur would likely be in the same locations as the minimum dilatant safety factor values. The maximum stress never reaches a positive or tensile value through five drawdowns.

Figure 2.15-4 plots the predicted average axial casing strain between the casing and top of salt for WH-115. The overall average strain is predicted to never exceed 1.6 millistrains even after five drawdowns, although the region above the top of the cavern, including the casing shoe, is predicted to have experienced localized strains above 1.6 mε by 2015 (Sobolik, 2015). The strain rate increases slightly once drawdowns begin, but not in an alarming fashion. Because of salt creep, casing integrity is an expected operational issue independent of the number of drawdowns for a particular cavern; because there is no significant change in strain behavior resulting from the drawdowns, there is nothing to indicate additional concern for the mechanical stability of the cavern.

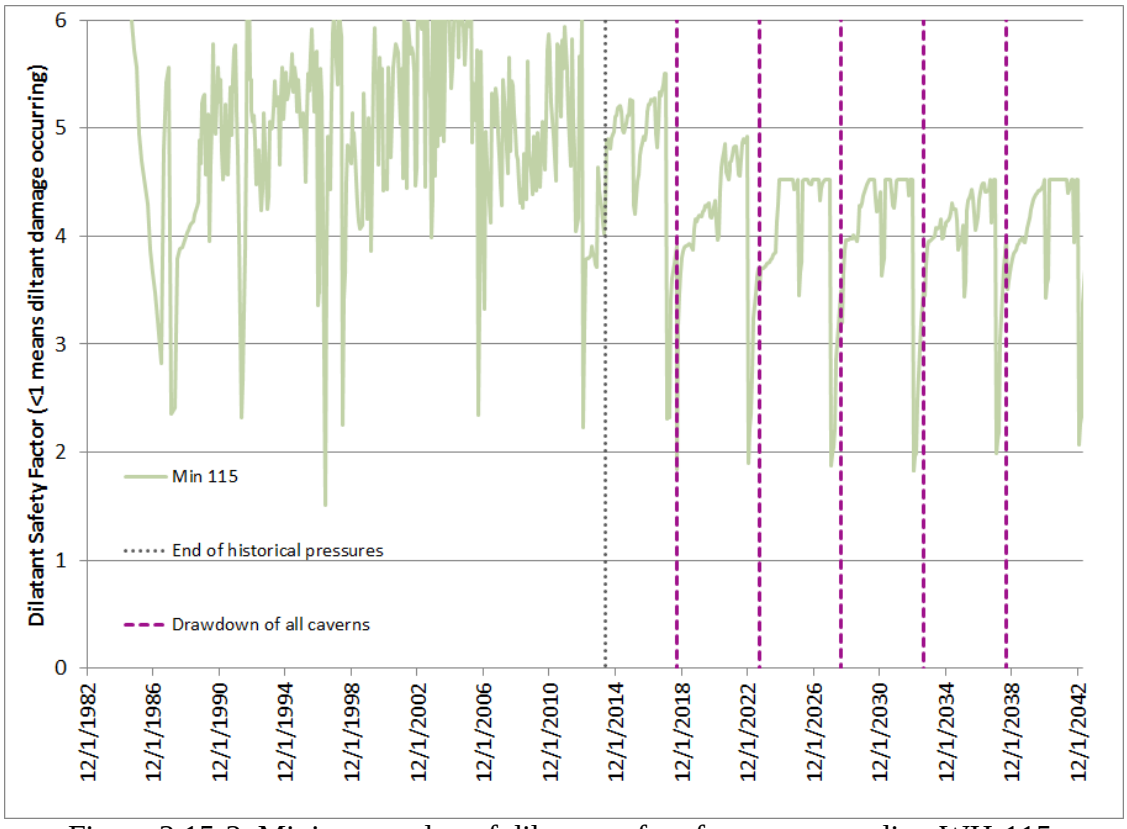

Figure 2.15-2. Minimum value of dilatant safety factor surrounding WH-115.

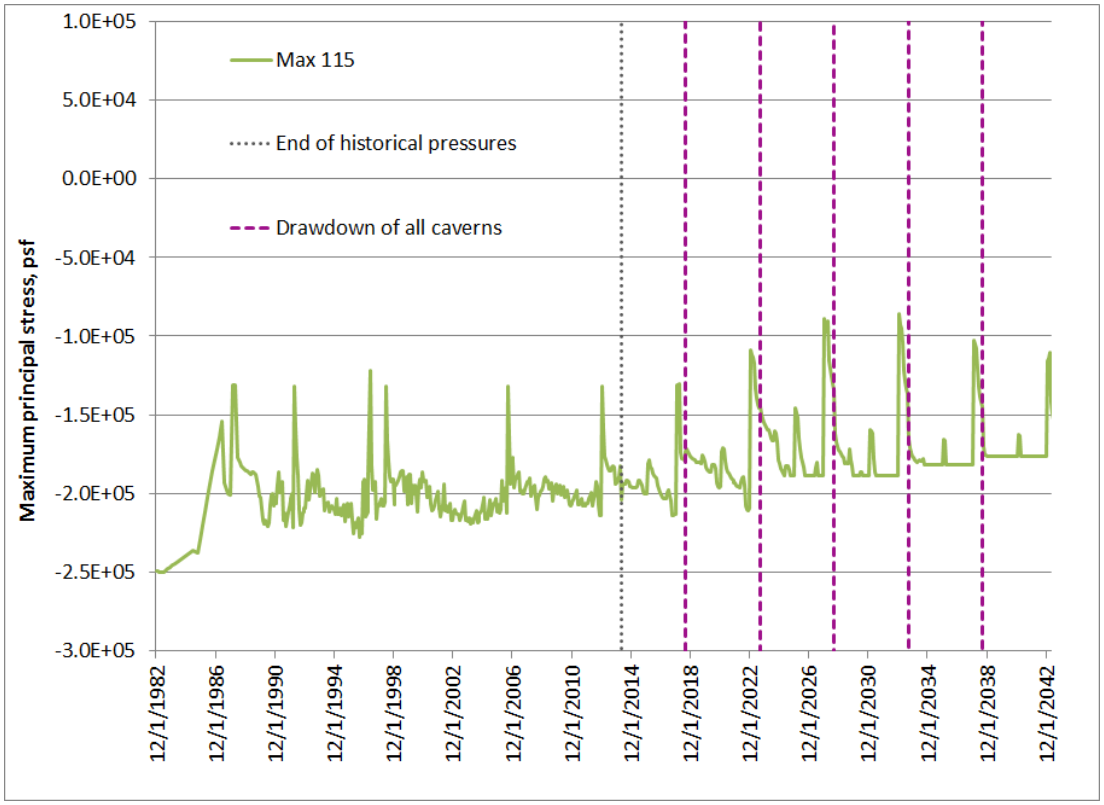

Figure 2.15-3. Maximum value of maximum principal stress surrounding WH-115.

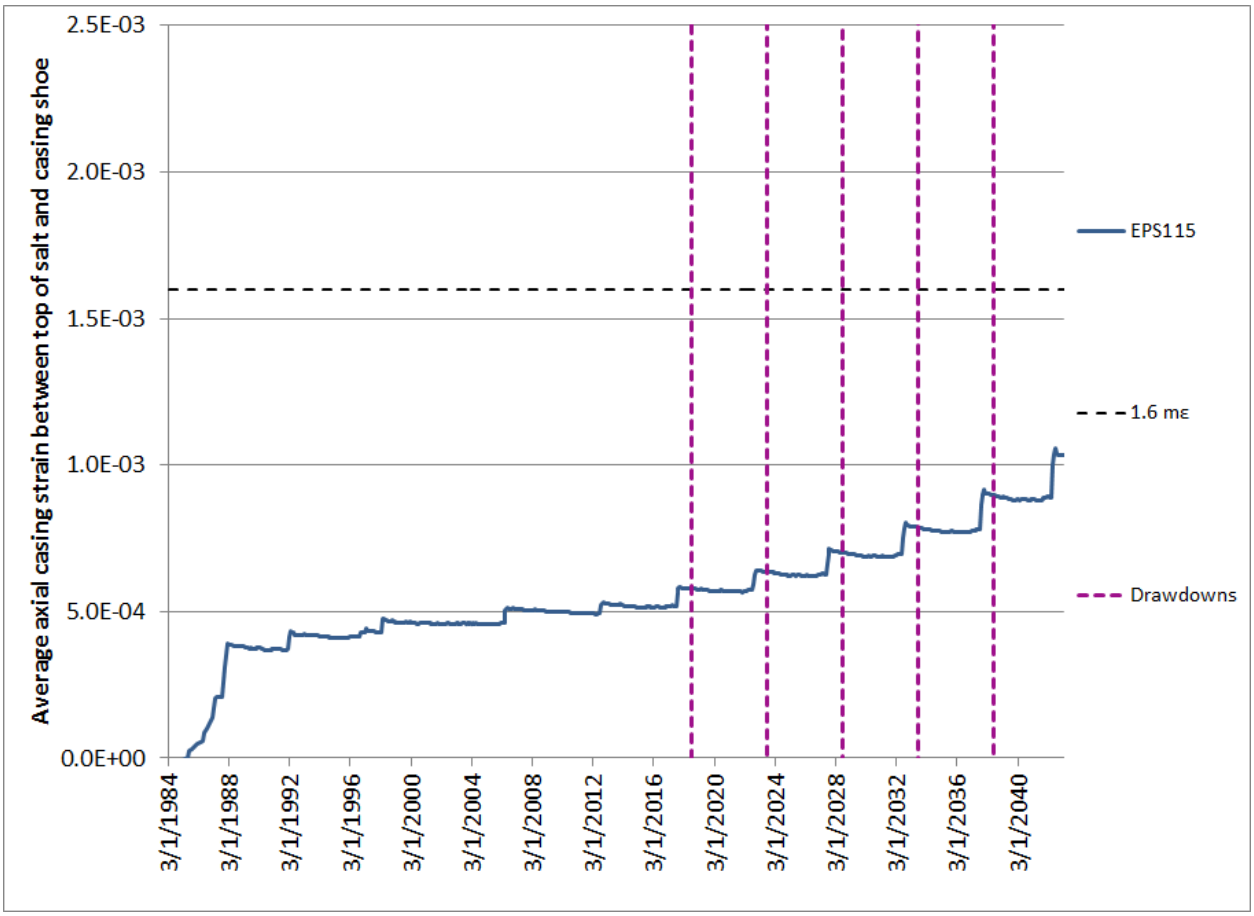

Figure 2.15-4. Predicted avg. axial casing strain between casing shoe and top of salt for WH-115.

As of July 2015, no salt falls have been recorded for WH-115 (Roberts et al., 2015). Salt falls are not unusual, even for otherwise mechanically-stable caverns, but a lack of salt falls supports the indications from the geomechanical calculations that WH-115 should be mechanically stable through five drawdowns. Therefore:

The updated estimate for WH-115 based on geomechanical analyses is that this cavern is stable through 5 drawdowns.

2.16 WH Cavern 116

WH Cavern 116 is a Phase 2 cavern surrounded by Phase 2 caverns. The previous best estimate for its number of available drawdowns was 5, based on P/D ratios with its nearby caverns. Table 2.16 summarizes the P/D and geomechanical estimates for available drawdowns for WH-116 in 2014. Figure 2.16-1 shows the volume of WH-116 in both its computational mesh geometry and its oldest available sonar geometry from 2000, and the geometries of the five drawdown layers built into the computational mesh. As is the case for all the Phase 2 caverns, the modeled drawdown layers extend for nearly the entire height of the cavern, and add approximately 15% to the volume of the cavern when they are removed.

Table 2.16. 2014 Estimates of available drawdowns, WH-116.

Cavern	Basis				2014 Best Estimate Basis (P/D or GM), Comments, Reference
	2D P/D < 1	3D P/D < 1	Geomechanics	Best Estimate	
WH116	4	5	5	5	P/D; Rudeen & Lord, 2013; Based on S&E, 2009b
					Nearest neighbors: 114 (W), 113 (NW), 111 (N), 110 (NE), 109 (SE), 107 (S)

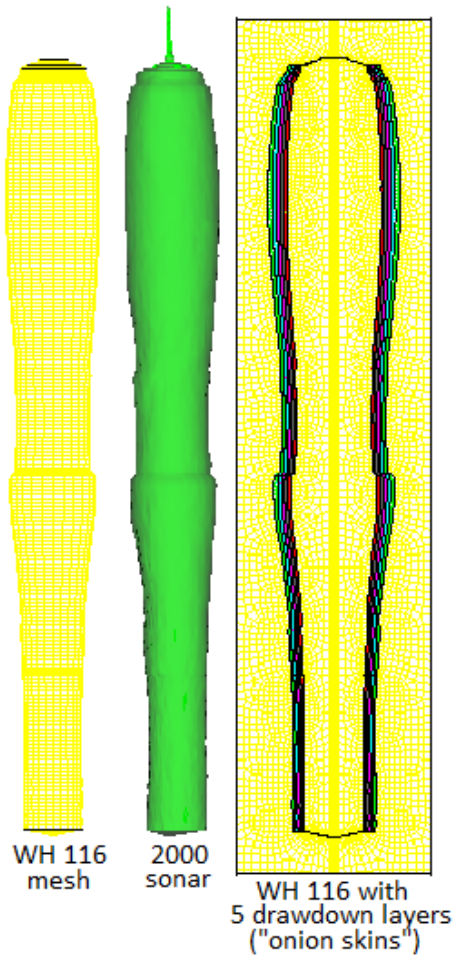

Figure 2.16-1. Computational mesh and sonar geometries for WH-116

Figure 2.16-2 plots the minimum value of dilatant damage factor, or safety factor, at any point around the cavern wall, as a function of time through five drawdowns. The lowest predicted value for the dilatant safety factor was 0.73, immediately after the first drawdown. The geomechanical analyses model the removal of material from the cavern wall as happening instantaneously; this is a more severe perturbation than what occurs in reality, the gradual dissolution of salt from fresh water. Therefore, although some stress perturbation is expected during a normal drawdown procedure, the magnitude if the stress differential as shown in Figure 2.16-2 is considered to be unrealistically extreme. The minimum value of safety factor occurs at the floor of the cavern, which has the similar pattern of high dilatant stresses and reduced safety factors during workovers. As usual, the more typical low peak values occur during workovers; the geomechanical predictions indicate that at all other times there are no excessive dilatant stress values. Because the time and location of the low safety factor values are in the floor of the cavern, and only for a brief period coincident with a workover, these occurrences are not believed to be significant enough to cause microcracking in the salt of a magnitude that would affect cavern stability. This conclusion is substantiated in Figure 2.16-3, which plots the maximum value of maximum principal stress around WH-116. Positive values indicate tension, which if they occur would likely be in the same locations as the minimum dilatant safety factor values. With the exception of the unusual peak value at the first drawdown, the maximum stress never reaches a positive or tensile value through five drawdowns.

Figure 2.16-4 plots the predicted average axial casing strain between the casing and top of salt for WH-116. The overall average strain is predicted to exceed 1.6 millistrains prior to the fourth drawdown, although the region above the top of the cavern, including the casing shoe, is predicted to have experienced localized strains above 1.6 mε by 2015 (Sobolik, 2015). The strain rate increases slightly once drawdowns begin, but not in an alarming fashion. Because of salt creep, casing integrity is an expected operational issue independent of the number of drawdowns for a particular cavern; because there is no significant change in strain behavior resulting from the drawdowns, there is nothing to indicate additional concern for the mechanical stability of the cavern.

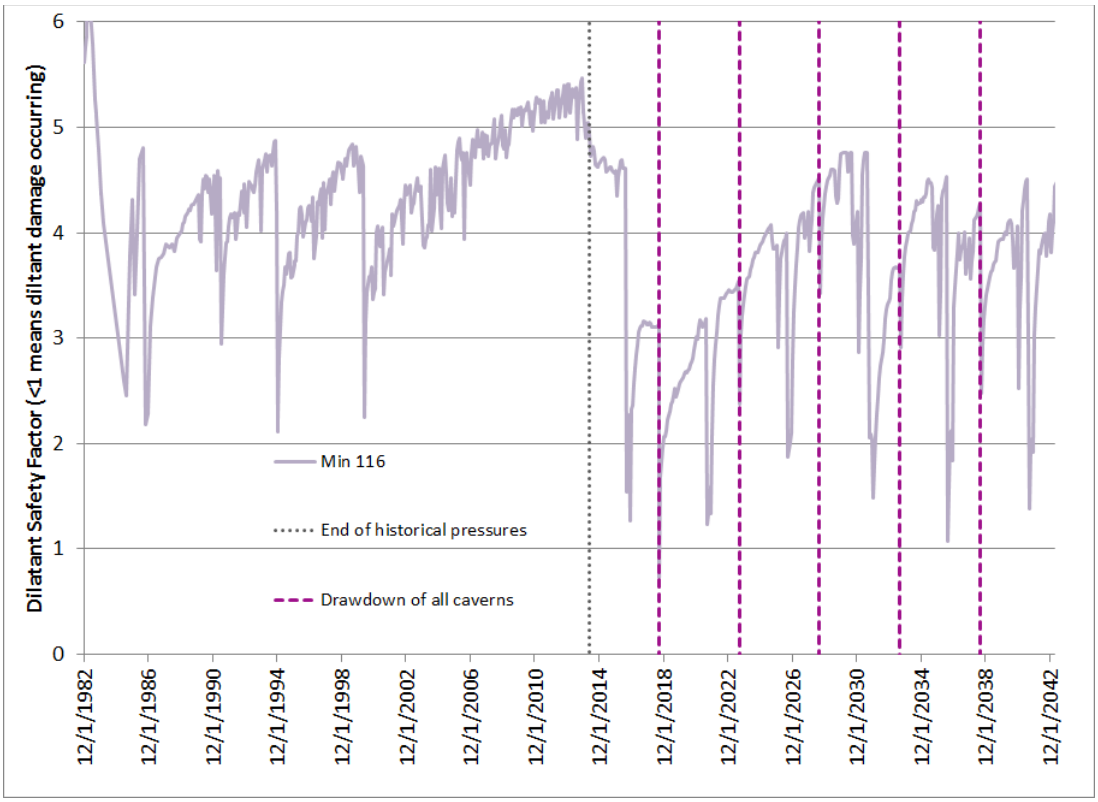

Figure 2.16-2. Minimum value of dilatant safety factor surrounding WH-116.

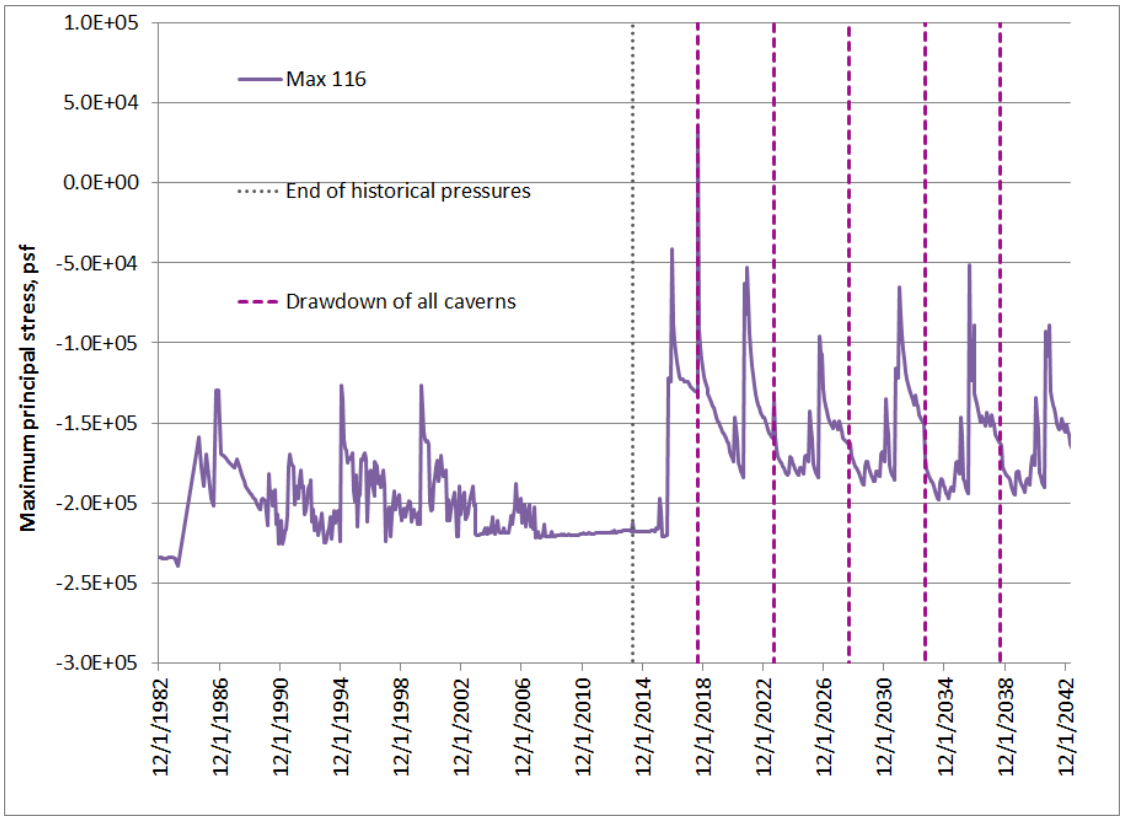

Figure 2.16-3. Maximum value of maximum principal stress surrounding WH-116.

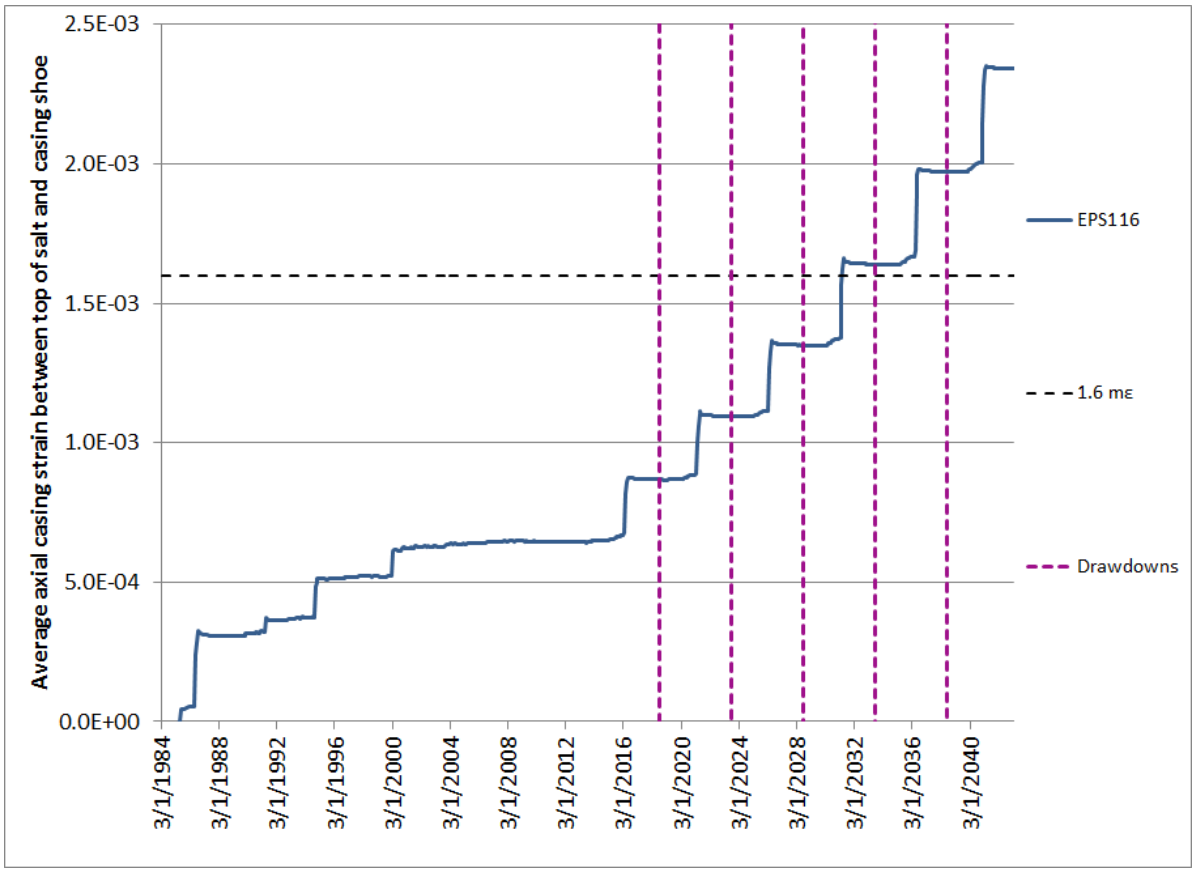

Figure 2.16-4. Predicted avg. axial casing strain between casing shoe and top of salt for WH-116.

As of July 2015, no salt falls have been recorded for WH-116 (Roberts et al., 2015). Salt falls are not unusual, even for otherwise mechanically-stable caverns, but a lack of salt falls supports the indications from the geomechanical calculations that WH-116 should be mechanically stable through five drawdowns. Therefore:

The updated estimate for WH-116 based on geomechanical analyses is that this cavern is stable through 5 drawdowns.

2.17 WH Cavern 117

WH Cavern 117 is a Phase 2 cavern surrounded by Phase 2 caverns. The previous best estimate for its number of available drawdowns was 5, based on P/D ratios with its nearby caverns. Table 2.17 summarizes the P/D and geomechanical estimates for available drawdowns for WH-117 in 2014. Figure 2.17-1 shows the volume of WH-117 in both its computational mesh geometry and its oldest available sonar geometry from 2004, and the geometries of the five drawdown layers built into the computational mesh. As is the case for all the Phase 2 caverns, the modeled drawdown layers extend for nearly the entire height of the cavern, and add approximately 15% to the volume of the cavern when they are removed.

Table 2.17. 2014 Estimates of available drawdowns, WH-117.

Cavern	Basis				2014 Best Estimate Basis (P/D or GM), Comments, Reference
	2D P/D < 1	3D P/D < 1	Geomechanics	Best Estimate	
WH117	5	5	5	5	P/D; Rudeen & Lord, 2013; Sobolik & Ehgartner, 2009b*
					Nearest neighbors: 114 (W), 113 (NW), 111 (N), 110 (NE), 109 (SE), 107 (S)

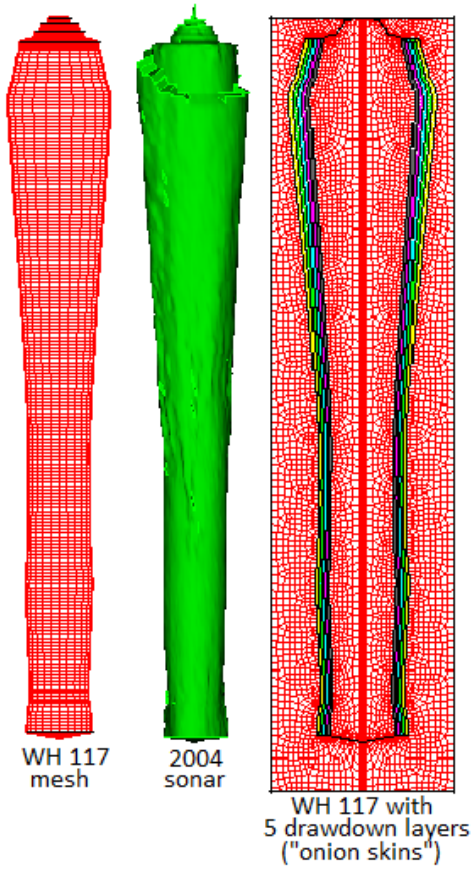

Figure 2.17-1. Computational mesh and sonar geometries for WH-117

Figure 2.17-2 plots the minimum value of dilatant damage factor, or safety factor, at any point around the cavern wall, as a function of time through five drawdowns. The lowest predicted value for the dilatant safety factor was 1.08, at the beginning of a workover after the fifth drawdown. This minimum value occurs at the floor of the cavern, which has the similar pattern of high dilatant stresses and reduced safety factors during workovers. Similarly low values occur near the corner of the cavern ceiling. As usual, these values occur during workovers; the geomechanical predictions indicate that at all other times there are no excessive dilatant stress values. Because the time and location of the low safety factor values are in the floor of the cavern, and only for a brief period coincident with a workover, these occurrences are not believed to be significant enough to cause microcracking in the salt of a magnitude that would affect cavern stability. This conclusion is substantiated in Figure 2.17-3, which plots the maximum value of maximum principal stress around WH-117. Positive values indicate tension, which if they occur would likely be in the same locations as the minimum dilatant safety factor values. The maximum stress never reaches a positive or tensile value through five drawdowns.

Figure 2.17-4 plots the predicted average axial casing strain between the casing and top of salt for WH-117. The overall average strain is predicted to exceed 1.6 millistrains before the fifth drawdown, although the region above the top of the cavern, including the casing shoe, is predicted to have experienced localized strains above 1.6 mε by 2015 (Sobolik, 2015). The strain rate increases slightly once drawdowns begin, but not in an alarming fashion. Because of salt creep, casing integrity is an expected operational issue independent of the number of drawdowns for a particular cavern; because there is no significant change in strain behavior resulting from the drawdowns, there is nothing to indicate additional concern for the mechanical stability of the cavern.

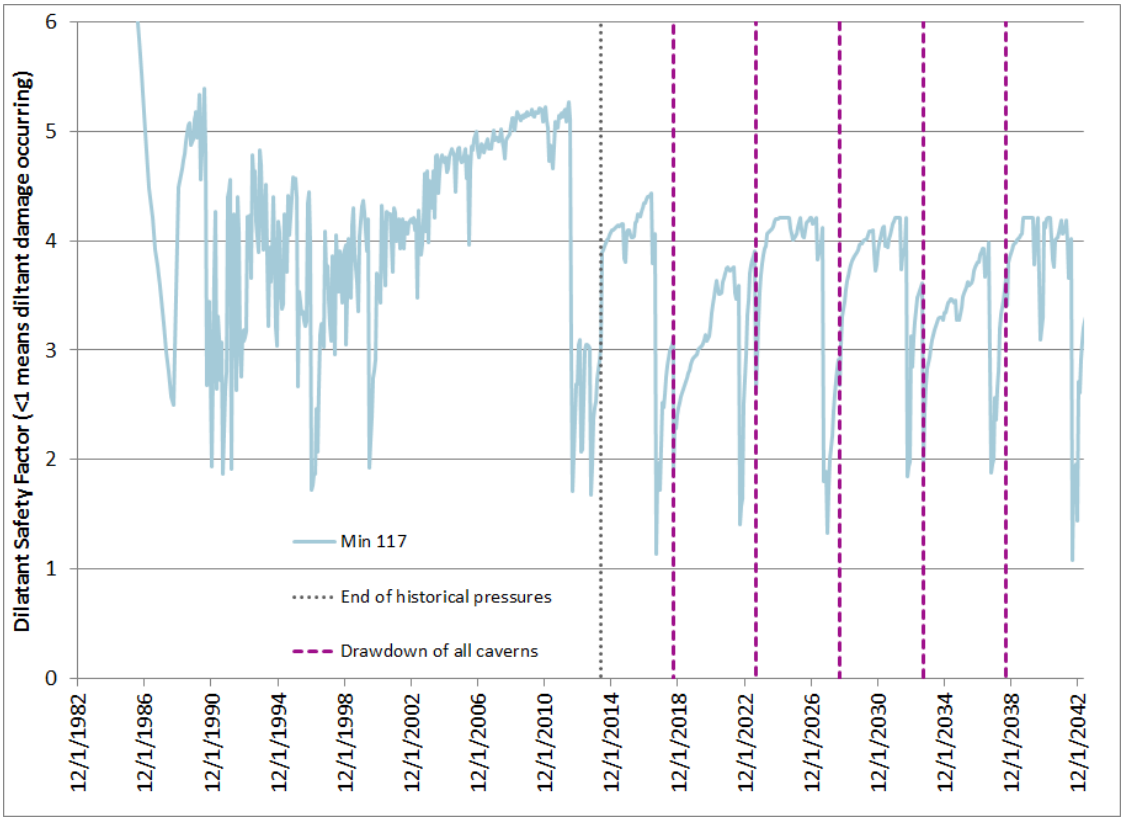

Figure 2.17-2. Minimum value of dilatant safety factor surrounding WH-117.

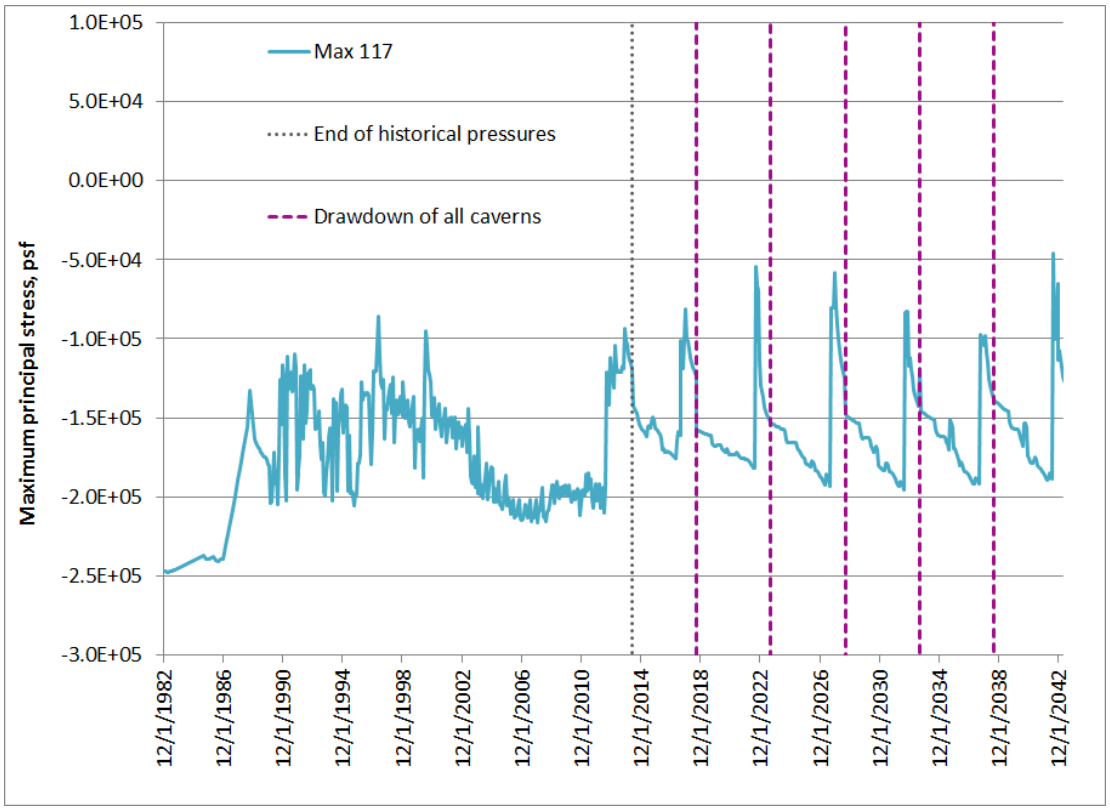

Figure 2.17-3. Maximum value of maximum principal stress surrounding WH-117.

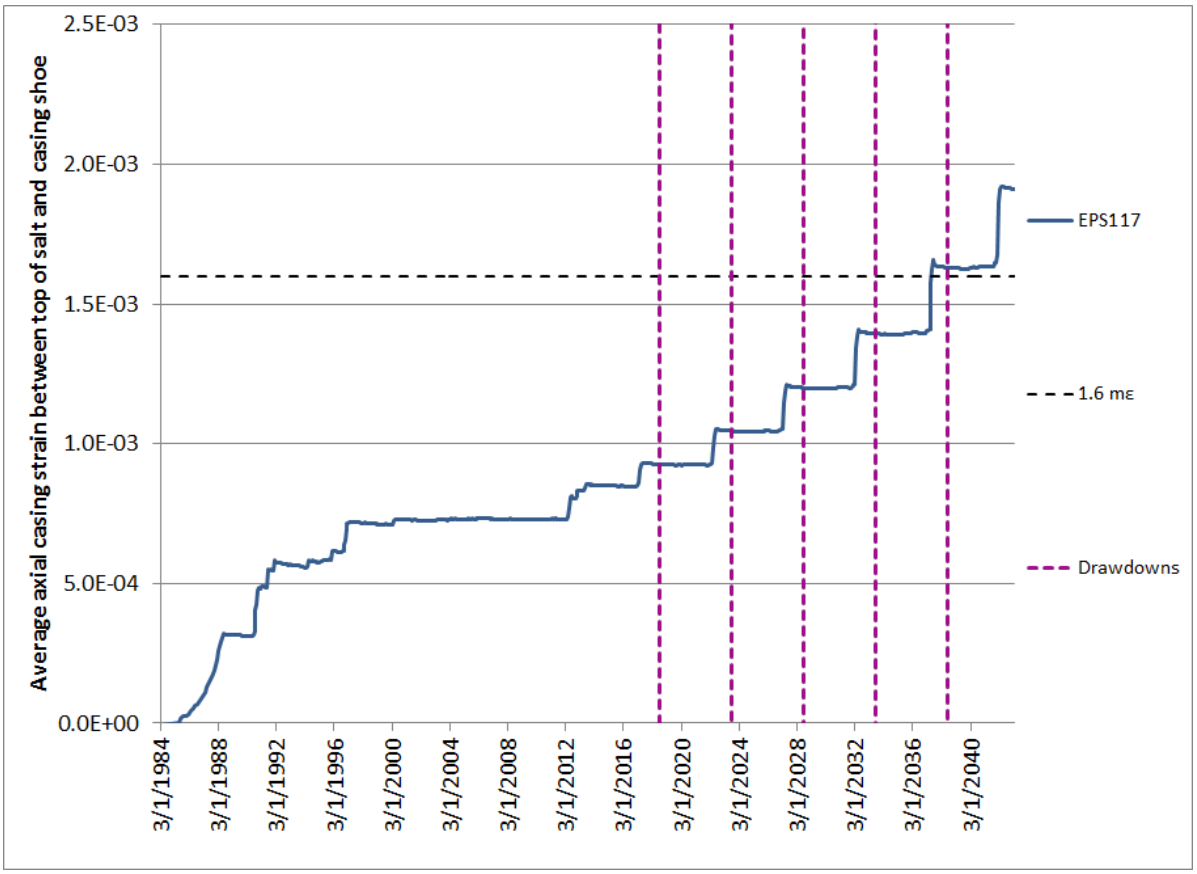

Figure 2.17-5. Predicted avg. axial casing strain between casing shoe and top of salt for WH-117.

As of July 2015, three salt falls have been recorded for WH-117 (Roberts et al., 2015). Salt falls are not unusual, even for otherwise mechanically-stable caverns, so this number of salt falls does not contradict the indications from the geomechanical calculations that WH-117 should be mechanically stable through five drawdowns. Therefore:

The updated estimate for WH-117 based on geomechanical analyses is that this cavern is stable through 5 drawdowns.

2.18 WH Cavern 7

WH Cavern 7 is a Phase 1 cavern located near other Phase 1 caverns. The previous best estimate for its number of available drawdowns was 5, based on P/D ratios with its nearby caverns. Table 2.18 summarizes the P/D and geomechanical estimates for available drawdowns for WH-7 in 2014. Figure 2.18-1 shows the volume of WH-7 in both its computational mesh geometry and its oldest available sonar geometry from 2005, and the geometries of the five drawdown layers built into the computational mesh. As is the case for all the Phase 2 caverns, the modeled drawdown layers extend for nearly the entire height of the cavern, and add approximately 15% to the volume of the cavern when they are removed.

Table 2.18. 2014 Estimates of available drawdowns, WH-7.

Cavern	Basis				2014 Best Estimate Basis (P/D or GM), Comments, Reference
	2D P/D < 1	3D P/D < 1	Geomechanics	Best Estimate	
WH7	0	0	5	5	GM; Green, Lord et al 2013; Sobolik & Ehgartner, 2009b
					Nearest neighbors: 6, 8, 9 (W)

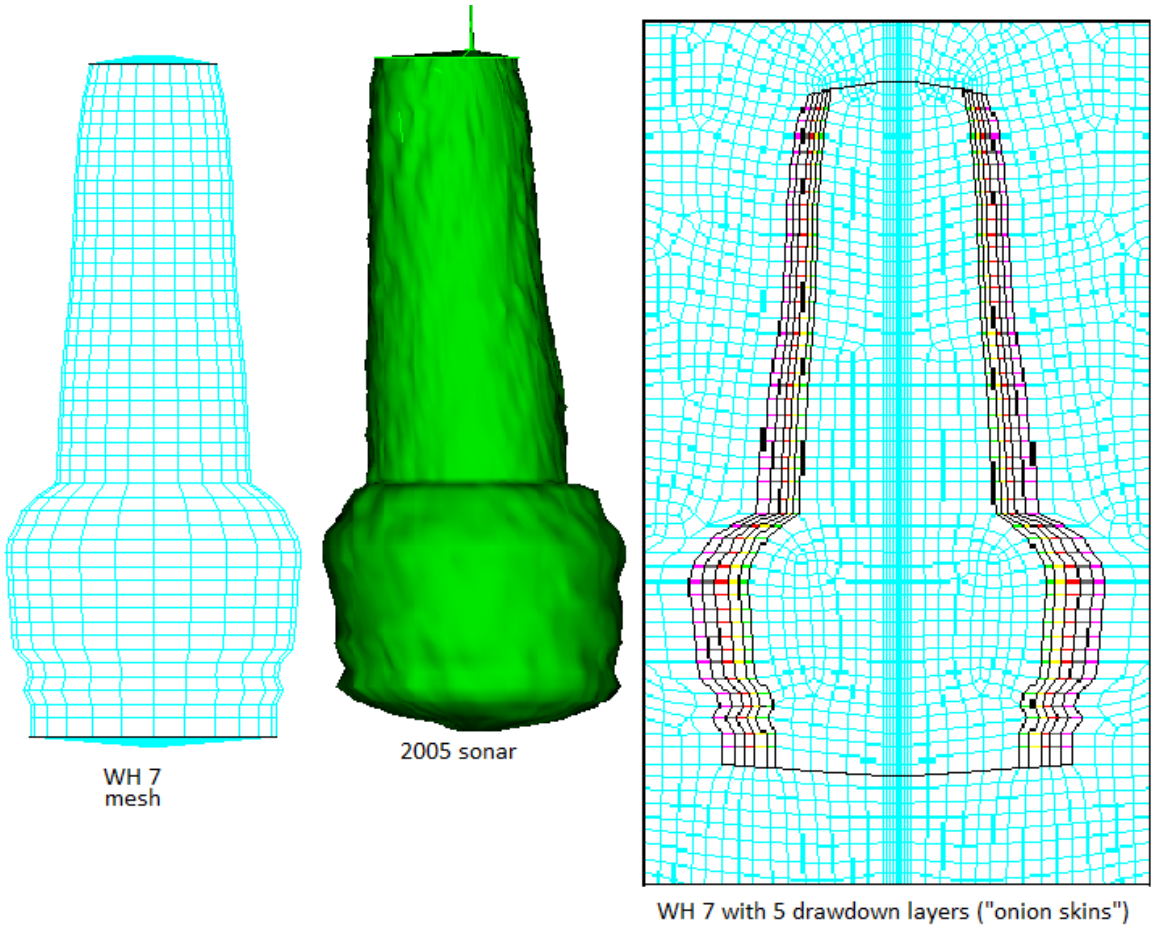

Figure 2.18-1. Computational mesh and sonar geometries for WH-7

Figure 2.18-2 plots the minimum value of dilatant damage factor, or safety factor, at any point around the cavern wall, as a function of time through five drawdowns. The lowest predicted value for the dilatant safety factor was 1.33, at the beginning of a workover after the fourth drawdown. Unlike most of the Phase 2 caverns, this minimum value occurs at the edge of the roof of the cavern. Other low values occur at about one-third the height of the cavern, where the diameter suddenly increases and there is a stress concentration, as shown in Figure 2.18-3. As usual, these lowest values occur during workovers; the geomechanical predictions indicate that at all times there are no excessive dilatant stress values. If safety factor values less than 1.0 occurred at the point of large diameter change, then this occurrence would be a potential concern for the initiation of microcracking or salt fracturing. However, because the low safety factor values are between 1.33 and 1.5, and they occur only for brief periods coincident with a workover, these occurrences are not believed to be significant enough to cause microcracking in the salt of a magnitude that would affect cavern stability. This conclusion is substantiated in Figure 2.18-4, which plots the maximum value of maximum principal stress around WH-7. Positive values indicate tension, which if they occur would likely be in the same locations as the minimum dilatant safety factor values. The maximum stress never reaches a positive or tensile value through five drawdowns.

Figure 2.18-5 plots the predicted average axial casing strain between the casing and top of salt for WH-7. The overall average strain is predicted to exceed 1.6 millistrains after the third drawdown, although the region above the top of the cavern, including the casing shoe, is predicted to have experienced localized strains above 1.6 mε by 2015 (Sobolik, 2015). The strain rate increases slightly once drawdowns begin, but not in an alarming fashion. Because of salt creep, casing integrity is an expected operational issue independent of the number of drawdowns for a particular cavern; because there is no significant change in strain behavior resulting from the drawdowns, there is nothing to indicate additional concern for the mechanical stability of the cavern.

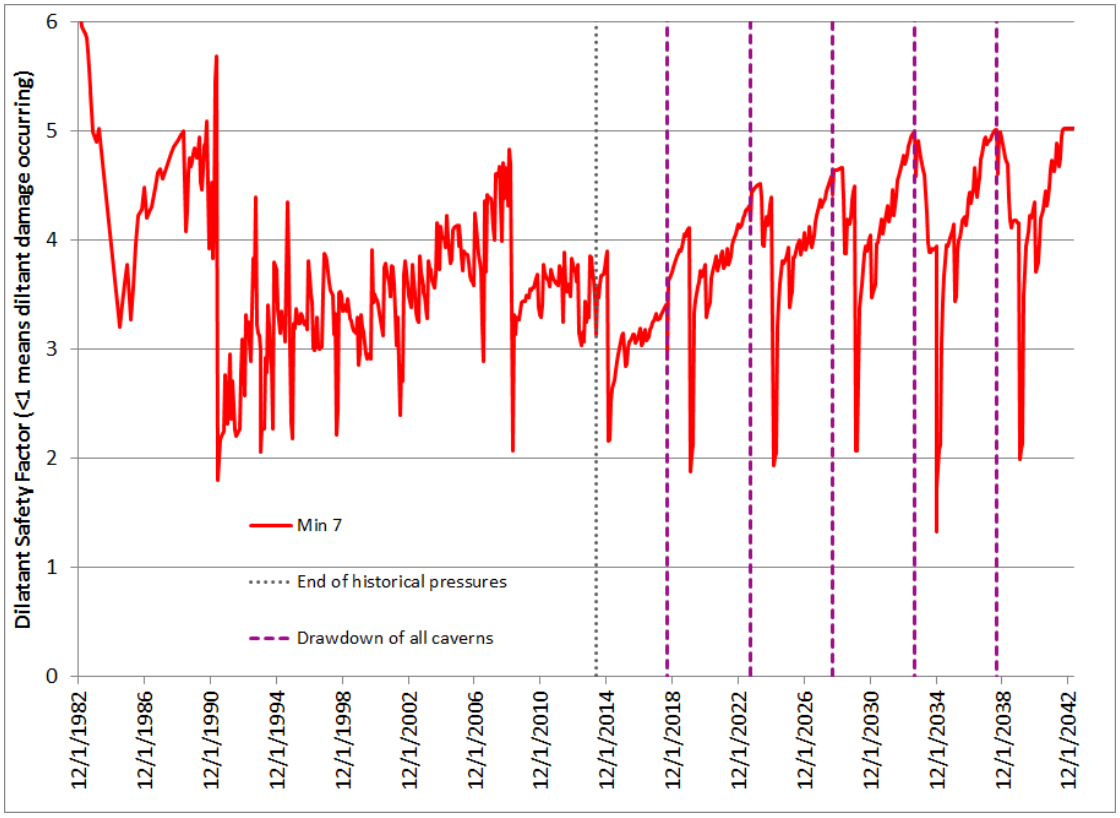

Figure 2.18-2. Minimum value of dilatant safety factor surrounding WH-7.

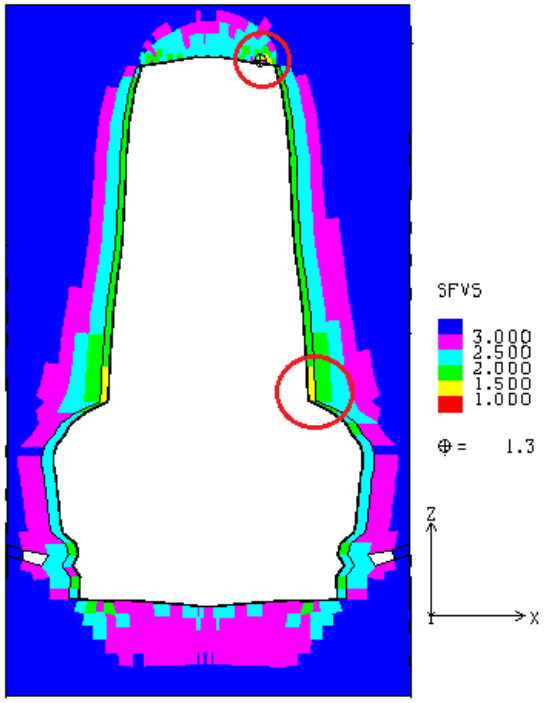

Figure 2.18-3. Locations of minimum value of dilatant safety factor in WH-7.

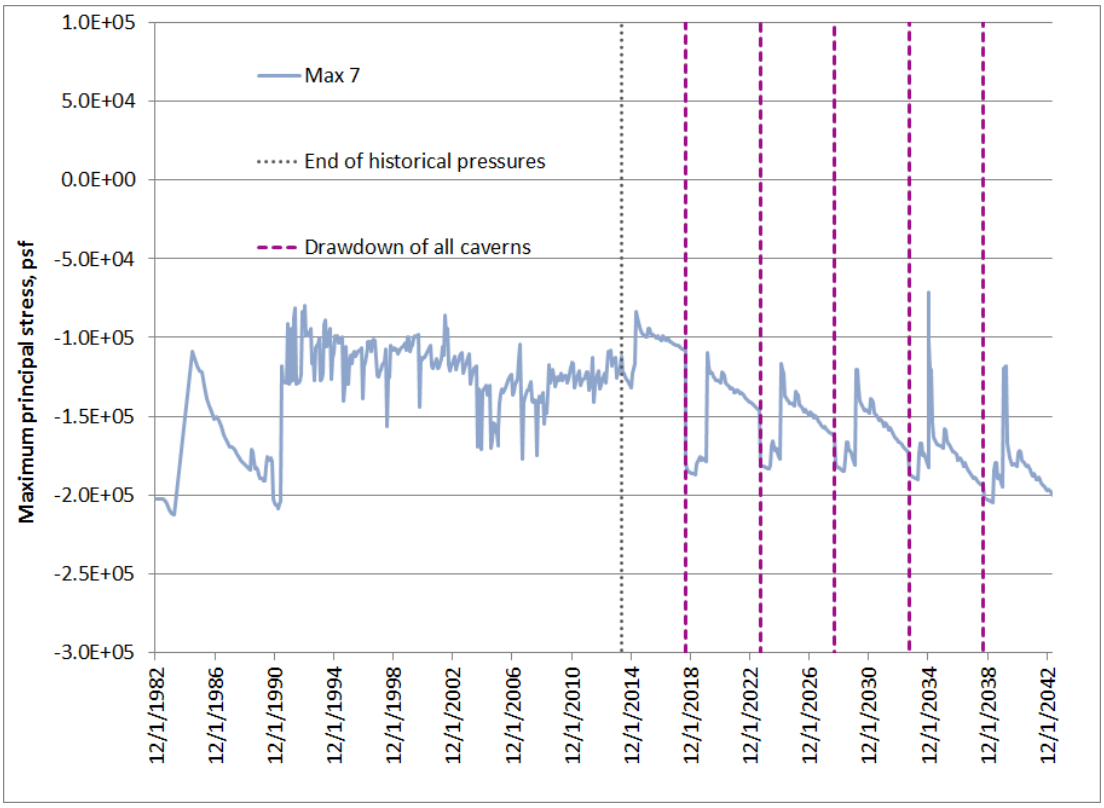

Figure 2.18-4. Maximum value of maximum principal stress surrounding WH-7.

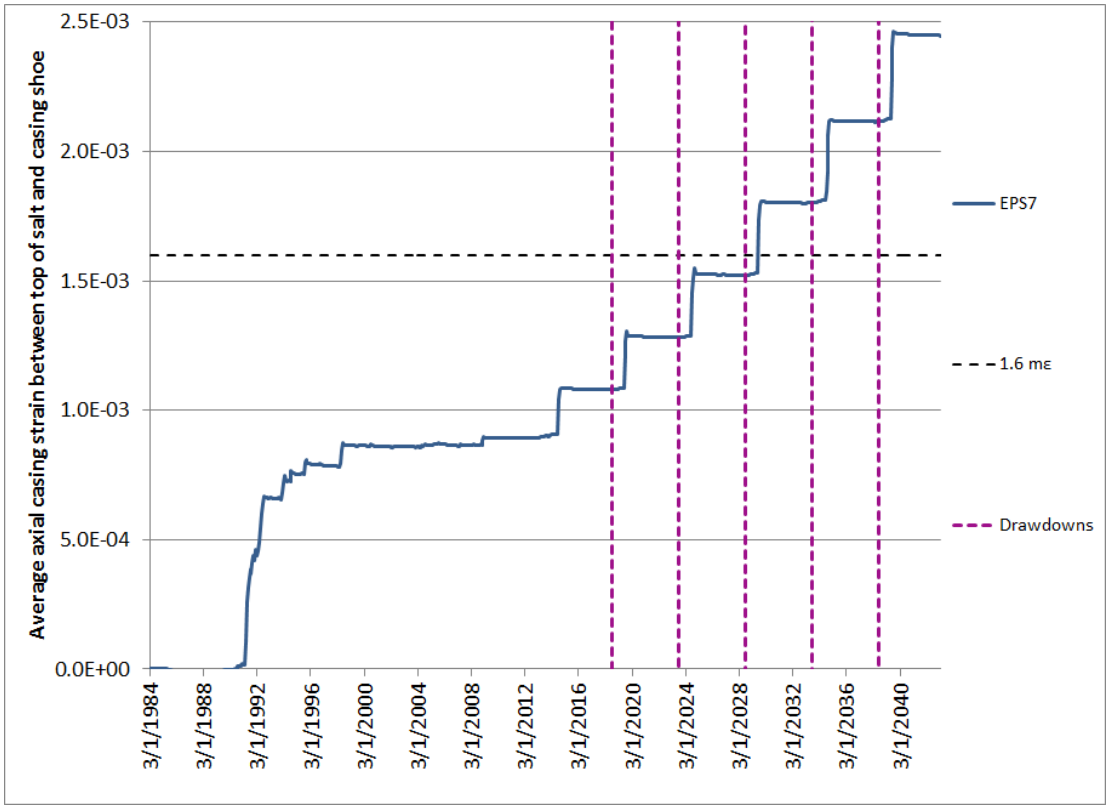

Figure 2.18-5. Predicted avg. axial casing strain between casing shoe and top of salt for WH-7.

As of July 2015, no salt falls have been recorded for WH-7 (Roberts et al., 2015). Salt falls are not unusual, even for otherwise mechanically-stable caverns, but a lack of salt falls supports the indications from the geomechanical calculations that WH-7 should be mechanically stable through five drawdowns. Therefore:

The updated estimate for WH-7 based on geomechanical analyses is that this cavern is stable through 5 drawdowns.

2.19 WH Cavern 8

WH Cavern 8 is a Phase 1 cavern located near other Phase 1 caverns. The previous best estimate for its number of available drawdowns was 2, based on P/D ratios with its nearby caverns. Table 2.19 summarizes the P/D and geomechanical estimates for available drawdowns for WH-8 in 2014. Figure 2.19-1 shows the volume of WH-8 in both its computational mesh geometry and its oldest available sonar geometry from 2004, and the geometries of the four drawdown layers built into the computational mesh (a fifth drawdown was not meshed due to mesh interference problems). As is the case for all the Phase 2 caverns, the modeled drawdown layers extend for nearly the entire height of the cavern, and add approximately 15% to the volume of the cavern when they are removed. Caverns WH-6, 8, and 9 are sufficiently large and in close proximity to each other that the operations of one have observable effects on the others.

Table 2.19. 2014 Estimates of available drawdowns, WH-8.

Cavern	Basis				2014 Best Estimate Basis (P/D or GM), Comments, Reference
	2D P/D < 1	3D P/D < 1	Geomechanics	Best Estimate	
WH8	0	0	2	2	GM; Green, Lord et al 2013; Sobolik & Ehgartner, 2009b
					Nearest neighbors: 9 (NW), 7 (E)

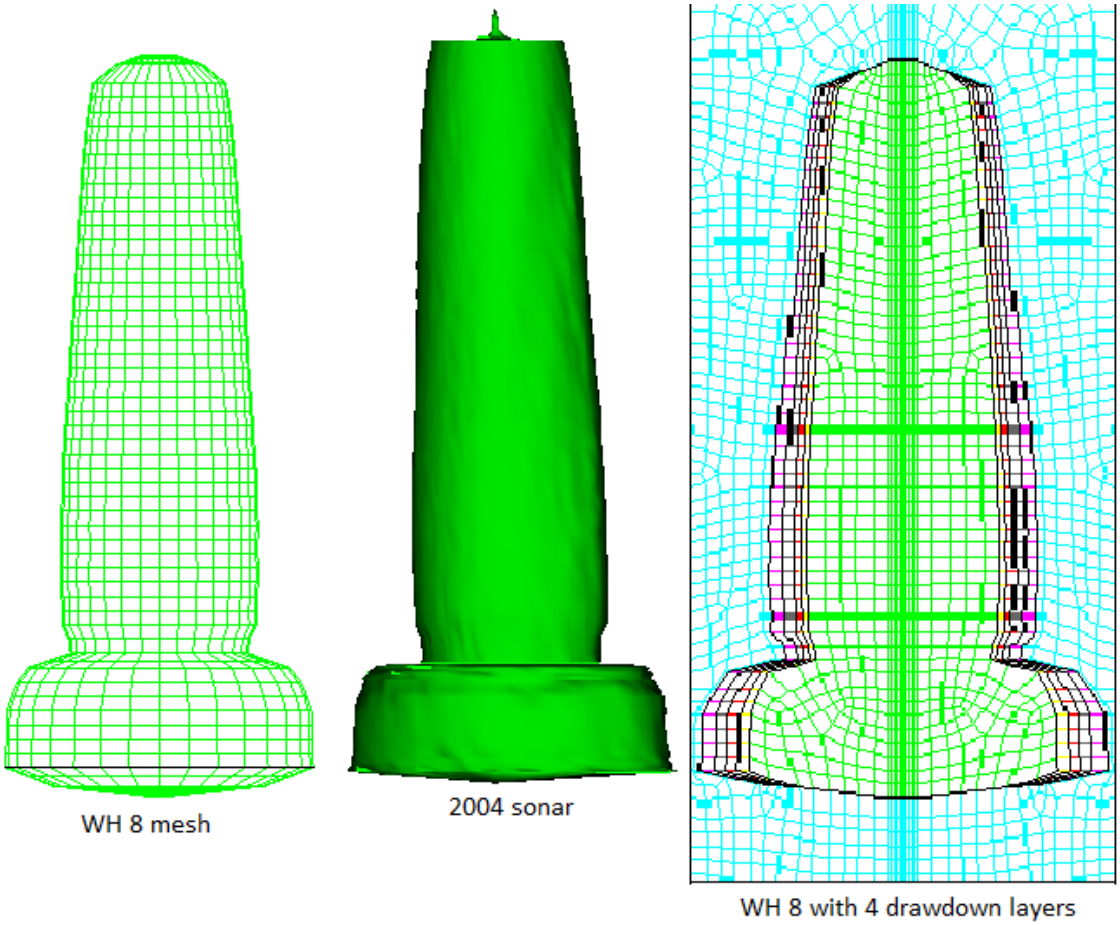

Figure 2.19-1. Computational mesh and sonar geometries for WH-8

Figure 2.19-2 plots the minimum value of dilatant damage factor, or safety factor, at any point around the cavern wall, as a function of time through five drawdowns. WH-8 has several instances when the minimum damage factor is below 1, at the cavern's workover following each drawdown. Similarly, the maximum value of maximum principal stress plotted in Figure 2.19-3 shows instances when tensile stress is recorded somewhere on the wall of the cavern. In addition, the overall trend of the minimum safety factor and maximum stress progresses toward less stable values, a trend not seen for the Phase 2 caverns. These results are curious, and require further investigation into the spatial extent of the extreme stress states. Figure 2.19-4 shows WH-8 and WH-9, and the location of the minimum safety factor near WH-8. The extreme stress state occurs at the bottom of WH-8 at its closest proximity to WH-9. Furthermore, Figures 2.19-2 and 2.19-3 show two peaks in the extreme stress states for WH-8; the first occurs at the workover for WH-8, and the second occurs for the workover in WH-9. The weak point for WH-8 is at the top of the enlarged portion at the bottom of the cavern, nearest to WH-9. Dilatant or tensile stresses in this region can potentially result in the formation of a fracture connecting the two caverns and rendering them as effectively gallery caverns. All other times and locations around WH-8 demonstrate a cavern much like WH-7: generally mechanically stable, with stress concentrations in the ceiling and at the large change in diameter, but with no stress states that exceed stability thresholds. If WH-8 had a larger standoff from WH-9, it would be considered mechanically stable and have five available drawdowns. However, because of the proximity of WH-9 and its effect on stresses around WH-8, the predictions in Figures 2.19-2 through 2.19-4 indicate that extreme care must be taken with WH-8. In addition, as WH-8 grows larger with each succeeding drawdown, the margin for error decreases with the decrease of the safety factor. The workover in WH-8 after the fourth drawdown creates conditions that exceed the stress thresholds (safety factor < 1.0; tensile stresses). Therefore, three drawdowns is automatically the maximum that can be considered for WH-8; because of the proximity issues with WH-9, it is considered prudent to limit the available drawdowns for WH-8 to two until a long-term plan for WH-9 operations is better established.

Figure 2.20-5 plots the predicted average axial casing strain between the casing and top of salt for WH-8. The overall average strain is predicted to never exceed 1.6 millistrains even after five drawdowns, although the region above the top of the cavern, including the casing shoe, is predicted to have experienced localized strains above 1.6 mε by 2015 (Sobolik, 2015). The strain rate increases slightly once drawdowns begin, but not in an alarming fashion. Because of salt creep, casing integrity is an expected operational issue independent of the number of drawdowns for a particular cavern; because there is no significant change in strain behavior resulting from the drawdowns, there is nothing to indicate additional concern for the mechanical stability of the cavern in regards to the casing.

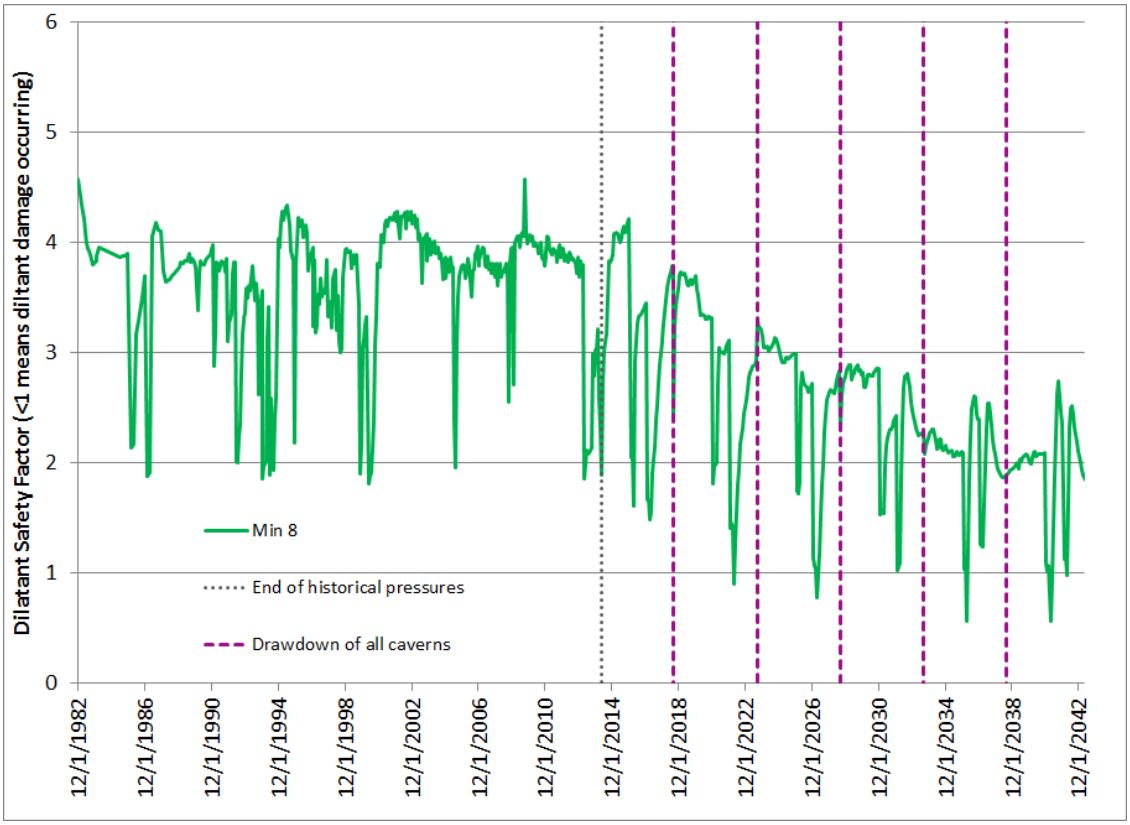

Figure 2.19-2. Minimum value of dilatant safety factor surrounding WH-8.

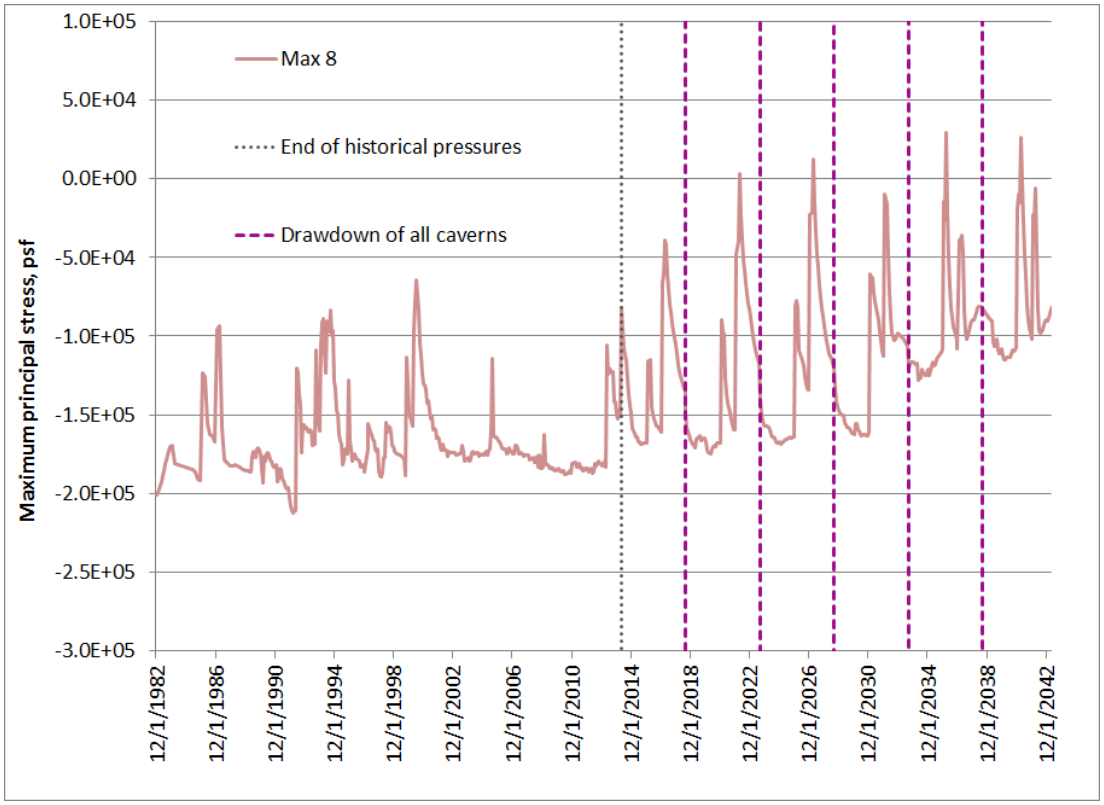

Figure 2.19-3. Maximum value of maximum principal stress surrounding WH-8.

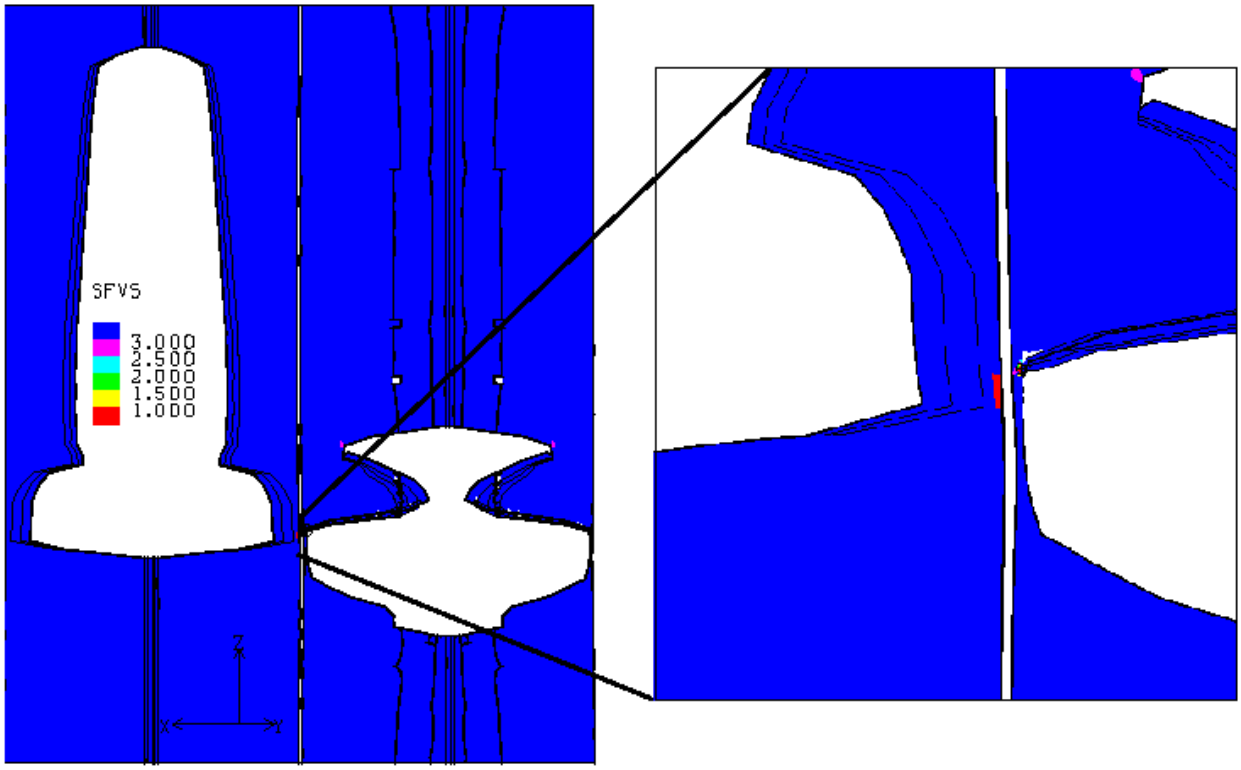

Figure 2.19-4. Locations of minimum value of dilatant safety factor in WH-8.

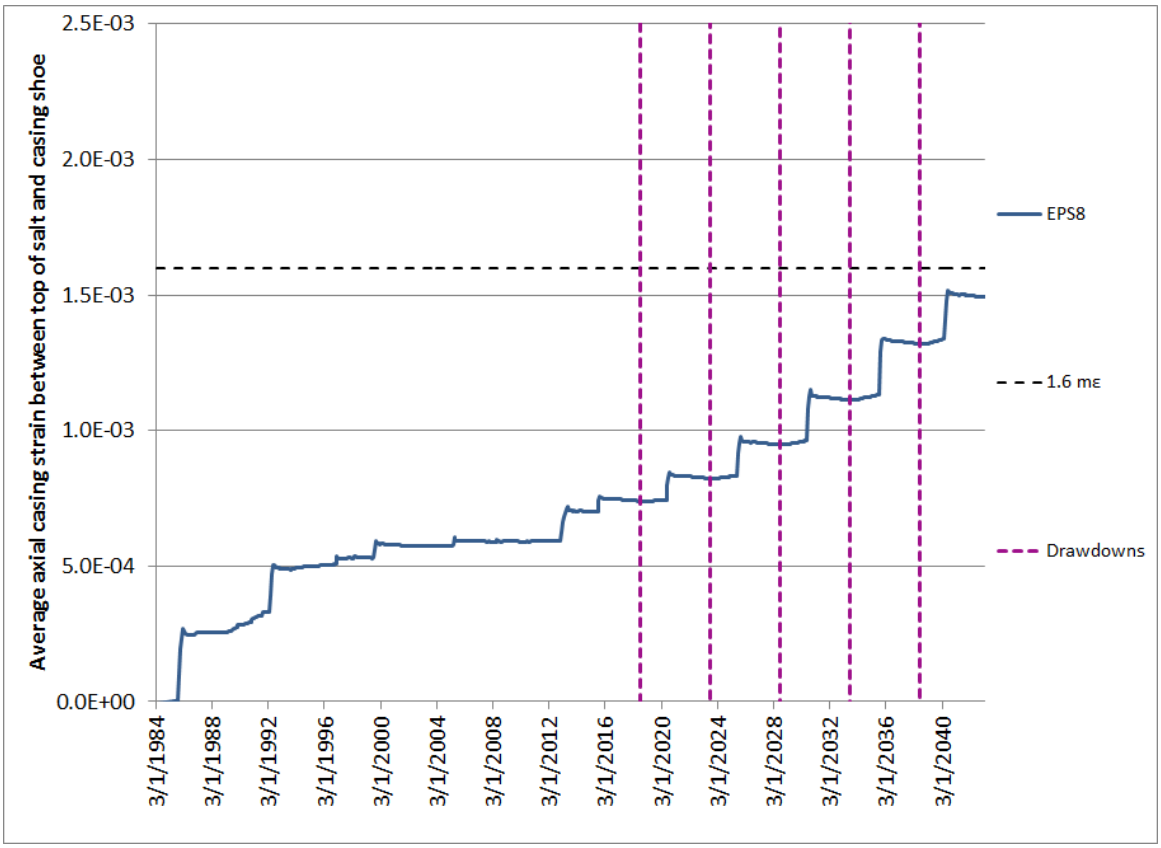

Figure 2.19-5. Predicted avg. axial casing strain between casing shoe and top of salt for WH-8.

As of July 2015, no salt falls have been recorded for WH-8 (Roberts et al., 2015). Salt falls are not unusual, even for otherwise mechanically-stable caverns. The stability issues related to the proximity of WH-9 to WH-8 have been described above. Therefore, on the basis of these analytical results:

The updated estimate for WH-8 based on geomechanical analyses is that this cavern should be stable through 2 drawdowns; any drawdowns of WH-8 should be considered as part of an overall plan that includes the continued operation of WH-9.

2.20 WH Cavern 9

WH Cavern 9 is a Phase 1 cavern located near other Phase 1 caverns. The previous best estimate for its number of available drawdowns was 1, based on P/D ratios with its nearby caverns. Table 2.20 summarizes the P/D and geomechanical estimates for available drawdowns for WH-9 in 2014. Figure 2.20-1 shows the volume of WH-9 in both its computational mesh geometry and its oldest available sonar geometry from 1977, and the geometries of the three drawdown layers built into the computational mesh (more drawdowns were not meshed due to uncertainties in leached volumes). Unlike the case for all the Phase 2 caverns, the modeled drawdown layers are only applied to the ledge between the upper and lower lobes. Caverns WH-6, 8, and 9 are sufficiently large and in close proximity to each other that the operations of one have observable effects on the others.

Table 2.20. 2014 Estimates of available drawdowns, WH-9.

Cavern	Basis				2014 Best Estimate Basis (P/D or GM), Comments, Reference
	2D P/D < 1	3D P/D < 1	Geomechanics	Best Estimate	
WH9	0	0	1	1	GM; Yellow, Lord et al 2013; Sobolik & Ehgartner, 2009b, Sobolik, 2013
					Nearest neighbors: 6 (N), 8 (SE)

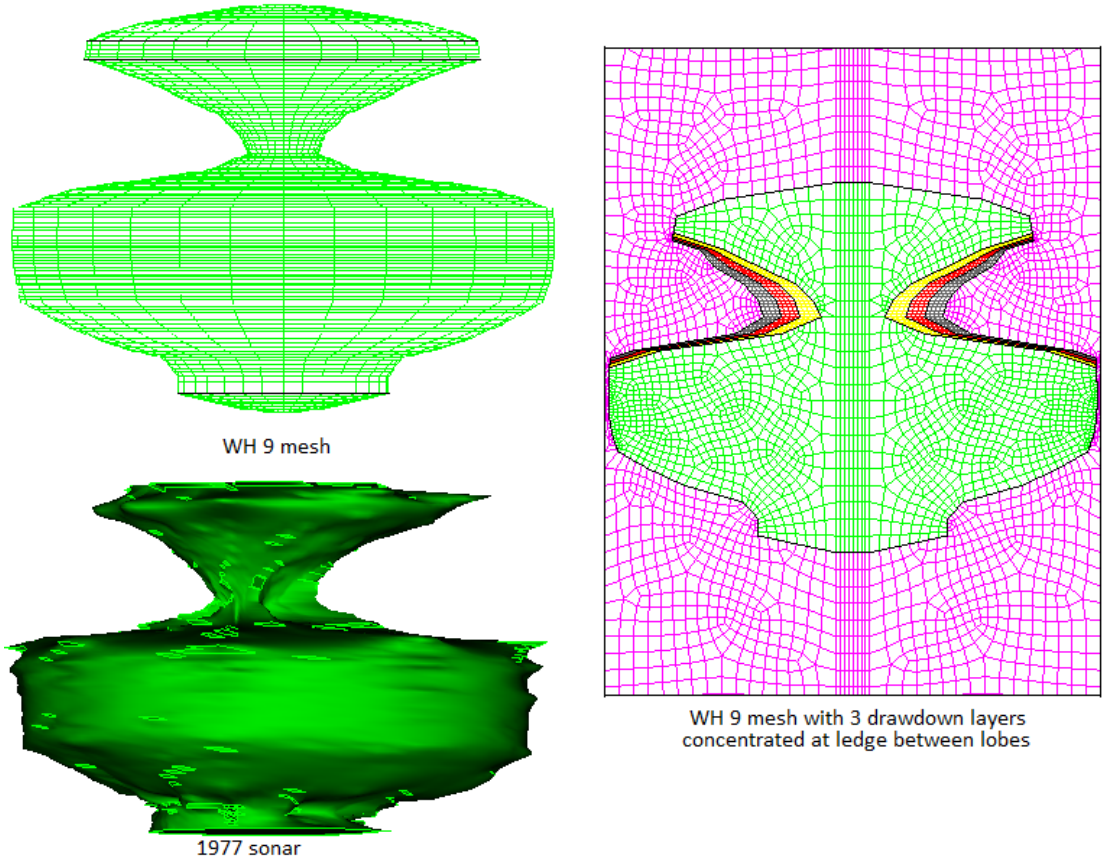

Figure 2.20-1. Computational mesh and sonar geometries for WH-9

Figure 2.20-2 plots the minimum value of dilatant damage factor, or safety factor, at any point around the cavern wall, as a function of time through five drawdowns. WH-9 has a lengthy period where at least one location on its wall has a predicted safety factor value of zero. Similarly, the maximum value of maximum principal stress plotted in Figure 2.20-3 shows a predicted tensile stress somewhere on the wall of the cavern for an extended period of time. Examination of the results of the calculations show that the upper corner of the lower lobe of WH-9, closest to the WH-8, is the location of this extreme stress state, as shown in Figure 2-19.4. In addition, several other locations around WH-9 achieve threshold or near-threshold stress conditions. Figure 2.20-4 shows the dilatant safety factor around WH-9 at the beginning of a workover. The top edge of the lower lobe around its entire circumference, the outer circumference of the upper lobe, and the ledge between the lobe all indicate values of dilatant safety factor that at times are wither below 1.0 (the onset of dilatant damage) or 1.5 (the target minimum safety factor). The maximum principal stress at these locations does also occasionally become positive during a workover. Two additional comments must be made regarding the modeling of the behavior of WH-9. First, the modeled workovers for this cavern included more gradual depressurization and repressurization procedures than were modeled for the other caverns; therefore, "spikes" in behavior are more realistic and believable. Second, the "onion skin" layers removed for each drawdown were assumed to occur only in the ledge. In actual practice, it will be very difficult to design a drawdown of WH-9 that does not enlarge the diameter of the bottom lobe to at least some extent. Because of the close proximity of WH-9 to both WH-8 and WH-6, an increase in the diameter of the lower lobe would magnify the potential for fracture creation and propagation between these caverns. Therefore, there can only be one recommended drawdown for WH-9, and that would be the drawdown that permanently removes oil from the cavern. In addition, whatever actions that are planned for WH-9 will have a significant influence on the behavior and stability of WH-8, and must be planned accordingly.

Figure 2.20-5 plots the predicted average axial casing strain between the casing and top of salt for WH-9. The overall average strain is predicted to exceed 1.6 millistrains after the first drawdown, although the region above the top of the cavern, including the casing shoe, is predicted to have experienced localized strains above 1.6 mε by 2015 (Sobolik, 2015). Much like WH-6, which is a cavern with a large diameter-to-height ratio, casing integrity is an ongoing issue, particularly as it relates to the enhanced strain effects that occur during a workover.

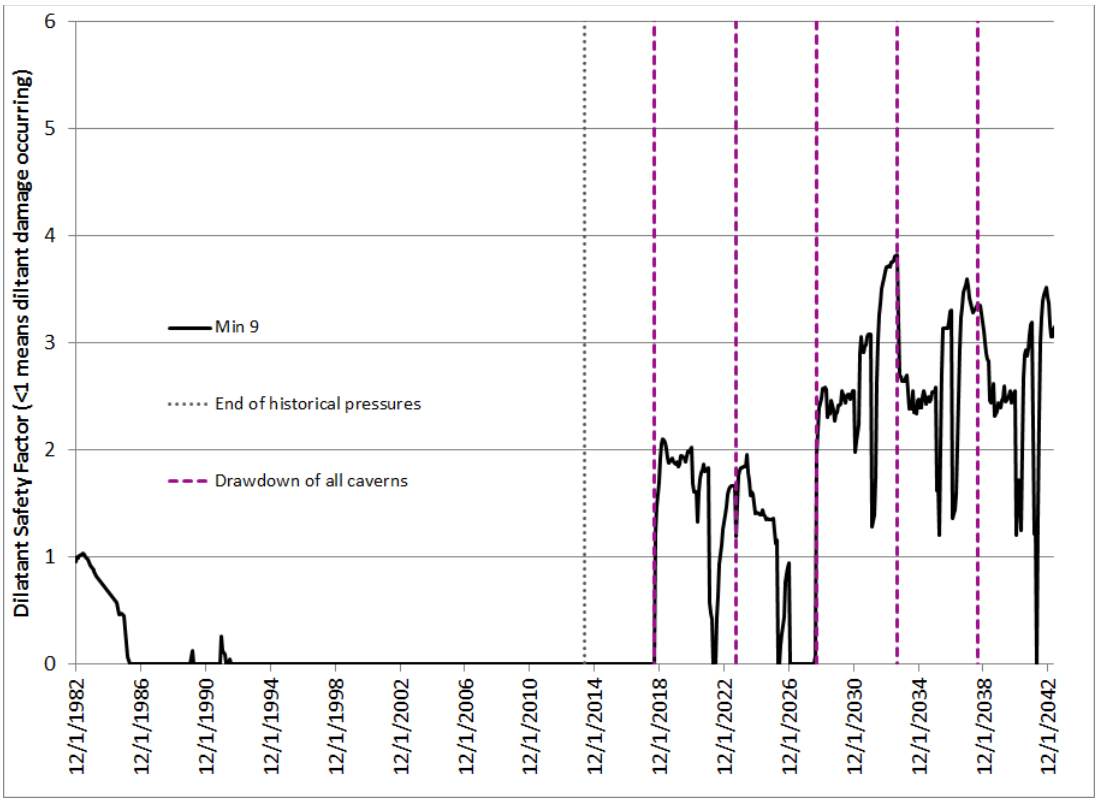

Figure 2.20-2. Minimum value of dilatant safety factor surrounding WH-9.

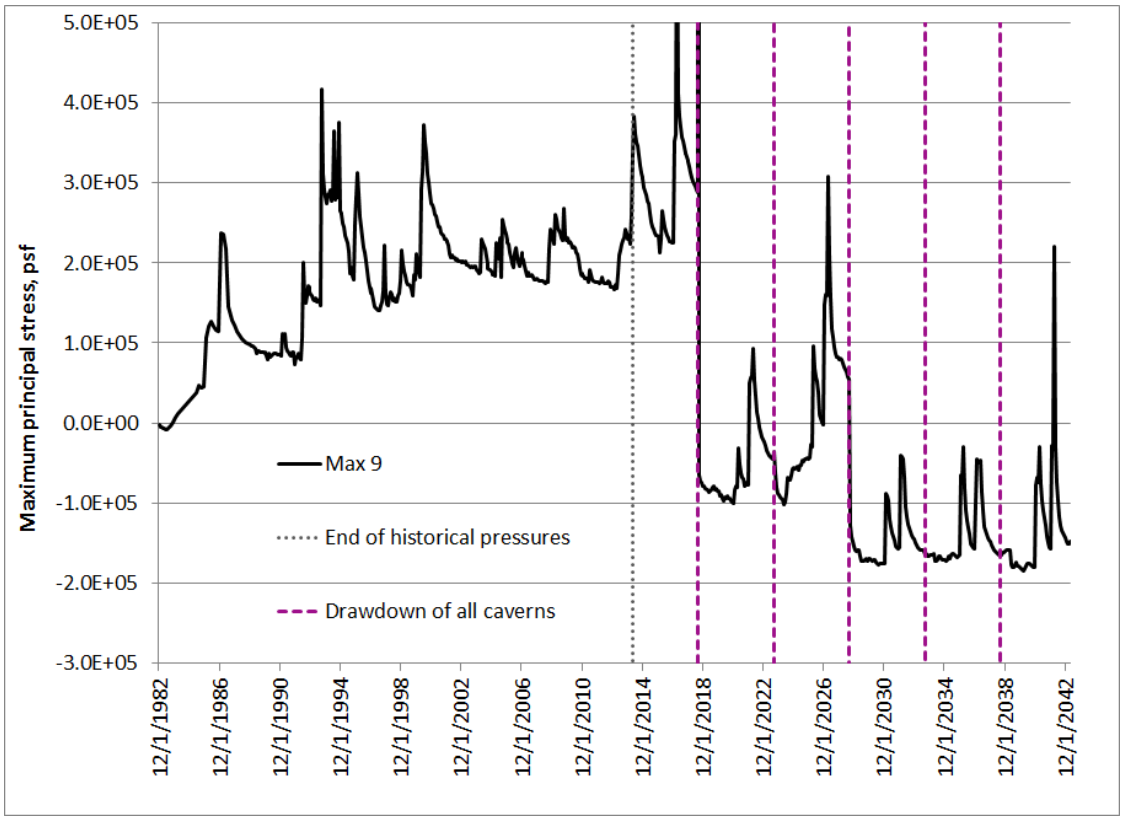

Figure 2.20-3. Maximum value of maximum principal stress surrounding WH-9.

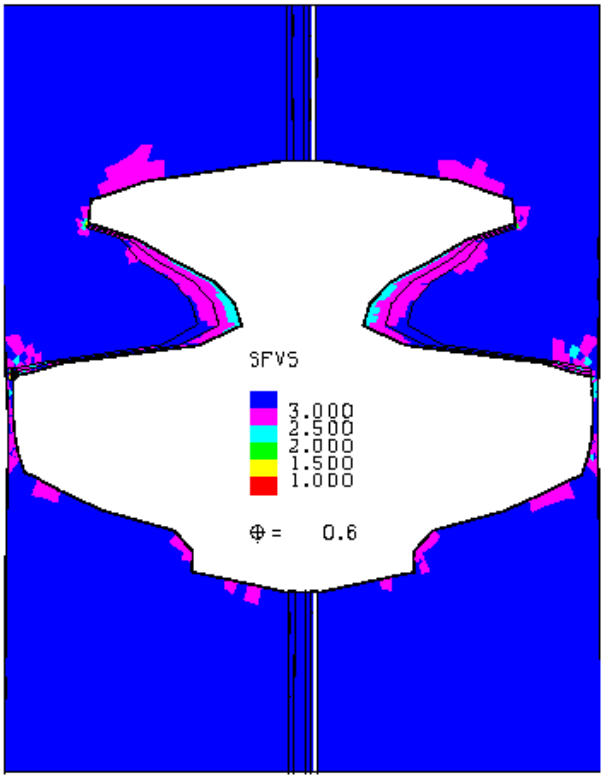

Figure 2.20-4. Locations of minimum value of dilatant safety factor in WH-9.

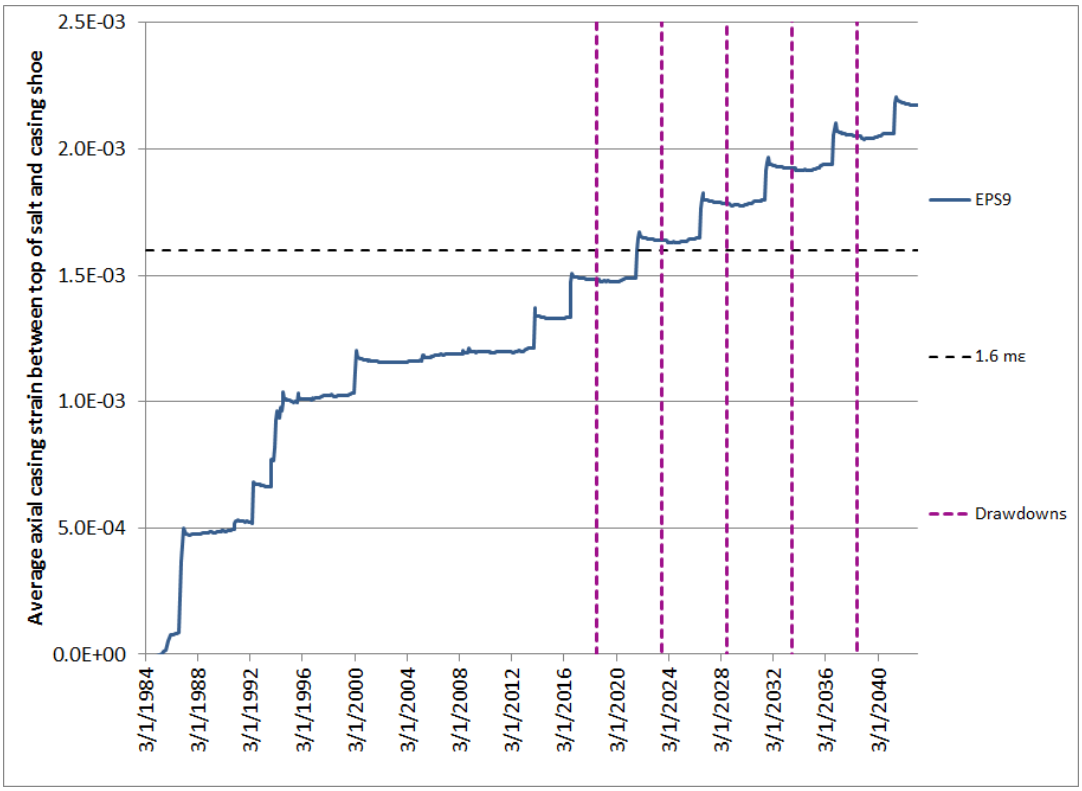

Figure 2.20-5. Predicted avg. axial casing strain between casing shoe and top of salt for WH-9.

As of July 2015, no salt falls has been recorded for WH-9 (Roberts et al., 2015). Salt falls are not unusual, even for otherwise mechanically-stable caverns. The stability issues related to the unusual geometry of WH-9, and the proximity of WH-9 to WH-8 have been described above. The estimate for the number of available drawdowns for WH-9 assumes that it will be very difficult to perform a drawdown without increasing the diameter of the lower lobe of WH-9, the portion of the cavern closest to WH-8. Therefore, on the basis of these analytical results:

The updated estimate for WH-9 based on geomechanical analyses is that this cavern, in its current configuration, has only 1 available drawdown. Additional drawdowns may be available only if such drawdowns can be effectively designed to remove the ledge between the upper and lower lobes, and not increase the diameter of the lower lobe. If it is desired to consider operating WH-9 and WH-8 as a gallery, this estimate may be reevaluated based on such an operation.

2.21 WH Cavern 11

WH Cavern 11 is a Phase 1 cavern located near Phase 2 caverns. The previous best estimate for its number of available drawdowns was 5, based on P/D ratios with its nearby caverns. Table 2.21 summarizes the P/D and geomechanical estimates for available drawdowns for WH-11 in 2014. Figure 2.21-1 shows the volume of WH-11 in both its computational mesh geometry and its oldest available sonar geometry from 2003, and the geometries of the three drawdown layers built into the computational mesh (more drawdowns were not meshed due to uncertainties in leached volumes). As is the case for all the Phase 2 caverns, the modeled drawdown layers extend for nearly the entire height of the cavern, and add approximately 15% to the volume of the cavern when they are removed.

Table 2.21. 2014 Estimates of available drawdowns, WH-11.

Cavern	Basis				2014 Best Estimate Basis (P/D or GM), Comments, Reference
	2D P/D < 1	3D P/D < 1	Geomechanics	Best Estimate	
WH11	5	5	5	5	GM; R&L, 2013; S&E, 2009b
					Nearest neighbors: 112 (S), 108 (SW)

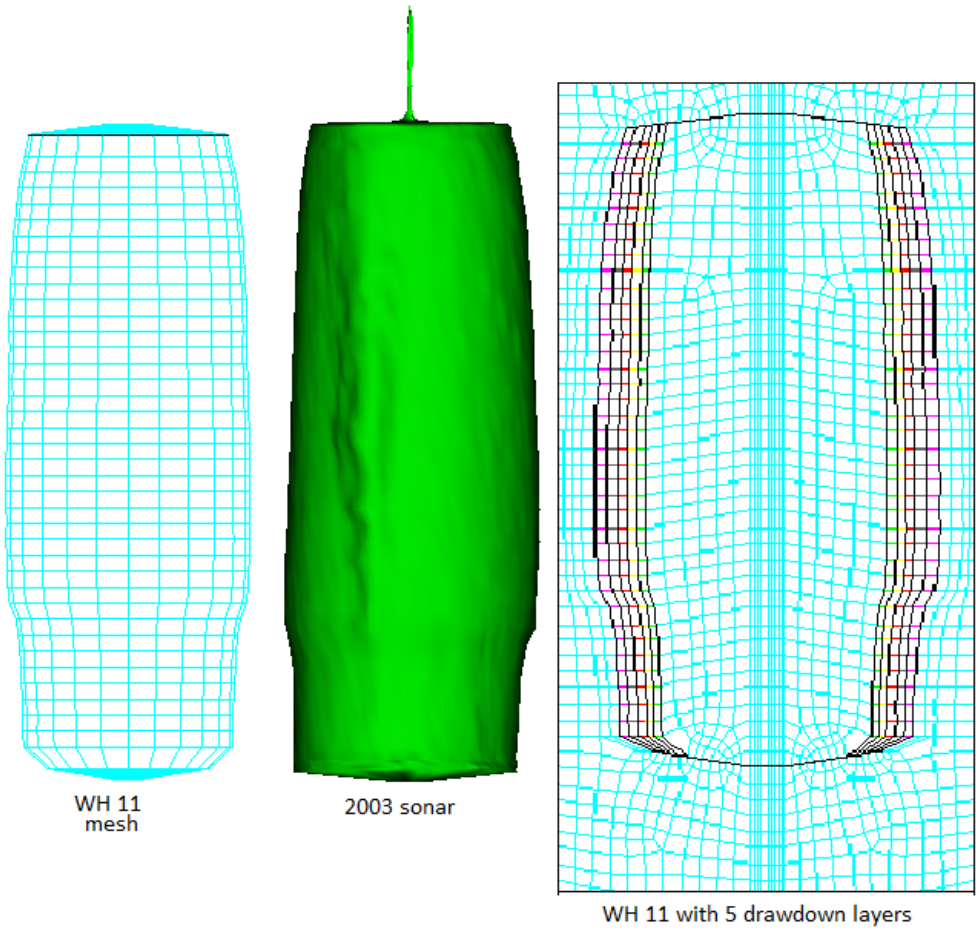

Figure 2.21-1. Computational mesh and sonar geometries for WH-11

Figure 2.21-2 plots the minimum value of dilatant damage factor, or safety factor, at any point around the cavern wall, as a function of time through five drawdowns. The lowest predicted value for the dilatant safety factor was 1.98, prior to the second drawdown; otherwise, the minimum safety factor never reaches values under 2.0. These values are not believed to be significant enough to cause microcracking in the salt of a magnitude that would affect cavern stability. This conclusion is substantiated in Figure 2.21-3, which plots the maximum value of maximum principal stress around WH-11. Positive values indicate tension, which if they occur would likely be in the same locations as the minimum dilatant safety factor values. The maximum stress never reaches a positive or tensile value through five drawdowns.

Figure 2.21-4 plots the predicted average axial casing strain between the casing and top of salt for WH-11. The overall average strain is predicted to exceed 1.6 millistrains prior to the third drawdown, although the region above the top of the cavern, including the casing shoe, is predicted to have experienced localized strains above 1.6 mε by 2015 (Sobolik, 2015). The strain rate increases slightly once drawdowns begin, but not in an alarming fashion. Because of salt creep, casing integrity is an expected operational issue independent of the number of drawdowns for a particular cavern; because there is no significant change in strain behavior resulting from the drawdowns, there is nothing to indicate additional concern for the mechanical stability of the cavern.

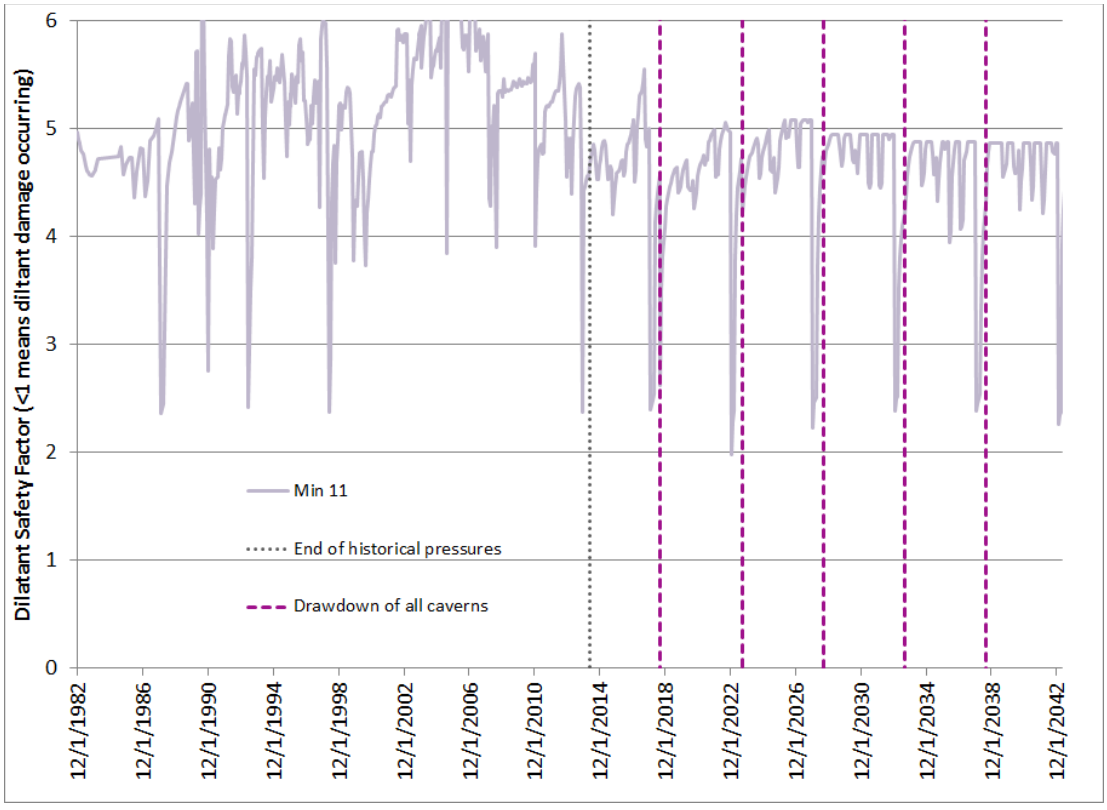

Figure 2.21-2. Minimum value of dilatant safety factor surrounding WH-11.

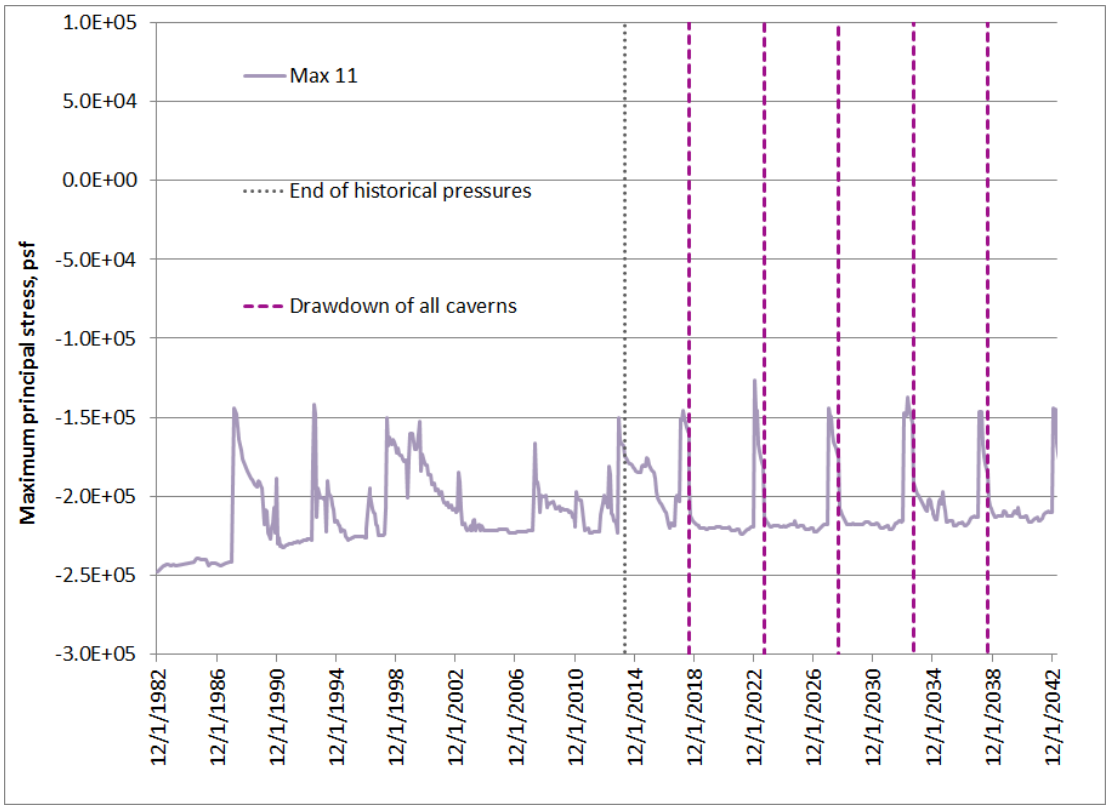

Figure 2.21-3. Maximum value of maximum principal stress surrounding WH-11.

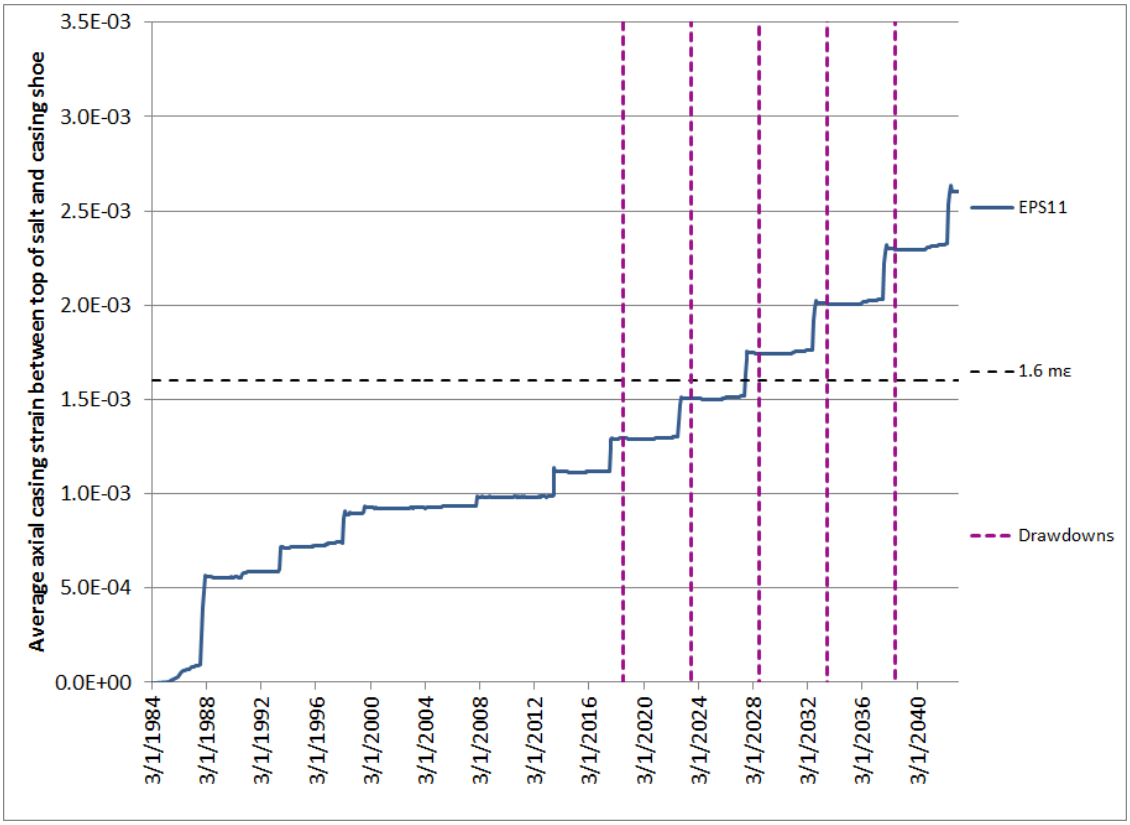

Figure 2.21-5. Predicted avg. axial casing strain between casing shoe and top of salt for WH-11.

As of July 2015, no salt falls have been recorded for WH-11 (Roberts et al., 2015). Salt falls are not unusual, even for otherwise mechanically-stable caverns, but a lack of salt falls supports the indications from the geomechanical calculations that WH-11 should be mechanically stable through five drawdowns. Therefore:

The updated estimate for WH-11 based on geomechanical analyses is that this cavern is stable through 5 drawdowns.

3. Conclusions - Summary of Available Drawdown

The estimates for the available drawdowns for each of the West Hackberry caverns have been updated based on the recently upgraded West Hackberry geomechanical model (Sobolik, 2015). The new estimates for West Hackberry are summarized in Table 3-1, and the updated estimates for all SPR sites are in Table 3-2. All of the Phase 2 caverns, and also caverns WH-7 and WH-11, are predicted to have five available drawdowns remaining. WH-8 has only two remaining drawdowns due to its proximity to WH-9, and WH-9 has only one remaining drawdown. WH-6 has been emptied of oil and will not likely be reutilized for oil storage, and therefore has been updated as "not available". As a follow-up to these recommendations, it is important for the SPR to develop a procedure to document the number and dates of full and partial drawdowns, so that this table may be a useful tool for planning future operations.

Table 3-1. Updated Number of Available Drawdowns – West Hackberry

Cavern	Basis				Best Estimate Basis (P/D or GM), Comments, Reference
	2D P/D < 1	3D P/D < 1	Geomechanics	Best Estimate	
WH101	3	3	5	5	GM; Sobolik, 2015
WH102	3	3	5	5	GM; Sobolik, 2015
WH103	2	4	5	5	GM; Sobolik, 2015
WH104	3	3	5	5	GM; Sobolik, 2015
WH105	2	2	5	5	GM; Sobolik, 2015
WH106	4	4	5	5	GM; Sobolik, 2015
WH107	2	5	5	5	GM; Sobolik, 2015
WH108	4	4	5	5	GM; Sobolik, 2015
WH109	2	4	5	5	GM; Sobolik, 2015
WH110	1	5	5	5	GM; Sobolik, 2015
WH111	5	5	5	5	GM; Sobolik, 2015
WH112	4	4	5	5	GM; Sobolik, 2015
WH113	4	4	5	5	GM; Sobolik, 2015
WH114	4	4	5	5	GM; Sobolik, 2015
WH115	4	5	5	5	GM; Sobolik, 2015
WH116	4	5	5	5	GM; Sobolik, 2015
WH117	5	5	5	5	GM; Sobolik, 2015
WH6	0	0	1	N/A	Cavern emptied of oil
WH7	0	0	5	5	GM; Sobolik, 2015
WH8	0	0	2	2	GM; Green, Lord et al 2013; Sobolik, 2015
WH9	0	0	1	1	GM; Yellow, Lord et al 2013; Sobolik, 2015
WH11	5	5	5	5	GM; Sobolik, 2015
P/D numbers from Rudeen & Lord (2013)					

Table 3-2. Summary of Number of Available Drawdowns for All SPR Sites, March 2016

Cavern	Best Estimate	Cavern	Best Estimate	Cavern	Best Estimate
BC15	1	BM101	5	WH101	5
BC17	1	BM102	5	WH102	5
BC18	1	BM103	5	WH103	5
BC19	1	BM104	5	WH104	5
BC101	1	BM105	5	WH105	5
BC102	5	BM106	5	WH106	5
BH101	3	BM107	5	WH107	5
BH102	4	BM108	5	WH108	5
BH103	4	BM109	5	WH109	5
BH104	3	BM110	5	WH110	5
BH105	4	BM111	5	WH111	5
BH106	4	BM112	5	WH112	5
BH107	4	BM113	5	WH113	5
BH108	5	BM114	5	WH114	5
BH109	5	BM115	5	WH115	5
BH110	5	BM116	5	WH116	5
BH111	4	BM1	1	WH117	5
BH112	3	BM2	1	WH6	N/A
BH113	3	BM4	1	WH7	5
BH114	5	BM5	1	WH8	2
				WH9	1
				WH11	5

4. References

- Eldredge, L. L., D. Checkai, G. Osborne, D. L. Lord, D. K. Rudeen, P. D. Weber and K. A. Gutierrez (2013). "Technical Basis for 2013 SPR Remedial Leach Plan." SPR Joint Working Group on Cavern Leaching. DM Petroleum Operations, New Orleans, LA. U.S. Strategic Petroleum Reserve.
- Lord, A. S., D. K. Rudeen and B. L. Ehgartner (2009). "List of P/D Ratios of all caverns and the allowable number of full drawdowns until P/D ratios of 1.78 and 1.0 are reached." *Milestone FY10-1.7(a1)*, Sandia National Laboratories. Albuquerque, NM 87125, USA. U.S. Strategic Petroleum Reserve.
- Lord, D.L., S.R. Sobolik, B.Y. Park and D.K. Rudeen (2013), "Impacts of First Water Drawdown on SPR Low P/D Caverns", Letter Report to Gilbert Shank DOE PMO dated December 20, 2013. Geotechnology & Engineering, Sandia National Laboratories. U.S. Strategic Petroleum Reserve.
- Lord, D. L. and S. R. Sobolik (2013). "Geotechnical Issues Concerning West Hackberry Cavern 6." presented at SPR Program Review, New Orleans, LA 31-Jul-2013, ed: Geotechnology & Engineering Department, Sandia National Laboratories.
- Osnes, J. D. (2010). "Technical Review of Pillar-to-Diameter Ratio Study Performed by Sandia National Laboratories by the Strategic Petroleum Reserve." RESPEC, Rapid City, SD 57709. U.S. Strategic Petroleum Reserve.
- Park, B. Y., B. L. Ehgartner and M. Y. Lee (2006). "Three Dimensional Simulation for Bayou Choctaw Strategic Petroleum Reserve." Unlimited Release SAND2006-7589, Sandia National Laboratories, Albuquerque, NM.
- Park, B. Y. and B. L. Ehgartner (2011). "Allowable Pillar to Diameter Ratio for Strategic Petroleum Reserve Caverns." Unlimited Release SAND2011-2896, Sandia National Laboratories, Albuquerque, NM 87185. U.S. Strategic Petroleum Reserve.
- Park, B.Y., 2013. Interface Modeling to Predict Wellbore Damage for Big Hill Strategic Petroleum Reserve. In *Proceedings of the 47th US Rock Mechanics Symposium, San Francisco, CA, June 23–26, 2010,* ARMA No. 13-223.
- Park, B.Y., 2014. *Geomechanical Analysis to Predict the Oil Leak at the Wellbores in Big Hill Strategic Petroleum Reserve*, SAND2014-0669, Sandia National Laboratories, Albuquerque, New Mexico.
- Rudeen, D.K. and D.L. Lord (2013). "SPR Cavern Pillar-to-Diameter 2013 Update," Letter Report to Gilbert Shank, DOE PMO dated October 1, 2013. Geotechnology & Engineering, Sandia National Laboratories. U.S. Strategic Petroleum Reserve.
- Sobolik, S. (2013a). "Pressure Differential between West Hackberry Caverns 6 and 9 During Oil Removal in 6." Memo to James Erskine, DM Cavern Operations, Geotechnology & Engineering Department, Sandia National Laboratories. U.S. Strategic Petroleum Reserve.
- Sobolik, S. (2013b). "Preliminary Recommendations Regarding the Maximum Length of Workover of West Hackberry Cavern 9 during Cavern 6 Oil Removal Process." Memo to Lionel Gele, December 20, 2013, DOE-SPR, Sandia National Laboratories. U.S. Strategic Petroleum Reserve.

- Sobolik, S. R. and B. L. Ehgartner (2009a). "Analysis of Cavern Stability at the Bryan Mound SPR Site." SAND2009-1986, Sandia National Laboratories, Albuquerque, NM USA. U.S. Strategic Petroleum Reserve.
- Sobolik, S. R. and B. L. Ehgartner (2009b). "Analysis of Cavern Stability at the West Hackberry SPR Site." SAND2009-2194, Sandia National Laboratories, Albuquerque, NM USA. U.S. Strategic Petroleum Reserve.
- Sobolik, S. R. and B. L. Ehgartner (2012). "Analysis of the Stability of Cavern 3 at the Bryan Mound SPR Site." *SAND2012-1953*, Sandia National Laboratories, Albuquerque, NM. U.S. Strategic Petroleum Reserve.
- Sobolik, S. (2014). "Current Recommendations Regarding ECP PM-00449, Baseline Remaining Drawdowns for all SPR Caverns." Letter to Lisa Nicholson, May 8, 2014, DOE-SPR, Sandia National Laboratories. U.S. Strategic Petroleum Reserve.
- Sobolik, S. R. (2015). "Analysis of Cavern and Well Stability at the West Hackberry SPR Site Using a Full-Dome Model." SAND2015-7401, Sandia National Laboratories, Albuquerque, NM USA. U.S. Strategic Petroleum Reserve.
- Van Sambeek, L.L., J.L. Ratigan, and F.D. Hansen, 1993. *Dilatancy of Rock Salt in Laboratory Tests*, Int. J. Rock Mech. Min. Sci. & Geomech. Abstr. Vol. 30, No. 7, pp 735-738.

- **DISTRIBUTION:**

External Distribution

Electronic copies to:

Wayne Elias (wayne.elias@hq.doe.gov)
for distribution to DOE SPR Program Office, Washington, D.C.
U.S. Department of Energy
Office of Fossil Energy
Forrestal Building
1000 Independence Ave., SW
Washington, DC 20585

Diane Willard (diane.willard@spr.doe.gov)
for distribution to DOE and FFPO SPR Project Management Office, New Orleans, LA.
U.S. Department of Energy
Strategic Petroleum Reserve Project Management Office
900 Commerce Road East
New Orleans, LA 70123

Sandia Distribution

Print copies to:

5	MS0750	Carolyn Kirby
1	MS0751	B. Y. Park
1	MS0751	Steven R. Sobolik

Electronic Copies:

Borns, David	djborns@sandia.gov
Halloran, Amy Randolph	arhallo@sandia.gov
Kirby, Carolyn	clkirby@sandia.gov
Lee, Moo	mylee@sandia.gov
Park, Byoung Yoon	bypark@sandia.gov
Sobolik, Steven R.	srsobol@sandia.gov
Webb, Erik K	ekwebb@sandia.gov
SPR Library	sprclk@sandia.gov
Technical Library	


Sandia National Laboratories